

Supporting Information

**Mechanism-Based Design of Quinoline Potassium Acyltrifluoroborates
for Rapid Amide-Forming Ligations at Physiological pH**

Matthias Tanriver, Yi-Chung Dzeng, Sara Da Ros, Erwin Lam, Jeffrey W. Bode*

Laboratorium für Organische Chemie, Department of Chemistry and Applied
Biosciences, ETH Zürich, Zürich 8093, Switzerland

bode@org.chem.ethz.ch

Table of Contents

GENERAL INFORMATION	3
PREPARATION OF POTASSIUM ACYLTRIFLUOROBORATES	4
SYNTHESIS OF PHENYL- AND PYRIDYL KATs	4
SYNTHESIS OF 8-QUINOLYL KATs	6
PREPARATION OF KAT PRECURSORS	9
PREPARATION OF HYDROXYLAMINES	11
EXTINCTION COEFFICIENT DETERMINATION OF KATs	13
UV-VIS MEASUREMENT OF KAT LIGATION RATE	25
KINETIC PLOTS	30
BUFFER PREPARATION.....	39
NMR COMPETITION EXPERIMENTS	40
COMPETITION RESULTS.....	41
REACTION OUTCOME AND MODEL PREDICTION.....	42
X-RAY - CRYSTALLOGRAPHIC DATA	46
PROTEIN EXPERIMENTS.....	50
EXPRESSION AND PURIFICATION OF SFGFP(S147C).....	50
SFGFP(S147C)-HYDROXYLAMINE BIOCONJUGATE	51
KAT LIGATION WITH SFGFP(S147C)-HYDROXYLAMINE BIOCONJUGATE 9	52
ACID-BASE TITRATION	53
COMPUTATIONAL MODEL.....	55
COMPUTED REACTION COORDINATE.....	57
REALTIME MASS SPECTROMETRY ANALYSIS OF THE LIGATION REACTION MIXTURE	58
NMR-SPECTRA OF SYNTHESIZED COMPOUNDS.....	59

General Information

All reagents were purchased from ABCR, Acros, Fisher Scientific, Fluorochem and Sigma Aldrich and used without further purification. Common solvents for flash column chromatography were of technical grade and distilled prior to use. Anhydrous solvents for chemical reactions were purchased from Sigma Aldrich. THF was dried by distillation over Na/benzophenone.

Air- and moisture sensitive reactions were carried out using standard techniques under an atmosphere of N₂. Thin layer chromatography (TLC) for reaction monitoring was conducted on glass-baked plates pre-coated with silica gel (Merck, Silica Gel 60 F254) and visualized by UV-quenching or staining with a KMnO₄-solution. Flash column chromatography was performed on Sigma Aldrich SiO₂ Type F60 (high-purity grade, 60 Å pore size, 230-400 mesh particle size) using a forced flow of air (0.5-1.0 bar). NMR spectra were recorded on Bruker Avance 600 MHz, Bruker Avance 500 MHz and Bruker Avance 400 MHz. Chemical shifts are reported in parts per million (ppm) and peaks were referenced to residual protonated solvents: CDCl₃ (δ = 7.26 ppm, 77.2 ppm); acetone-d₆ (δ = 2.05 ppm, 29.8 ppm, 206.3 ppm); DMSO-d₆ (δ = 2.05, 39.5 ppm); CD₃OD (δ = 3.31 ppm, 49.0 ppm). ¹⁹F-NMR and ¹¹B-NMR spectra are referenced to an external standard of trifluoroacetic acid and BF₃·OEt₂, respectively. NMR data is reported as follows: chemical shift, multiplicity (br, broad; s, singlet; d, doublet; t, triplet; q, quartet; p, pentet; m, multiplet), coupling constants in Hertz (Hz), integration.

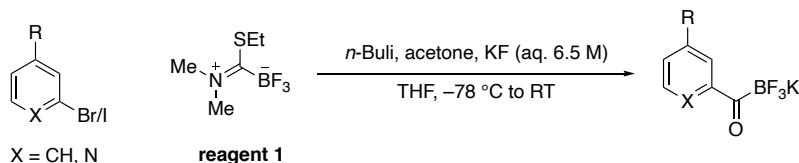
IR spectra were recorded on a JASCO FT-IR-4100 spectrometer and reported as wavenumbers in cm⁻¹. LC-MS was measured on a Waters Acquity UPLC connected to a SQ detector 2. High-resolution mass measurements were performed by the Molecular and Biomolecular Analysis Service MoBiAS at ETH Zurich on either a Bruker Daltonics maXis ESI-QTOF mass spectrometer or on a Bruker solariX ESI/MALDI-FTICR instrument with 4-hydroxy- α -cyanocinnamic acid as matrix. Preparative and analytical HPLC (high performance liquid chromatography) were performed on a Shiseido Proteonavi C4 (50 mm I.D. x 250 mm) at a flow rate of 40 mL/min and on a Shiseido Capcell pak UG 120 C18 (4.6 mm I.D. x 250 mm) with a flow rate of 1.0 mL/min, respectively. For the mobile phase, HPLC grade CH₃CN and Millipore-H₂O both containing 0.1% (v/v) TFA were used. UV-Vis spectra were recorded on a Thermo NanoDrop 2000c spectrophotometer.

Preparation of Potassium acyltrifluoroborates

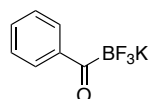
Synthesis of phenyl- and pyridyl KATs

Phenyl- and pyridyl-KATs were synthesized according to the procedure published in 2014.¹ For already reported compounds, only ¹H-NMR spectra and HRMS are listed.

General procedure for the synthesis of phenyl- and pyridyl KATs:

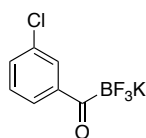


A heat-dried round-bottom flask under nitrogen was charged with aryl halide (1.08 mmol, 1.00 equiv) and reagent **1** (1.08 mmol, 1.00 equiv) and dissolved in 2 mL of anhydrous THF. The mixture was cooled to $-78\text{ }^{\circ}\text{C}$ using a dry ice/acetone bath. *n*-Butyllithium (675 μL , 1.00 equiv, 1.6 M in hexanes) was added over 30 min via syringe pump and the reaction was allowed to stir for one hour at $-78\text{ }^{\circ}\text{C}$. To quench the residual *n*-butyllithium, 1.00 equiv of acetone was added followed by 0.5 mL of aqueous KF (6.5 M, 3.00 equiv). The cooling bath was removed and the reaction was stirred for one hour. CH_2Cl_2 was added to the heterogenous mixture and the suspension was filtered. The residue was washed with CH_2Cl_2 (3 x 5 mL), followed by acetone (2-50 mL, the solution containing the product is yellow) until the filtrate was colorless. Acetone was removed under reduced pressure to obtain the product as a white or yellow solid.

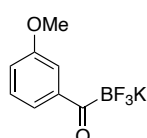


Potassium benzoyltrifluoroborate (3a): Prepared from iodobenzene (300 mg, 1.47 mmol) and reagent **1** (272 mg, 1.47 mmol) according to the general procedure and isolated as a colorless solid (183 mg, 59%). Compound **3a** has been fully characterized in a previous report.¹ **¹H-NMR** (600 MHz, DMSO-d_6): δ [ppm] δ 7.94 – 7.86 (m, 2H), 7.46 – 7.35 (m, 3H). **HRMS** (ESI neg.): calculated for $\text{C}_7\text{H}_5\text{BF}_3\text{O}$ [M-K]: 173.0391, found: 173.0393.

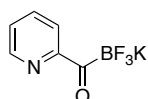
¹ Erős, G.; Kushida, Y.; Bode, J. W., A Reagent for the One-Step Preparation of Potassium Acyltrifluoroborates (KATs) from Aryl- and Heteroarylhalides. *Angewandte Chemie International Edition* **2014**, 53 (29), 7604-7607.



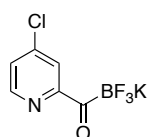
Potassium 3-chlorobenzoyltrifluoroborate (3b): Prepared from 3-chloriodobenzene (300 mg, 1.26 mmol) and reagent **1** (209 mg, 1.13 mmol) according to the general procedure and isolated as a colorless solid (211 mg, 68%). **¹H-NMR** (600 MHz, DMSO-*d*₆): δ [ppm] 7.86 (t, *J* = 1.6 Hz, 1H), 7.83 (d, *J* = 7.5 Hz, 1H), 7.50 (ddd, *J* = 7.8, 2.2, 1.1 Hz, 1H), 7.44 (t, *J* = 7.7 Hz, 1H). **¹³C-NMR** (151 MHz, DMSO-*d*₆): δ [ppm] 230.8 (br), 142.8, 132.9, 130.4, 129.9, 127.5, 127.5, 126.1, 126.1. **¹⁹F-NMR** (470 MHz, DMSO-*d*₆): δ [ppm] -141.89 (q, *J* = 46 Hz). **¹¹B-NMR** (160 MHz, DMSO-*d*₆): δ [ppm] -1.20 (q, *J* = 53.0 Hz). **IR** (ν/cm⁻¹, neat): 2360, 2341, 1638, 1587, 1565, 1465, 1423, 1250, 1078, 1022. 956; **m.p.**: 236 °C. **HRMS** (ESI neg.): calculated for C₇H₄BClF₃O [M-K]⁻: 207.0003, found: 207.0001.



Potassium 3-methoxybenzoyltrifluoroborate (3c): Prepared from 3-iodoanisole (500 mg, 2.14 mmol) and reagent **1** (395 mg, 2.14 mmol) according to the general procedure and isolated as a colorless solid (386 mg, 71%). Compound **3c** has been fully characterized in a previous report.² **¹H-NMR** (500 MHz, DMSO-*d*₆): δ [ppm] δ 7.56 (d, *J* = 8.0 Hz, 1H), 7.43 – 7.39 (m, 1H), 7.30 (t, *J* = 7.8 Hz, 1H), 7.00 (dd, *J* = 8.1, 2.8 Hz, 1H), 3.76 (s, 3H). **HRMS** (ESI neg.): calculated for C₈H₇BF₃O₂ [M-K]⁻: 203.0498, found: 203.0498.



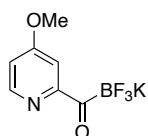
Potassium 2-isonicotinoyltrifluoroborate (4a): Prepared from 2-bromopyridine (200 mg, 1.27 mmol) and reagent **1** (234 mg, 1.27 mmol) according to the general procedure, with a slight modification and isolated as a yellow solid (110 mg, 41%). Compound **4a** has been fully characterized in a previous report.¹ **¹H-NMR** (600 MHz, DMSO-*d*₆): δ [ppm] 8.61 – 8.59 (m, 1H), 7.87 – 7.82 (m, 2H), 7.41 – 7.37 (m, 1H). **HRMS** (ESI neg.): calculated for C₆H₄BF₃NO [M-K]⁻: 174.0344, found: 174.0346.



Potassium 4-chloro-2-isonicotinoyltrifluoroborate (4b): Prepared from 2-bromo-4-chloropyridine (300 mg, 1.56 mmol) and reagent **1** (288 mg, 1.56 mmol) according to the general procedure, with a slight modification. The reaction mixture was filtered, washed with CH₂Cl₂ (3 x 5 mL) followed by acetone (3 x 5 mL).

² Jackl, M. K.; Schuhmacher, A.; Shiro, T.; Bode, J. W., Synthesis of N,N-Alkylated α-Tertiary Amines by Coupling of α-Aminoalkyltrifluoroborates and Grignard Reagents. *Organic Letters* **2018**, *20* (13), 4044-4047.

The residual filter cake was washed with DMF until the filtrate was colorless. DMF was evaporated under reduced pressure to give **4b** as a yellow solid (205 mg, 53%). **¹H-NMR** (600 MHz, DMSO-*d*₆): δ [ppm] 8.59 (dd, *J* = 5.2, 0.6 Hz, 1H), 7.84 (d, *J* = 1.6 Hz, 1H), 7.56 (dd, *J* = 5.2, 2.2 Hz, 1H). **¹³C-NMR** (151 MHz, DMSO-*d*₆): δ [ppm] 231.7 (br), 159.3, 150.6, 143.2, 124.7, 122.8. **¹⁹F-NMR** (470 MHz, DMSO-*d*₆): δ [ppm] -142.83 (q, *J* = 48.6 Hz). **¹¹B-NMR** (160 MHz, DMSO-*d*₆): δ [ppm] -1.30 (q, *J* = 51.3 Hz). **IR** (ν/cm⁻¹, neat): 3300, 3066, 1656, 1566, 1550, 1466, 1389, 1241, 1226, 1132, 1109, 1076, 1034, 1000, 919; **m.p.**: 195 °C. **HRMS** (ESI neg.): calculated for C₆H₃BClF₃NO [M-K]⁻: 207.9955, found: 207.9953.



Potassium 4-methoxy-2-isonicotinoyltrifluoroborate (4c): Prepared from 2-bromo-4-methoxypyridine (200 mg, 1.06 mmol) and reagent **1** (197 mg, 1.06 mmol) according to the general procedure, with a slight modification. Compound **4c** is insoluble in acetone. After washing the filter cake with acetone (3 x 5 mL) the residual filter cake was allowed to dry overnight and the product isolated as pale yellow solid (220 mg, 85%). **¹H-NMR** (600 MHz, DMSO-*d*₆): δ [ppm] 8.41 (d, *J* = 5.6 Hz, 1H), 7.38 (d, *J* = 2.6 Hz, 1H), 6.97 (dd, *J* = 5.6, 2.7 Hz, 1H), 3.83 (s, 3H). **¹³C-NMR** (151 MHz, DMSO-*d*₆): δ [ppm] 232.9 (br), 165.5, 159.9, 150.2, 110.5, 108.9, 55.1. **¹⁹F-NMR** (470 MHz, DMSO-*d*₆): δ [ppm] -142.5 (q, *J* = 45.5 Hz). **¹¹B-NMR** (160 MHz, DMSO-*d*₆): δ [ppm] -1.26 (q, *J* = 52.9 Hz). **IR** (ν/cm⁻¹, neat): 3069, 3018, 2974, 2944, 1660, 1584, 1564, 1481, 1469, 1301, 1285, 1200, 1173, 1116, 1100, 1072, 1034, 1004; **m.p.**: >230 °C. **HRMS** (ESI neg.): calculated for C₇H₆BF₃NO₂ [M-K]⁻: 204.0449, found: 204.0452.

Synthesis of 8-quinolyl KATs

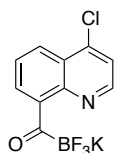
General procedure for the synthesis of 8-quinolyl KATs:

A flame-dried 10 mL Schlenk-flask equipped with magnetic stir bar and septum under an inert nitrogen atmosphere was charged with 8-quinolyl halide (1.20 mmol, 1.00 equiv) and dissolved in 8 mL anhydrous Et₂O:THF (4:1 v/v). The solution was cooled to -110 °C in a dry ice/acetone/nitrogen bath. *n*-Butyllithium (1.6 M in hexane, 1.00 equiv) was added dropwise over 30 min via syringe pump. After the mixture was stirred for 45 min, reagent **1** (1.20 mmol, 1.00 equiv) was dissolved in 2 mL Et₂O:THF (4:1 v/v) and added dropwise over 30 min via syringe pump. The reaction was allowed to stir for 60 min at -110 °C. Residual

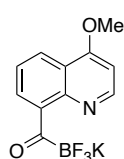
n-butyllithium was quenched with acetone (50 μ L) followed by the addition of an aqueous solution of $\text{KF}_{(\text{aq})}$ (923 μ L, 6.5 M, 5.00 equiv). The flask was removed from the cooling bath and the mixture was stirred overnight at room temperature. To the resulting heterogeneous mixture was added Et_2O (10 mL). The mixture was filtered and washed with additional CH_2Cl_2 (3 x 10 mL) and acetone (2 x 10 mL). The remaining filter cake was washed with DMF until the filtrate was colorless. DMF was removed under reduced pressure at 50 – 60 $^\circ\text{C}$ to yield the product as a yellow or brown solid.



Potassium 8-quinolinoyltrifluoroborate (5a): Prepared from 8-bromoquinoline (400 mg, 1.92 mmol) according to the general procedure. Product **5a** was isolated as a light brown solid (100 mg, 20%). **$^1\text{H-NMR}$** (600 MHz, DMSO-d_6): δ [ppm] 8.81 (dd, $J = 4.1, 1.9$ Hz, 1H), 8.30 (dd, $J = 8.3, 1.8$ Hz, 1H), 7.87 (dd, $J = 7.4, 2.3$ Hz, 1H), 7.59 – 7.51 (m, 2H), 7.47 (dd, $J = 8.3, 4.1$ Hz, 1H). **$^{13}\text{C-NMR}$** (151 MHz, DMSO-d_6): δ [ppm] 241.5 (br), 149.6, 147.0, 144.9, 135.7, 127.8, 127.4, 125.6, 125.5, 125.5, 120.9. **$^{19}\text{F-NMR}$** (470 MHz, DMSO-d_6): δ [ppm] -144.6 – -145.2 (m). **$^{11}\text{B-NMR}$** (160 MHz, DMSO-d_6): δ [ppm] -1.54 (q, $J = 53.1$ Hz). **IR** (v/cm^{-1} , neat): 3063, 3041, 1645, 1597, 1567, 1492, 1249, 1183, 1126, 1059, 1028, 1012, 1002, 985; **m.p.**: 195 $^\circ\text{C}$. **HRMS** (ESI neg.): calculated for $\text{C}_{10}\text{H}_6\text{BF}_3\text{NO}$ [M-K] $^-$: 224.0502, found: 224.0501.

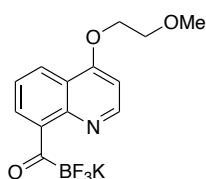


Potassium 4-chloro-8-quinolinoyltrifluoroborate (5b): Prepared from 4-chloro-8-iodoquinoline (400 mg, 1.38 mmol) according to the general procedure. Product **5b** was isolated as a brown solid (212 mg, 52%). **$^1\text{H-NMR}$** (600 MHz, DMSO-d_6): δ [ppm] 8.76 (d, $J = 4.6$ Hz, 1H), 8.13 (dd, $J = 8.4, 1.4$ Hz, 1H), 7.74 – 7.68 (m, 2H), 7.61 (dd, $J = 6.9, 1.5$ Hz, 1H). **$^{13}\text{C-NMR}$** (151 MHz, DMSO-d_6): δ [ppm] 241.2 (br), 149.5, 147.8, 145.7, 140.7, 127.3, 126.3, 125.3, 122.7, 121.1. **$^{19}\text{F-NMR}$** (470 MHz, DMSO-d_6): δ [ppm] -144.8 – -145.5 (m). **$^{11}\text{B-NMR}$** (160 MHz, DMSO-d_6): δ [ppm] -0.28 – -2.74 (br). **IR** (v/cm^{-1} , neat): 1646, 1586, 1557, 1485, 1387, 1291, 1063, 1024, 991; **m.p.**: 190 $^\circ\text{C}$. **HRMS** (ESI neg.): calculated for $\text{C}_{10}\text{H}_5\text{BClF}_3\text{NO}$ [M-K] $^-$: 258.0112, found: 258.0112.



Potassium 4-methoxy-8-quinolinoyltrifluoroborate (5c): Prepared from 8-iodo-4-methoxyquinoline (450 mg, 1.58 mmol) according to the general procedure. Product **5c** was isolated as a yellow solid (151 mg, 33%). **$^1\text{H-NMR}$** (600 MHz, DMSO-d_6): δ [ppm] 8.64 (d, $J = 5.1$ Hz, 1H), 8.04 (dd, $J = 7.7, 2.1$ Hz, 1H), 7.51

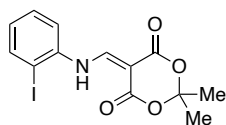
– 7.44 (m, 2H), 6.97 (d, $J = 5.1$ Hz, 1H), 4.02 (s, 3H). $^{13}\text{C-NMR}$ (151 MHz, DMSO- d_6): δ [ppm] 241.6 (br), 161.1, 150.6, 146.9, 145.7, 125.5, 124.7, 120.5, 120.4, 100.5, 55.9. $^{19}\text{F-NMR}$ (470 MHz, DMSO- d_6): δ [ppm] -144.5 – -145.2 (m). $^{11}\text{B-NMR}$ (160 MHz, DMSO- d_6): δ [ppm] -0.12 – -3.13 (br). **IR** (ν/cm^{-1} , neat): 3066, 3017, 2962, 2831, 1645, 1610, 1594, 1568, 1500, 1409, 1307, 1109, 991; **m.p.**: >220 °C (decomp.). **HRMS** (ESI neg.): calculated for $\text{C}_{11}\text{H}_8\text{BF}_3\text{NO}_2$ [M–K] $^-$: 254.0608, found: 254.0611.



Potassium 4-(2-methoxyethoxy)-8-quinolinoyltrifluoroborate (5d):

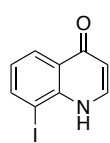
Prepared from 8-iodo-4-(2-methoxyethoxy)quinoline **P5** (370 mg, 1.12 mmol) according to the general procedure. Product **5d** was isolated as a yellow solid (95 mg, 25%). $^1\text{H-NMR}$ (600 MHz, DMSO- d_6): δ [ppm] 8.62 (d, $J = 5.1$ Hz, 1H), 8.06 (dd, $J = 7.4, 2.4$ Hz, 1H), 7.60 – 7.45 (m, 2H), 6.98 (d, $J = 5.1$ Hz, 1H), 4.42 – 4.29 (m, 2H), 3.88 – 3.78 (m, 2H), 3.38 (s, 3H). $^{13}\text{C-NMR}$ (151 MHz, DMSO- d_6): δ [ppm] 241.91, 160.29, 150.54, 146.92, 145.82, 125.64, 124.72, 120.62, 120.58, 101.12, 70.07, 67.76, 58.39. $^{19}\text{F-NMR}$ (470 MHz, DMSO- d_6): δ [ppm] -144.6 – -145.2 (m). $^{11}\text{B-NMR}$ (160 MHz, DMSO- d_6): δ [ppm] -0.14 – -2.54 (br). **IR** (ν/cm^{-1} , neat): 3075, 2975, 2926, 2899, 2817, 2360, 2343, 1645, 1594, 1571, 1308, 1112, 1081; **m.p.**: 174 °C. **HRMS** (ESI neg.): calculated for $\text{C}_{13}\text{H}_{12}\text{BF}_3\text{NO}_3$ [M–K] $^-$: 298.0870, found: 298.0866.

Preparation of KAT precursors



5-(((2-iodophenyl)amino)methylene)-2,2-dimethyl-1,3-dioxane-4,6-dione (**P1**):

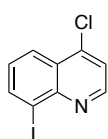
Following a reported procedure with slight modifications³, a 200 mL round-bottomed flask was charged with 2-iodoaniline (5.00 g, 22.83 mmol, 1.00 equiv) and dissolved in 80 mL anhydrous acetonitrile. Meldrum's acid (3.62 g, 25.11 mmol, 1.10 equiv) was added, followed by triethyl orthoformate (4.56 mL, 27.39 mmol, 1.20 equiv). The reaction was stirred at 95 °C until TLC analysis indicated full conversion. After cooling the reaction mixture to room temperature, crystals formed that were filtrated and washed with cold acetonitrile leaving behind **P1** as yellow crystals (8.15 g, 96%). **¹H-NMR** (400 MHz, DMSO-*d*₆): δ [ppm] 11.37 (d, *J* = 13.9 Hz, 1H), 8.65 (d, *J* = 13.9 Hz, 1H), 7.93 (dd, *J* = 7.9, 1.4 Hz, 1H), 7.73 (dd, *J* = 8.3, 1.4 Hz, 1H), 7.53 – 7.41 (m, 1H), 7.04 (td, *J* = 7.6, 1.4 Hz, 1H), 1.69 (s, 6H). **¹³C-NMR** (101 MHz, DMSO-*d*₆): δ [ppm] 164.6, 162.3, 153.5, 139.6, 139.2, 129.9, 128.0, 118.5, 104.6, 90.6, 87.7, 26.6. **HRMS** (ESI pos.): calculated for C₁₃H₁₂INNaO₄ [M+Na]⁺: 395.9703, found: 395.9706.



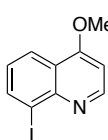
8-Iodoquinolin-4(1*H*)-one (**P2**):

Following a reported procedure with slight modifications³, a 100 mL round bottomed flask was charged with 15 mL diphenyl ether and heated to 210 °C. **P1** (3.00 g, 8.04 mmol) was added in portions over 5 minutes and the mixture was stirred for 30 min until full consumption of the starting material (TLC). The dark brown mixture was cooled to room temperature and poured into hexane to form a precipitate. After filtration, the precipitate was dissolved in acetone and dry loaded onto celite. The crude material was purified via flash column chromatography (hexanes:EtOAc 4:1 v/v to 2:1 to 1:1, then THF:EtOAc 1:1 v/v) to yield **P2** (1.63 g, 75%) as a light brown solid. **¹H-NMR** (400 MHz, DMSO-*d*₆): δ [ppm] 10.72 (s, 1H), 8.17 (dd, *J* = 7.5, 1.5 Hz, 1H), 8.11 (dd, *J* = 8.1, 1.5 Hz, 1H), 7.11 (t, *J* = 7.8 Hz, 1H), 6.11 (d, *J* = 7.5 Hz, 1H). **¹³C-NMR** (101 MHz, DMSO-*d*₆): δ [ppm] 176.8, 142.3, 140.6, 140.2, 126.6, 125.7, 124.8, 109.1, 87.2. **HRMS** (ESI pos.): calculated for C₉H₇INO [M+H]⁺: 271.9567, found: 271.9569.

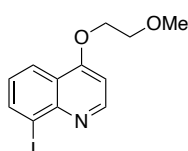
³ Broumidis, E.; Koutentis, P. A., A one-pot, two-step synthesis of 3-deazacanthin-4-ones via sequential Pd-catalyzed Suzuki-Miyaura and Cu-catalyzed Buchwald-Hartwig reactions. *Tetrahedron Letters* **2017**, *58* (27), 2661-2664.



4-Chloro-8-iodoquinoline (P3): **P2** (1.30 g, 4.80 mmol, 1.00 equiv) was suspended in 4.38 mL phosphorus oxychloride (48.0 mmol, 10.0 equiv) and heated to 105 °C and stirred for 90 min. The hot mixture was poured into ice water and the mixture was carefully neutralized with a saturated $\text{NaHCO}_3(\text{aq})$ solution. The precipitate was filtered off and washed with additional 50 mL water and dried under vacuum to give **P3** as a brown solid (1.18 g, 85%). **$^1\text{H-NMR}$** (400 MHz, DMSO-d_6): δ [ppm] 8.92 (d, $J = 4.7$ Hz, 1H), 8.49 (dd, $J = 7.4, 1.3$ Hz, 1H), 8.21 (dd, $J = 8.4, 1.3$ Hz, 1H), 7.85 (d, $J = 4.7$ Hz, 1H), 7.50 (dd, $J = 8.4, 7.4$ Hz, 1H). **$^{13}\text{C-NMR}$** (101 MHz, DMSO-d_6): δ [ppm] 151.3, 147.0, 141.5, 141.2, 129.5, 126.0, 124.6, 122.4, 104.2. **HRMS** (ESI pos.): calculated for $\text{C}_9\text{H}_6\text{ClIN}$ [$\text{M}+\text{H}$] $^+$: 298.9228, found: 298.9227.



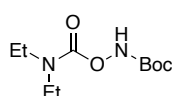
8-Iodo-4-methoxyquinoline (P4): A microwave tube was charged with **P3** (250 mg, 864 μmol , 1.00 equiv), sodium methoxide (233 mg, 4.32 mmol, 5.00 equiv) and suspended in 2.5 mL anhydrous DMF. The tube was sealed and stirred at 95 °C for 24 h. The mixture was removed from the oil bath and cooled to room temperature. The reaction was diluted with EtOAc, washed with H_2O , brine and extracted with EtOAc. The collected organic extracts were dried over Na_2SO_4 . The crude mixture was purified via flash column chromatography (hexanes:EtOAc 4:1 v/v to 2:1) to give **P4** as a colorless solid (219 mg, 89%). **$^1\text{H-NMR}$** (400 MHz, DMSO-d_6): δ [ppm] 8.81 (d, $J = 5.2$ Hz, 1H), 8.35 (dd, $J = 7.3, 1.3$ Hz, 1H), 8.15 (dd, $J = 8.2, 1.4$ Hz, 1H), 7.30 (dd, $J = 8.3, 7.3$ Hz, 1H), 7.11 (d, $J = 5.2$ Hz, 1H), 4.05 (s, 3H). **$^{13}\text{C-NMR}$** (101 MHz, DMSO-d_6): δ [ppm] 161.7, 152.5, 147.1, 140.1, 127.1, 122.3, 121.1, 103.4, 101.7, 56.5. **IR** (v/cm^{-1} , neat): 3022, 2981, 2940, 1601, 1584, 1551, 1497, 1400, 1297; **m.p.**: 96 °C. **HRMS** (ESI pos.): calculated for $\text{C}_{10}\text{H}_8\text{INNaO}$ [$\text{M}+\text{Na}$] $^+$: 307.9543, found: 307.9543.



8-Iodo-4-(2-methoxyethoxy)quinoline (P5): A microwave tube was charged with **P3** (100 mg, 345 μmol , 1.00 equiv), potassium tert-butoxide (58.1 mg, 518 μmol , 1.50 equiv) and 2-methoxyethanol (1.05 g, 13.8 mmol, 40.0 equiv) and sealed under an argon atmosphere. The reaction mixture was heated to 80 °C. After LCMS indicated full conversion (3 h), the reaction mixture was allowed to cool to room temperature and diluted with CH_2Cl_2 , washed with H_2O , brine, extracted with CH_2Cl_2 . The collected organic extracts were dried over Na_2SO_4 . The crude mixture was purified via flash column chromatography (hexanes:EtOAc 4:1 v/v to 2:1) to give **P5** as a colorless solid

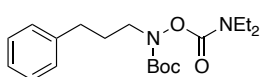
(96 mg, 84%). **¹H NMR** (500 MHz, CDCl₃): δ [ppm] 8.85 (d, *J* = 5.3 Hz, 1H), 8.31 (dd, *J* = 7.3, 1.4 Hz, 1H), 8.26 (dd, *J* = 8.3, 1.4 Hz, 1H), 7.21 (dd, *J* = 8.3, 7.4 Hz, 1H), 6.80 (d, *J* = 5.3 Hz, 1H), 4.42 – 4.26 (m, 2H), 3.95 – 3.83 (m, 2H), 3.48 (s, 3H). **¹³C-NMR** (126 MHz, CDCl₃): δ [ppm] 161.9, 152.1, 147.9, 140.8, 126.9, 123.1, 122.0, 102.2, 101.4, 70.7, 68.5, 59.5. **IR** (ν/cm⁻¹, neat): 2984, 2954, 2889, 2810, 1604, 1588, 1554, 1496, 1400, 1368, 1301, 1130, 1030; **m.p.**: 75 °C. **HRMS** (ESI pos.): calculated for C₁₂H₁₃INO₂ [M+H]⁺: 329.9986, found: 329.9986.

Preparation of Hydroxylamines



N-tert-Butoxycarbonyl-*O*-diethylcarbamoylhydroxylamine (**P6**):

Following a reported procedure⁴, a heat-dried flask was charged with *N*-Boc-hydroxylamine (6.00 g, 45.1 mmol, 1.30 equiv) and Et₃N (6.28 mL, 45.1 mmol, 1.30 equiv) in dry CH₂Cl₂ (70 mL). *N,N*-Diethylcarbamoyl chloride (4.39 mL, 34.7 mmol, 1.00 equiv) was added over 5 min, followed by DMAP (423 mg, 3.47 mmol, 0.10 equiv) and the reaction mixture was stirred at 40 °C for 12 h. The mixture was allowed to cool to room temperature and diluted with 1 M HCl. The aqueous phase was extracted with CH₂Cl₂ and the combined organic phases were washed with brine and dried over Na₂SO₄. Evaporation of CH₂Cl₂ yields **P6** (7.70 g, 96%) as a colorless oil. **¹H NMR** (500 MHz, CDCl₃): δ [ppm] 7.80 (s, 1H), 3.33 (q, *J* = 7.1 Hz, 4H), 1.48 (s, 9H), 1.24 – 1.12 (m, 6H). **HRMS** (ESI pos.): calculated for C₁₀H₂₀N₂NaO₄ [M+H]⁺: 255.1315, found: 255.1313.

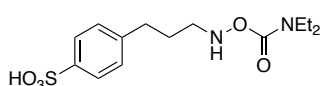


Tert-butyl ((diethylcarbamoyl)oxy)(3-phenylpropyl)carbamate (**P7**):

A heat-dried round bottom flask under nitrogen atmosphere was charged with **P6** (2.50 g, 10.8 mmol, 1.00 equiv), K₂CO₃ (3.72 g, 26.9 mmol, 2.50 equiv) and dissolved in dry DMF (5.0 mL) followed by the addition of 1-bromo-3-phenylpropane (1.96 mL, 12.9 mmol, 1.20 equiv). The reaction mixture was stirred until TLC indicated full conversion of the starting material (12 h). The reaction was diluted with Et₂O (30 mL) and H₂O (30 mL). The aqueous phase was extracted with Et₂O and the combined organic phases were washed with brine and dried over Na₂SO₄. The crude mixture was purified via flash column chromatography (hexanes:EtOAc 9:1 v/v to 4:1) to yield **P7** (3.69 g, 98%) as a

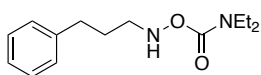
⁴ Noda, H.; Erős, G.; Bode, J. W., Rapid Ligations with Equimolar Reactants in Water with the Potassium Acyltrifluoroborate (KAT) Amide Formation. *Journal of the American Chemical Society* **2014**, *136* (15), 5611-5614.

colorless oil. **¹H NMR** (400 MHz, CDCl₃): δ [ppm] δ 7.48 – 7.03 (m, 5H), 3.72 (s, 2H), 3.38 (q, *J* = 7.7 Hz, 4H), 2.79 – 2.70 (m, 2H), 2.03 – 1.93 (m, 2H), 1.52 (s, 9H), 1.24 (t, *J* = 5.1 Hz, 6H). **¹³C-NMR** (101 MHz, CDCl₃): δ [ppm] 155.2, 154.3, 141.6, 128.5, 128.4, 125.9, 81.7, 50.0, 43.0, 41.7, 33.0, 29.1, 28.3, 14.3, 13.5. **IR** (v/cm⁻¹, neat): 3086, 3063, 3027, 2976, 2934, 2875, 1739, 1709, 1604, 1497, 1474, 1391, 1380, 1365, 1267, 1138. **HRMS** (ESI pos.): calculated for C₁₉H₃₁N₂O₄ [M+H]⁺: 351.2278, found: 351.2275.



4-(3-(((diethylcarbamoyl)oxy)amino)propyl)benzenesul-

fonic acid (6): To a solution of **7** (800 mg, 3.20 mmol) in CH₂Cl₂ (7 mL) was added dropwise chlorosulfonic acid (931 mg, 7.99 mmol) at 0 °C. After completion the solvent was evaporated and the crude was dissolved in 8 mL CH₃CN:H₂O (1:1 v/v), filtered and injected into preparative HPLC (Shiseido Proteonavi C4 column 50 x 250 mm) with a gradient of 25 to 90% MeCN with 0.1% TFA in 30 min. The fractions containing the product were collected and lyophilized to yield **6** (673 mg, 63%) as a colorless solid. **¹H-NMR** (500 MHz, DMSO-d₆): δ [ppm] 7.56 – 7.49 (m, 2H), 7.18 – 7.13 (m, 2H), 3.25 (s, 4H), 3.18 – 3.07 (m, 2H), 2.65 (t, *J* = 7.6 Hz, 2H), 1.90 – 1.79 (m, 2H), 1.08 (t, *J* = 7.1 Hz, 6H). **¹³C-NMR** (126 MHz, DMSO-d₆): δ [ppm] 153.2, 146.1, 141.5, 127.6, 125.8, 49.7, 42.5, 41.2, 31.8, 26.4, 13.8, 13.3; **m.p.**: 82 °C. **HRMS** (ESI pos.) calculated for C₁₄H₂₃N₂O₅S [M+H]⁺: 331.1313, found: 331.1322.

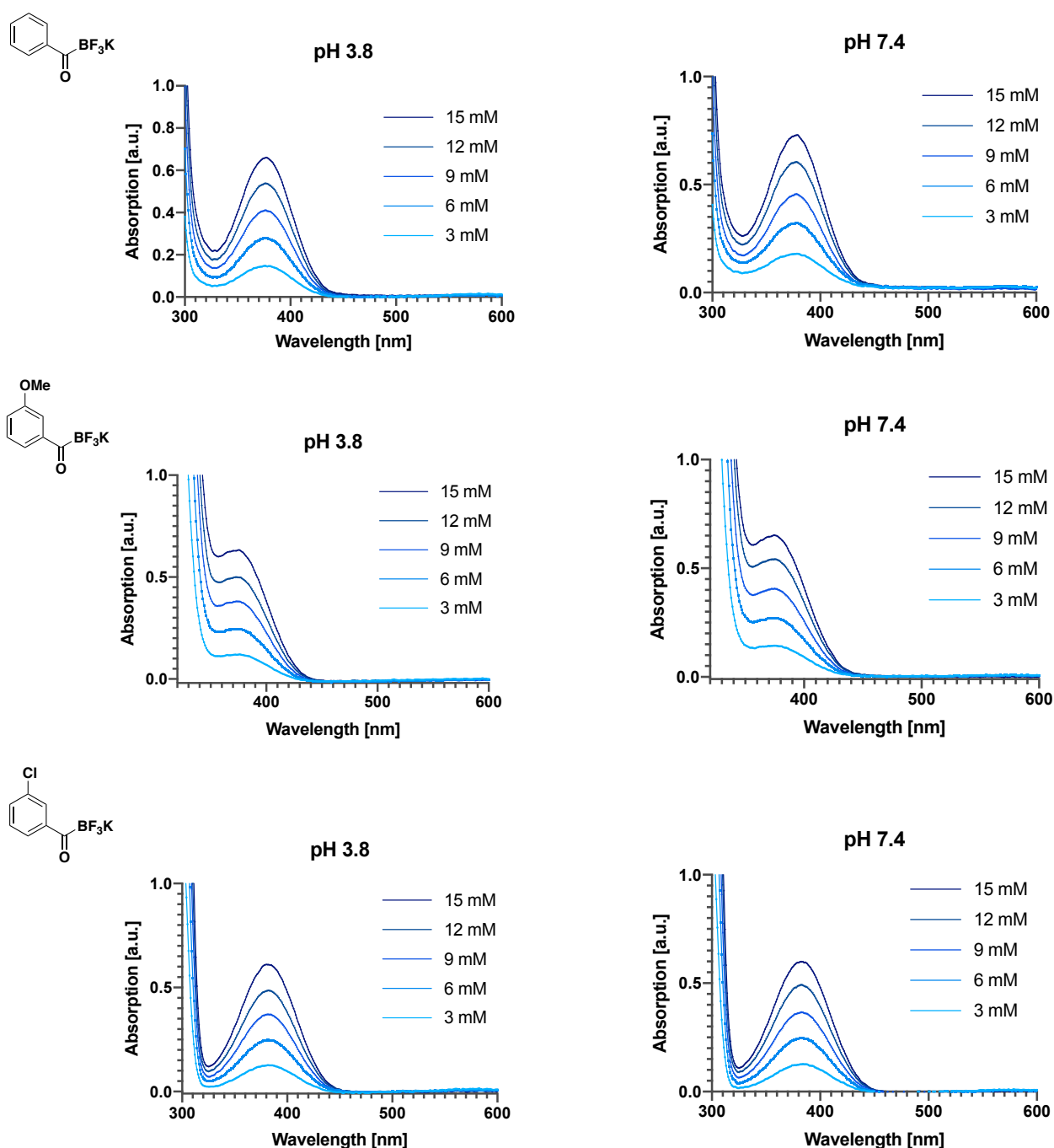


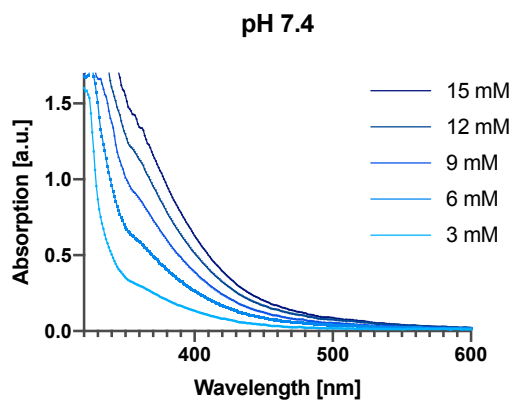
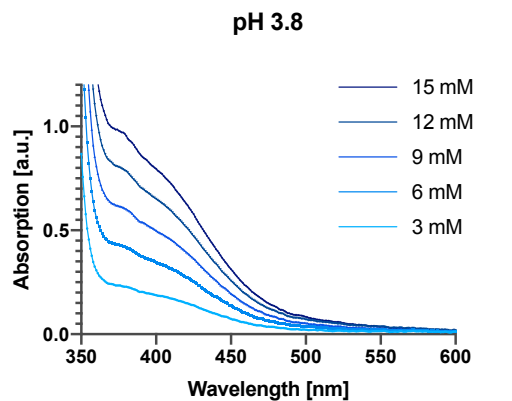
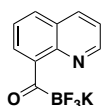
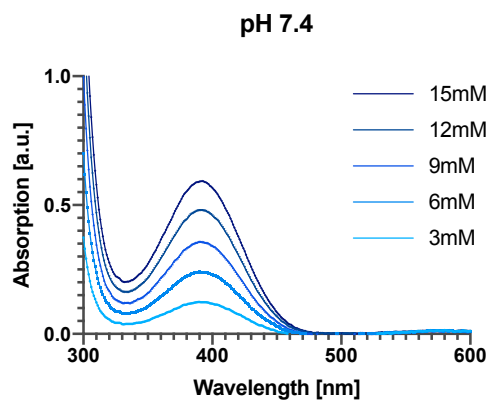
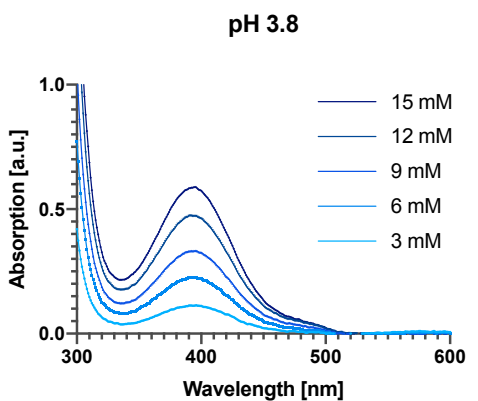
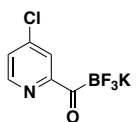
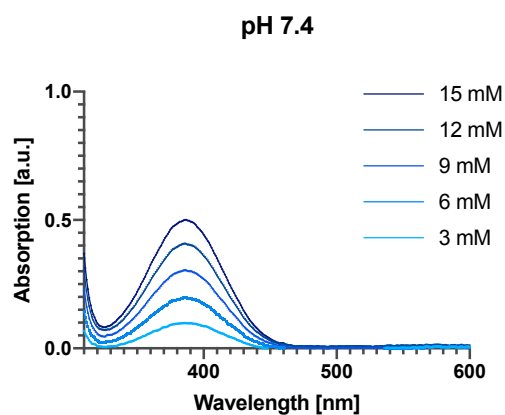
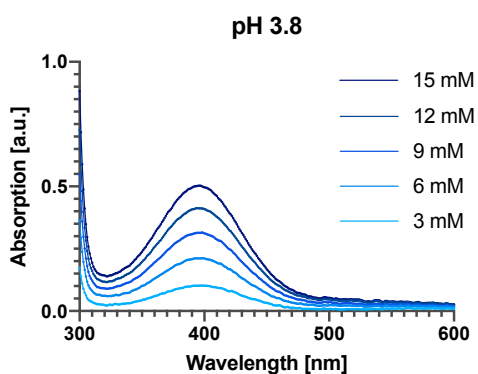
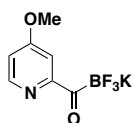
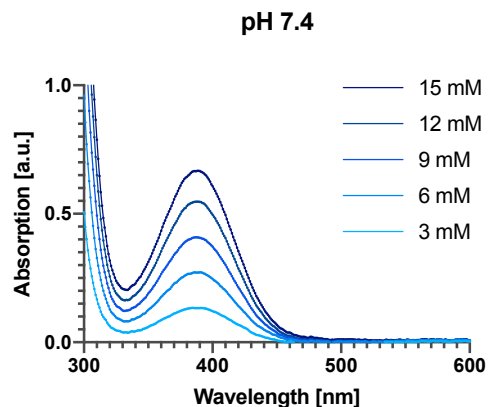
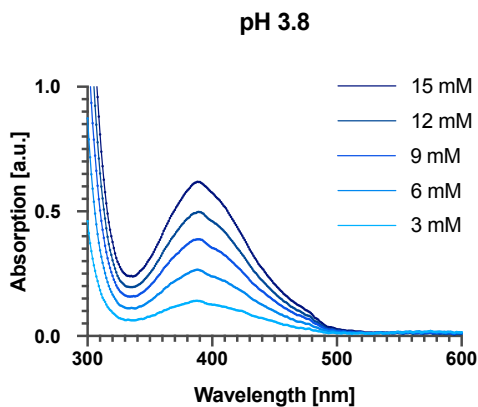
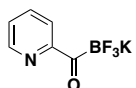
N-ethyl-N-(((3-phenylpropyl)amino)oxy)carbonyl)ethanamine (7): A

solution of **P7** (1.12 g, 3.20 mmol, 1.00 equiv) in a mixture of CH₂Cl₂ and TFA (1:1 v/v, 6 mL) was stirred for 2 h at 0 °C. After completion, the reaction mixture was diluted with 5 mL CH₂Cl₂ and the solution was neutralized with a saturated solution of NaHCO_{3(aq)}. The aqueous phase was extracted three times with CH₂Cl₂ (5 mL). The combined organic phases were washed with brine (20 mL) and dried over Na₂SO₄. The crude was purified via flash column chromatography (hexanes:EtOAc 4:1 v/v to 1:1) to yield **7** (720 mg, 90%) as a colorless liquid. **¹H NMR** (400 MHz, CDCl₃): δ [ppm] 7.39 – 7.21 (m, 5H), 3.34 (s, 4H), 3.10 – 3.02 (m, 2H), 2.82 – 2.73 (m, 2H), 2.00 – 1.87 (m, 2H), 1.19 (t, *J* = 7.1 Hz, 6H). **¹³C-NMR** (101 MHz, CDCl₃): δ [ppm] 156.9, 141.3, 128.5, 128.5, 126.0, 52.4, 42.5, 41.1, 33.4, 28.9, 14.0. **IR** (v/cm⁻¹, neat): 3232, 3062, 3026, 2973, 2934, 2872, 1698, 1419, 1271, 1156. **HRMS** (ESI pos.): calculated for C₁₄H₂₂KN₂O₂ [M+K]⁺: 289.1313, found: 289.1318.

Extinction coefficient determination of KATs

A dilution series of KATs with concentrations 15 mM, 12 mM, 9 mM, 6 mM and 3 mM were prepared as follows: 30 μmol of the respective KAT was weighted out and diluted with potassium phosphate buffer – CH_3CN 1:1 (v/v, 0.1 M) and potassium acetate buffer – CH_3CN 1:1 (v/v, 0.1 M) to 2 mL, giving a 15 mM solution, which was used to prepare a serial dilutions of KATs. The absorption spectra of the KAT solutions were measured with NanoDrop a in quartz cuvette at room temperature at pH 3.8 and pH 7.4. The recorded absorption curves were plotted against wavelength:





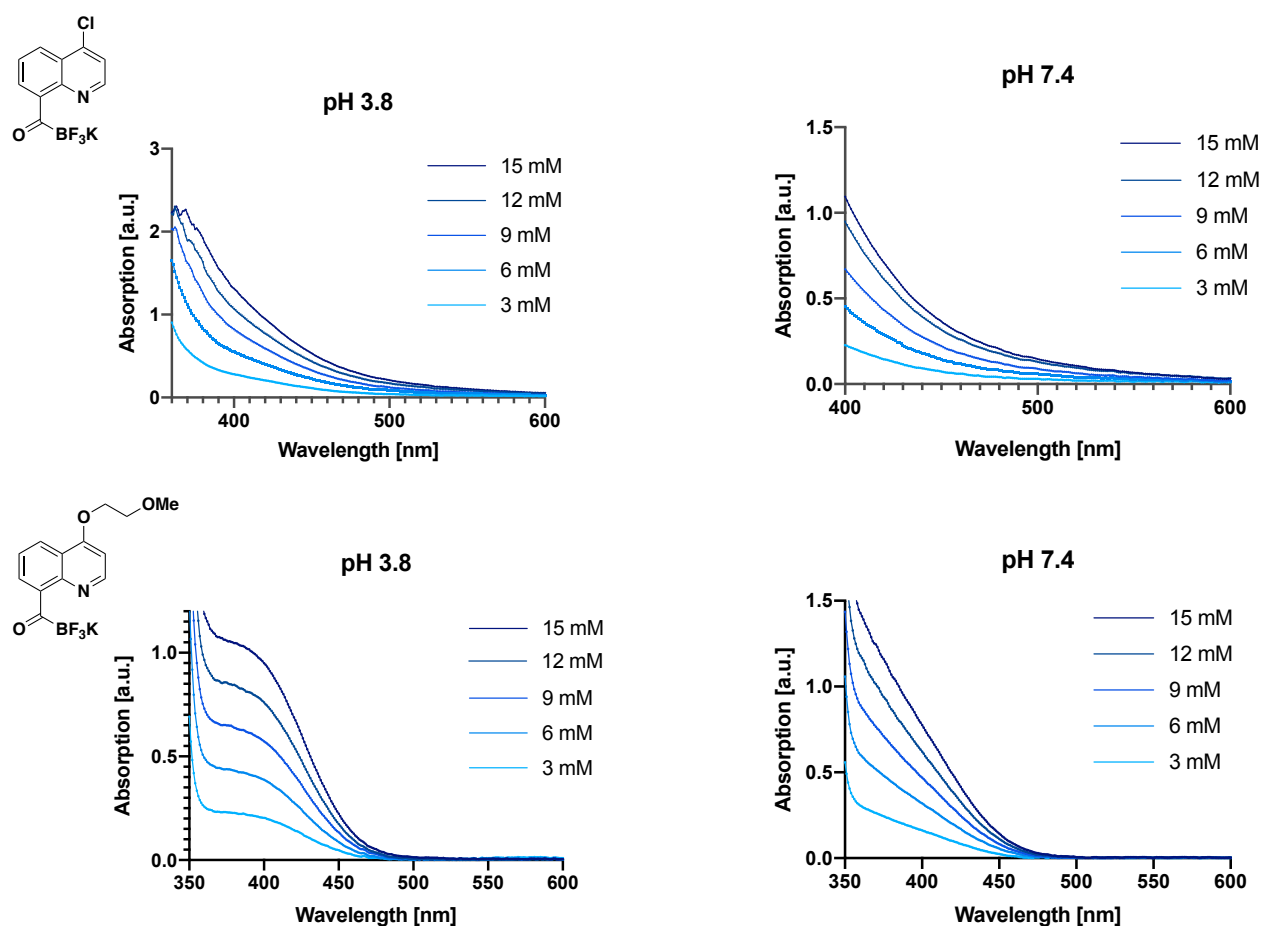
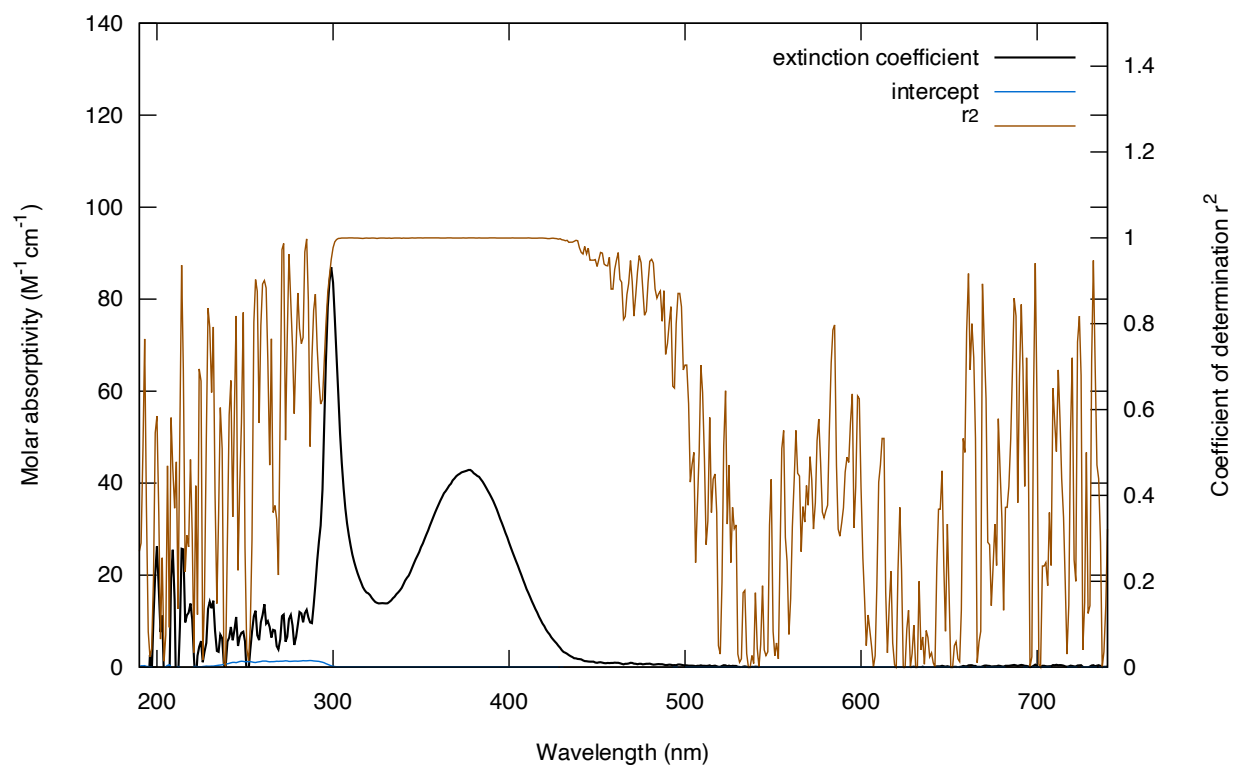
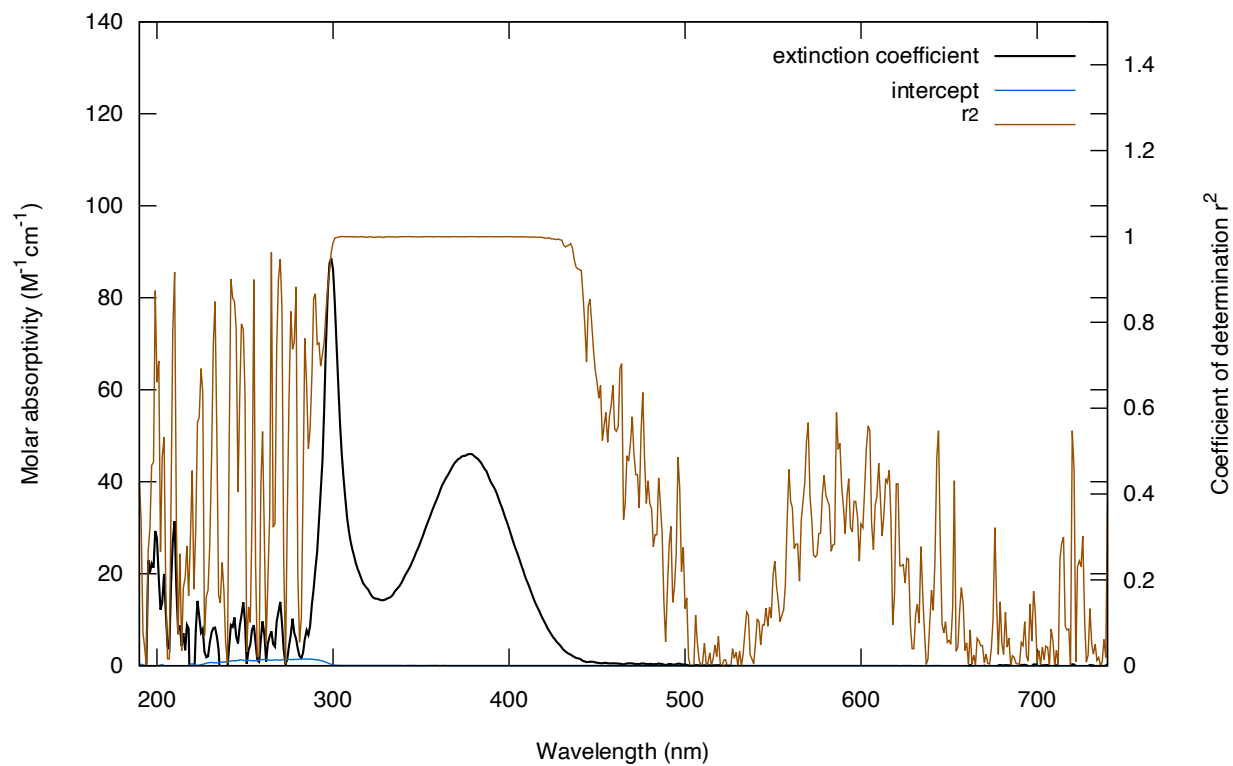


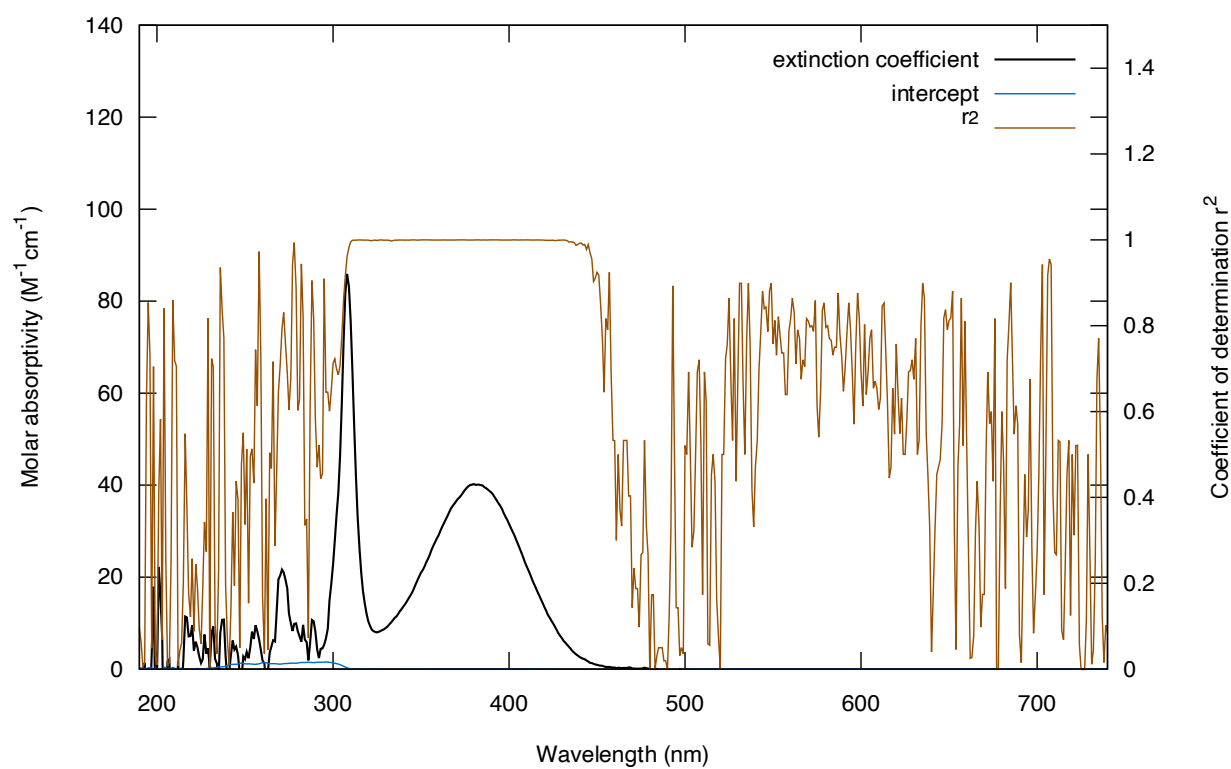
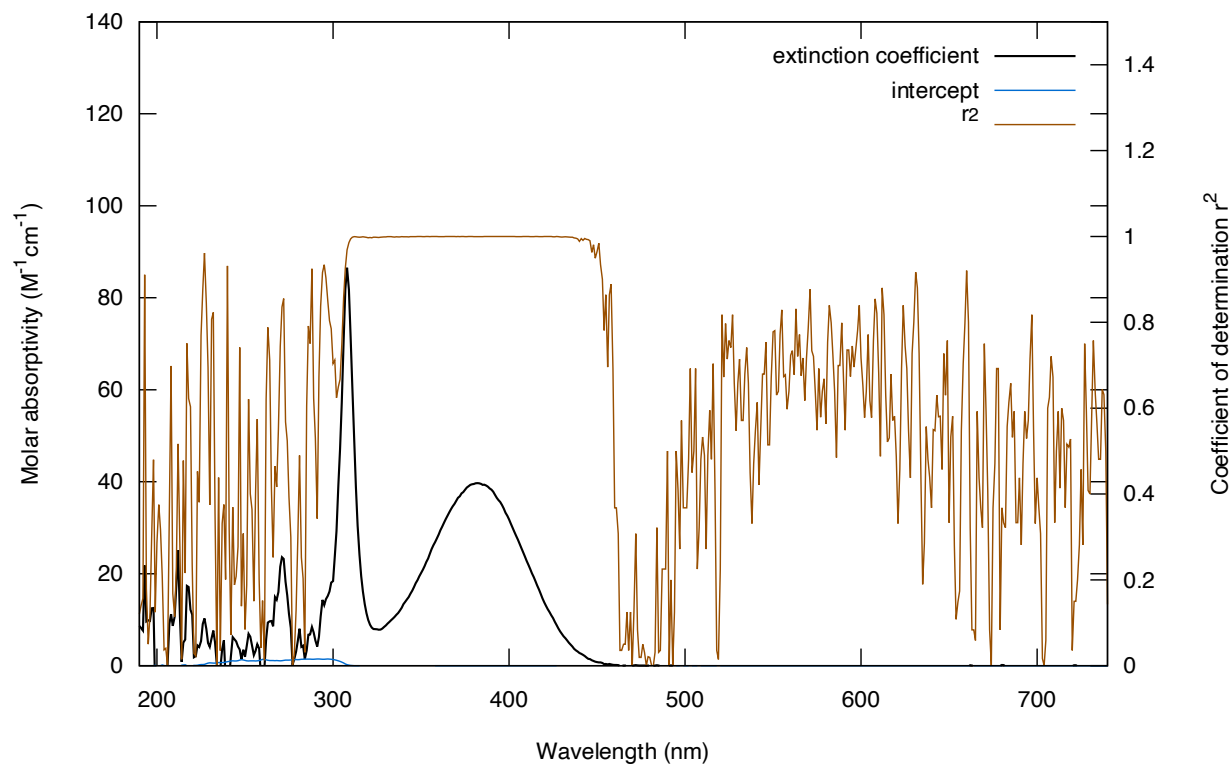
Figure 1. Absorption spectra of dilution series of potassium acyltrifluoroborates (KATs).

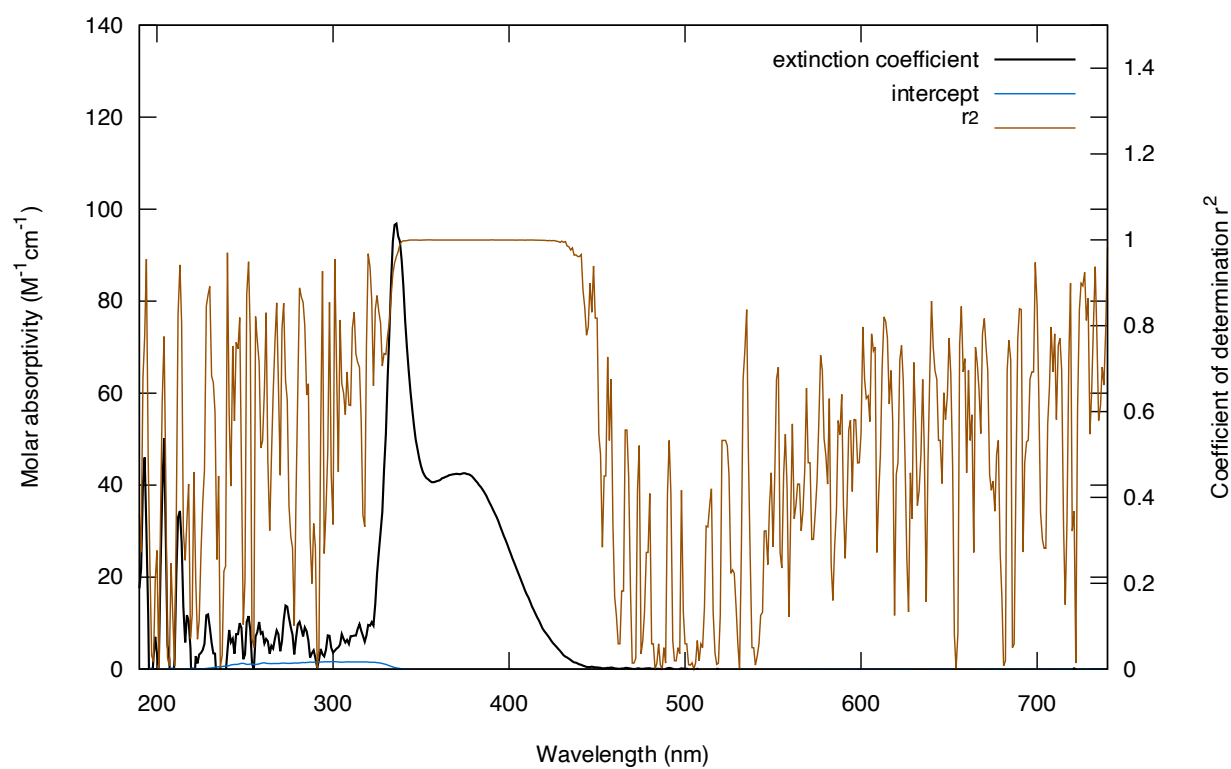
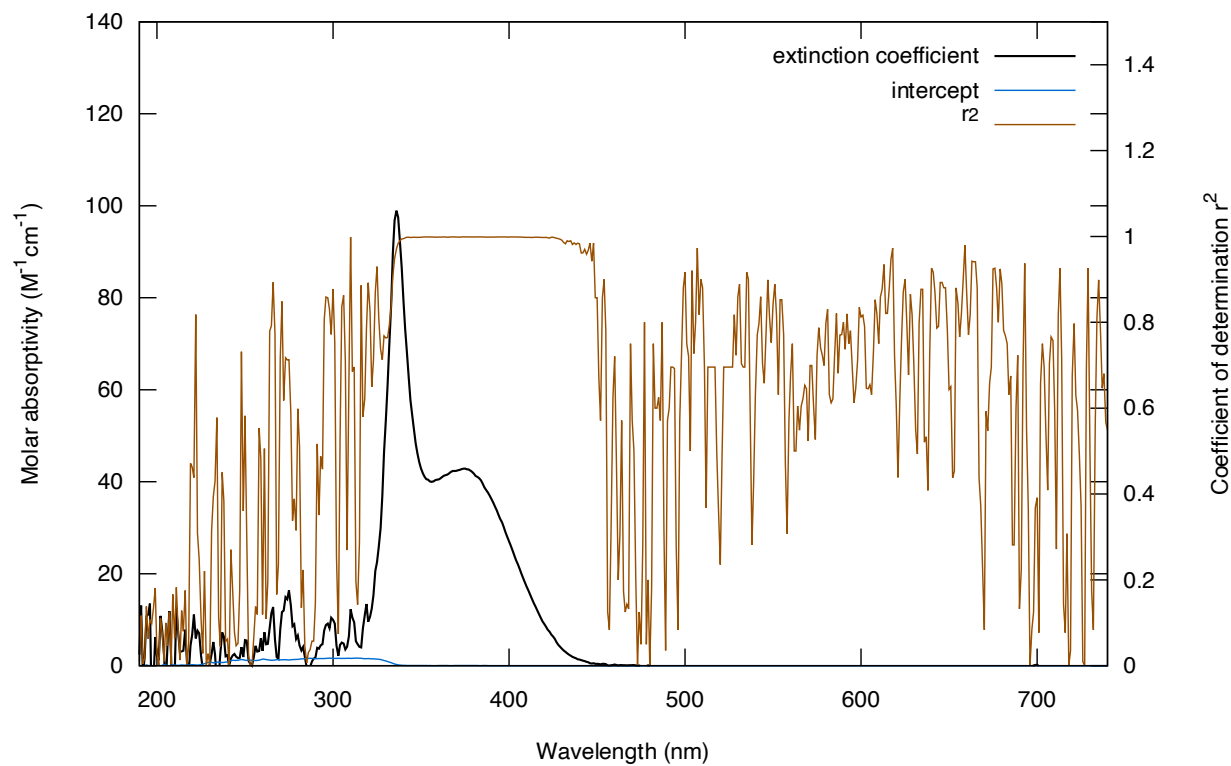
The recorded absorption value at each wavelength was then fitted to the following model derived from Beer's law to solve for molar absorption as a function of wavelength:

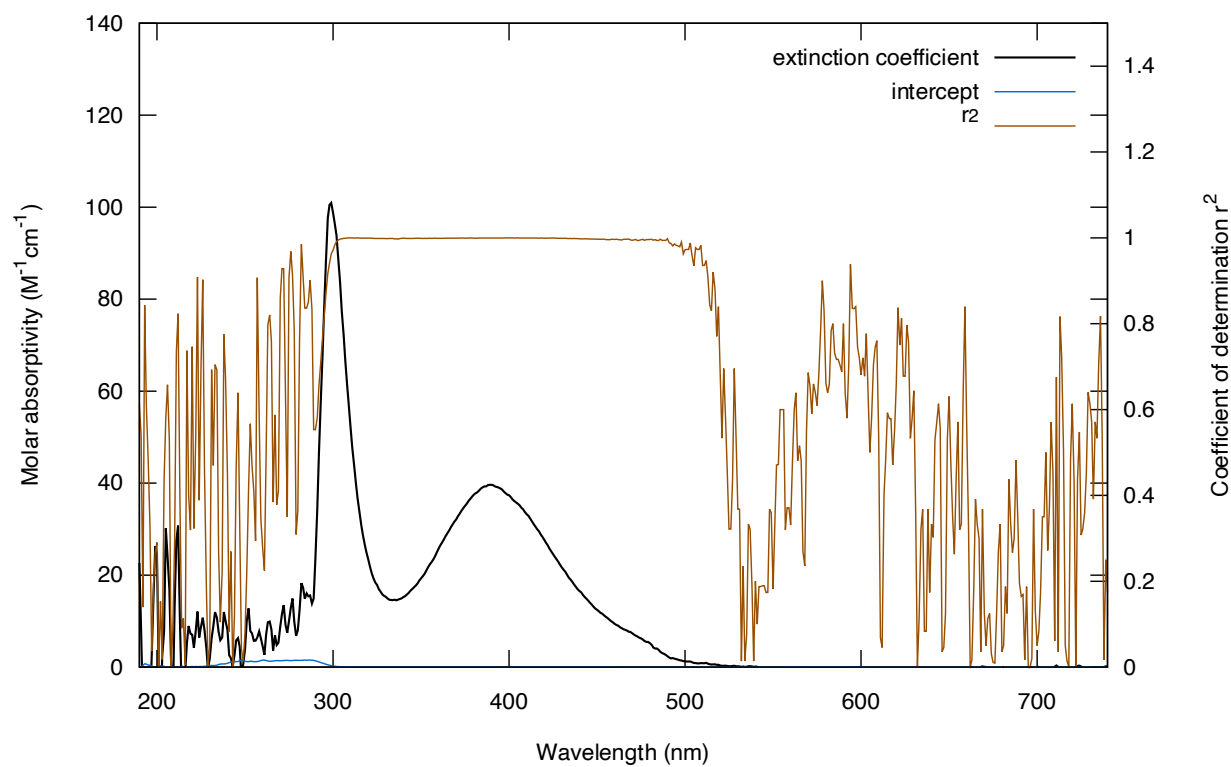
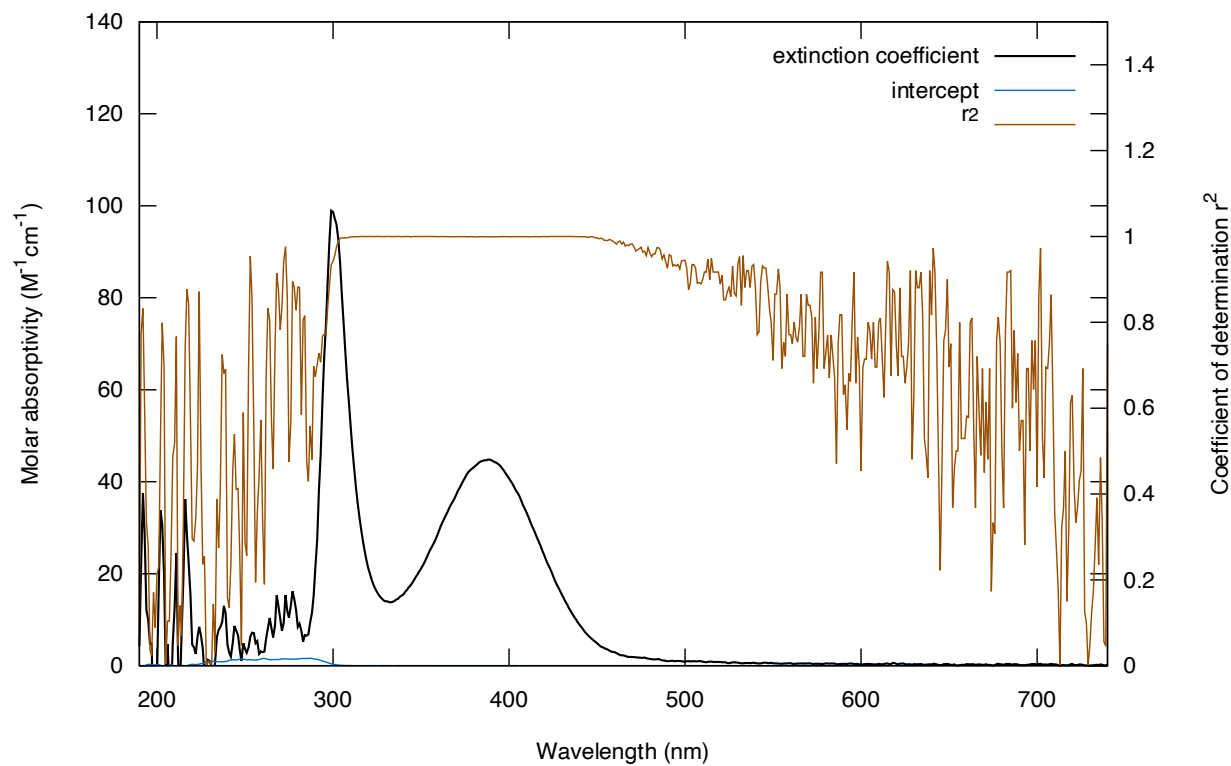
$$A = \varepsilon cl + \varepsilon_0 + z$$

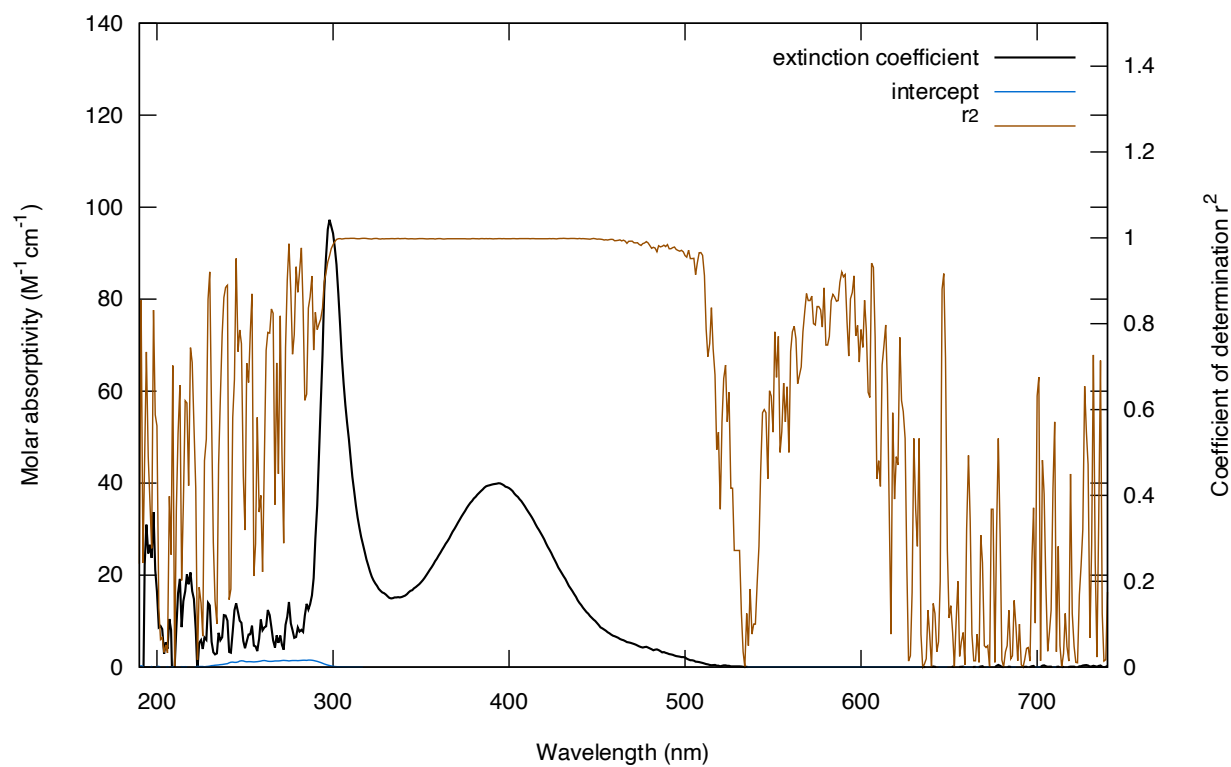
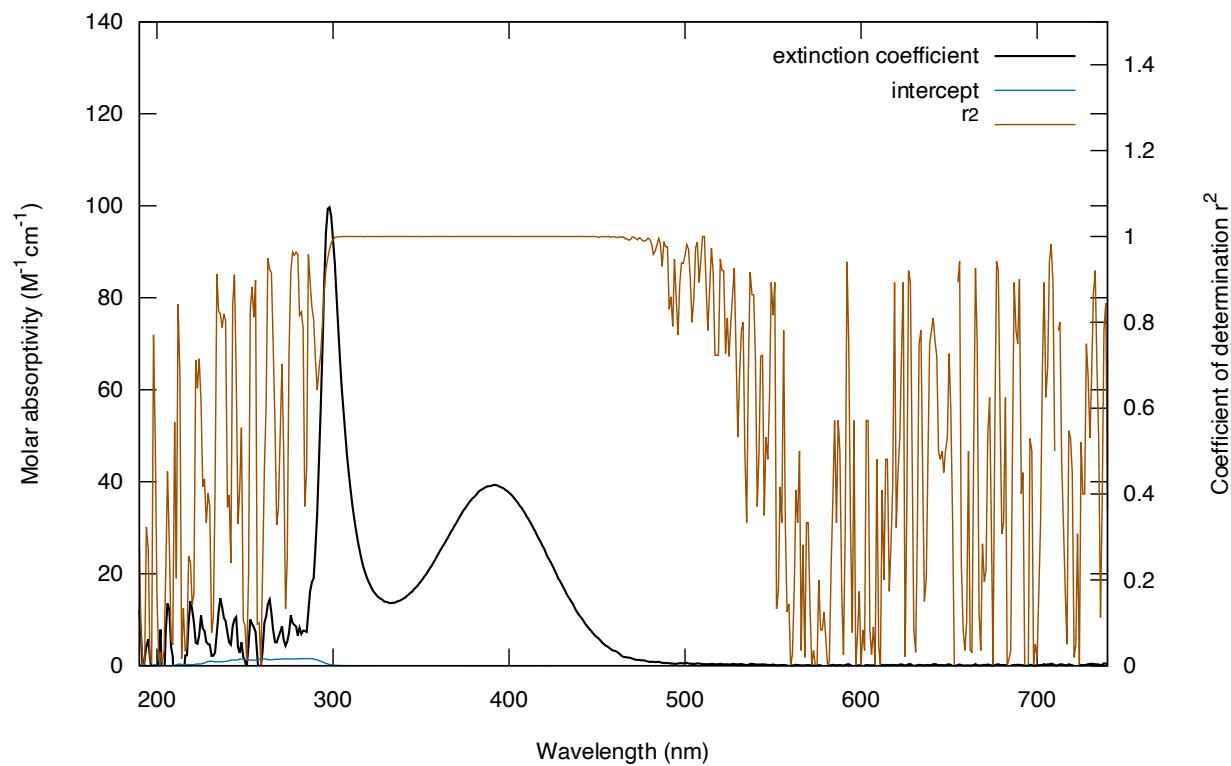
where A is the measured absorbance, ε is the molar extinction coefficient with unit $M^{-1} \text{ cm}^{-1}$, c is the molar concentration of the absorbing substance, l is the light path (1 cm), ε_0 is the systematic error term (intercept), and z is the random error term. A wavelength is considered suitable for kinetic study for a specific KAT if the fitting r^2 is larger than 0.95 at that wavelength. The extinction coefficient (in black), the r^2 value (in brown), and the intercept ε_0 were plotted against wavelength below in Figure 2.

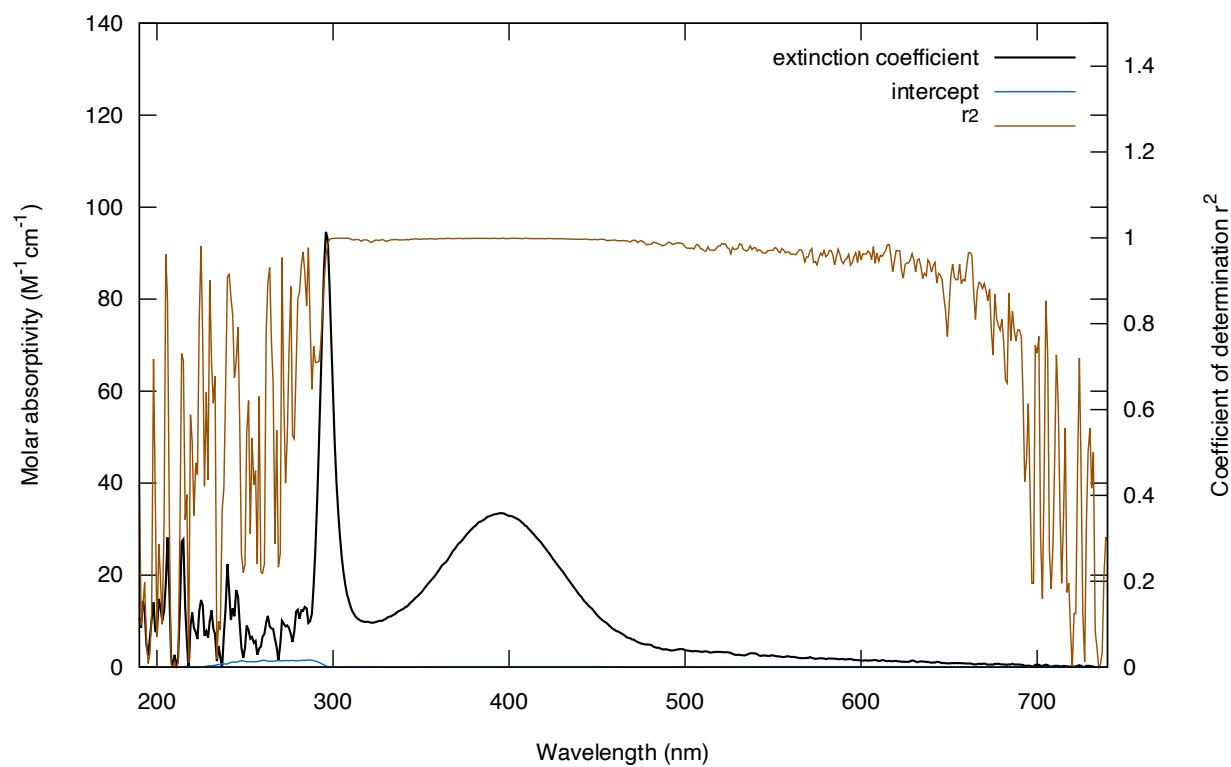
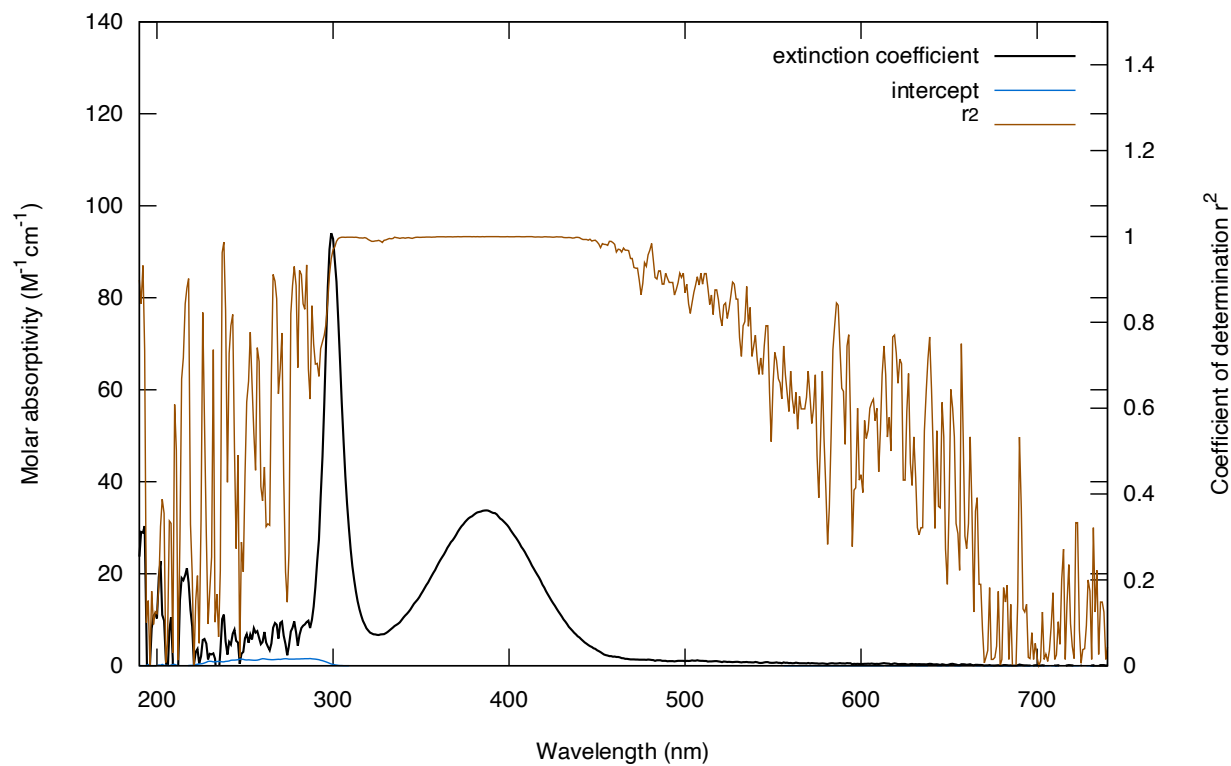
UV absorption linearity of **3a** at pH 3.8UV absorption linearity of **3a** at pH 7.4

UV absorption linearity of **3b** at pH 3.8UV absorption linearity of **3b** at pH 7.4

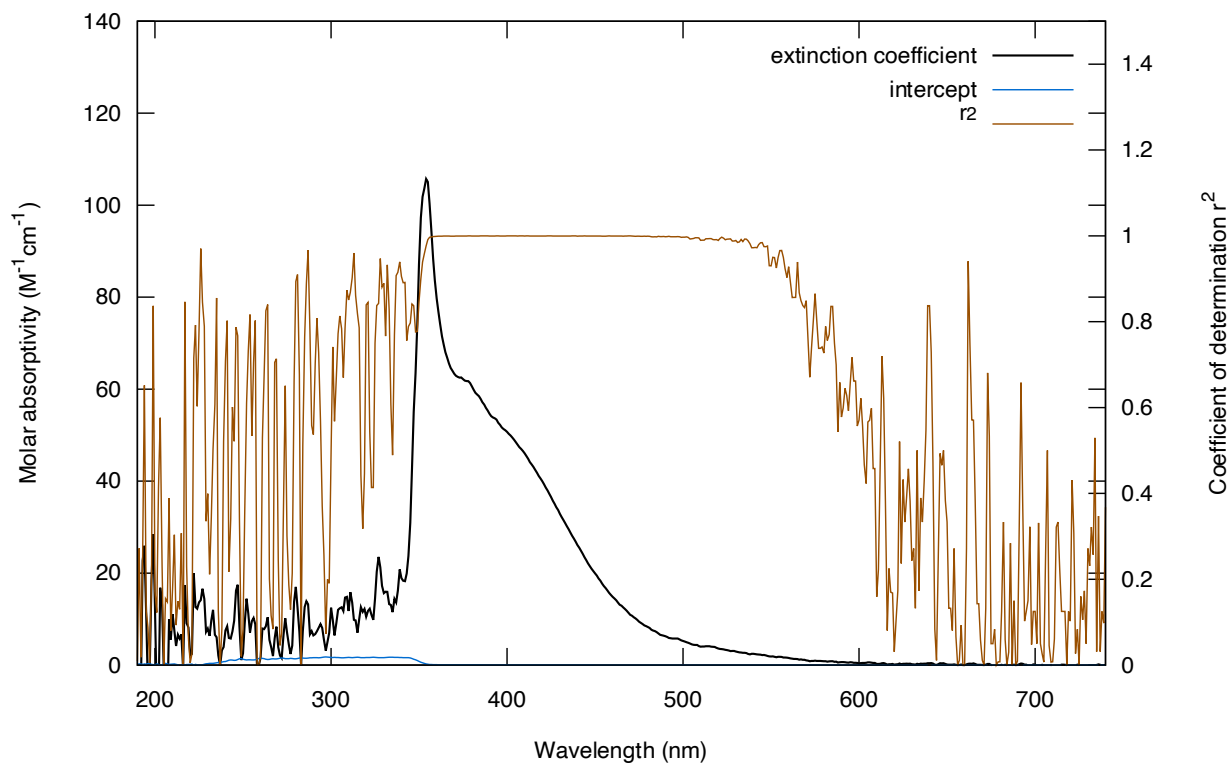
UV absorption linearity of **3c** at pH 3.8UV absorption linearity of **3c** at pH 7.4

UV absorption linearity of **4a** at pH 3.8UV absorption linearity of **4a** at pH 7.4

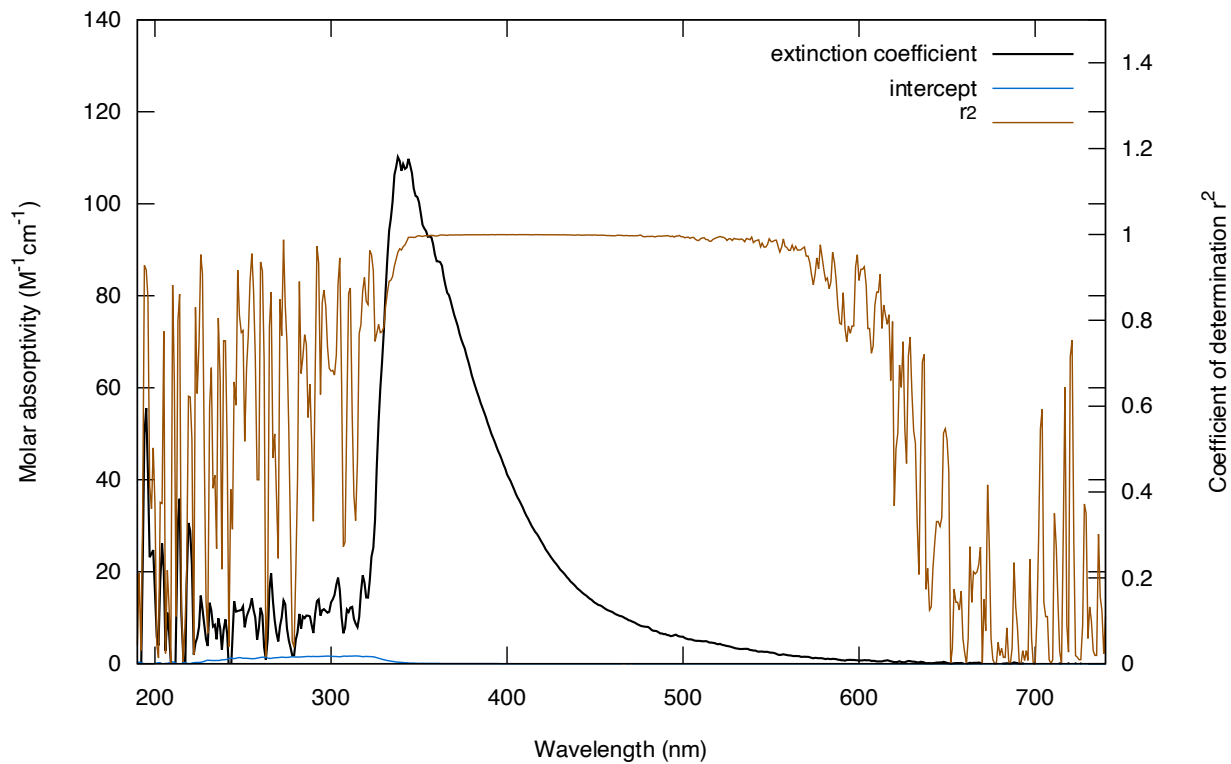
UV absorption linearity of **4b** at pH 3.8UV absorption linearity of **4b** at pH 7.4

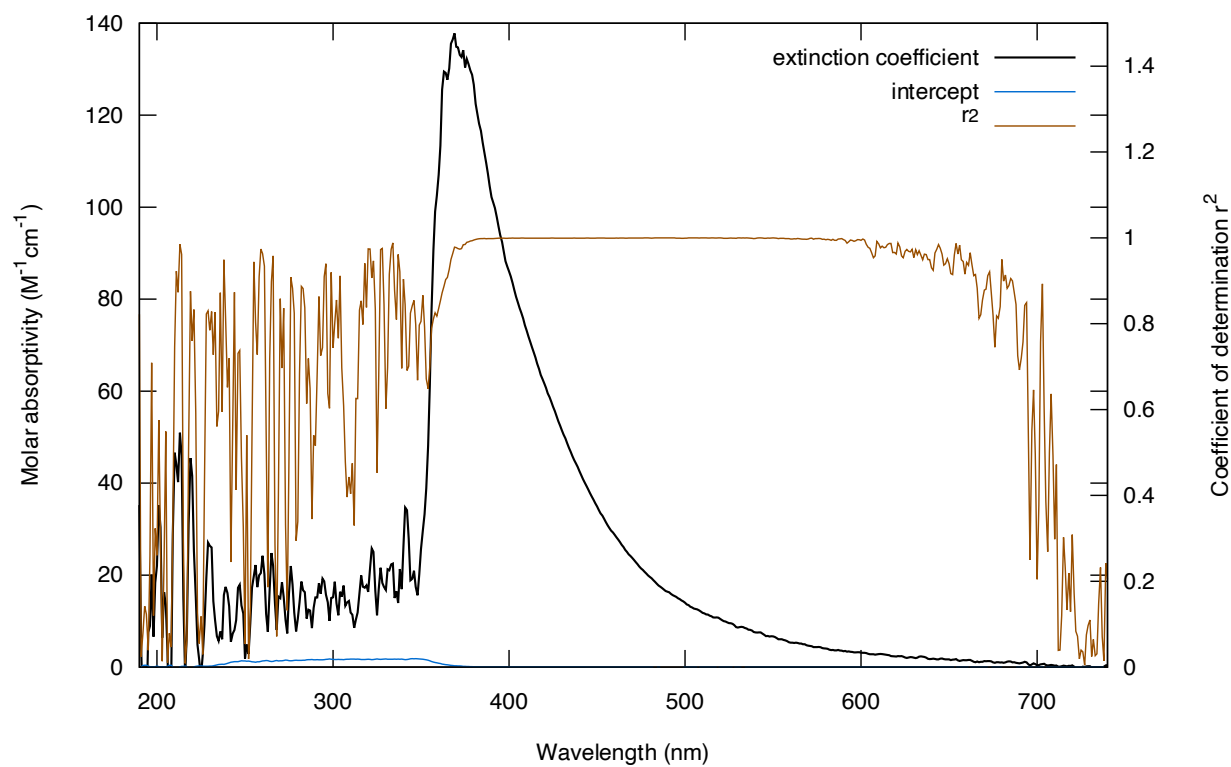
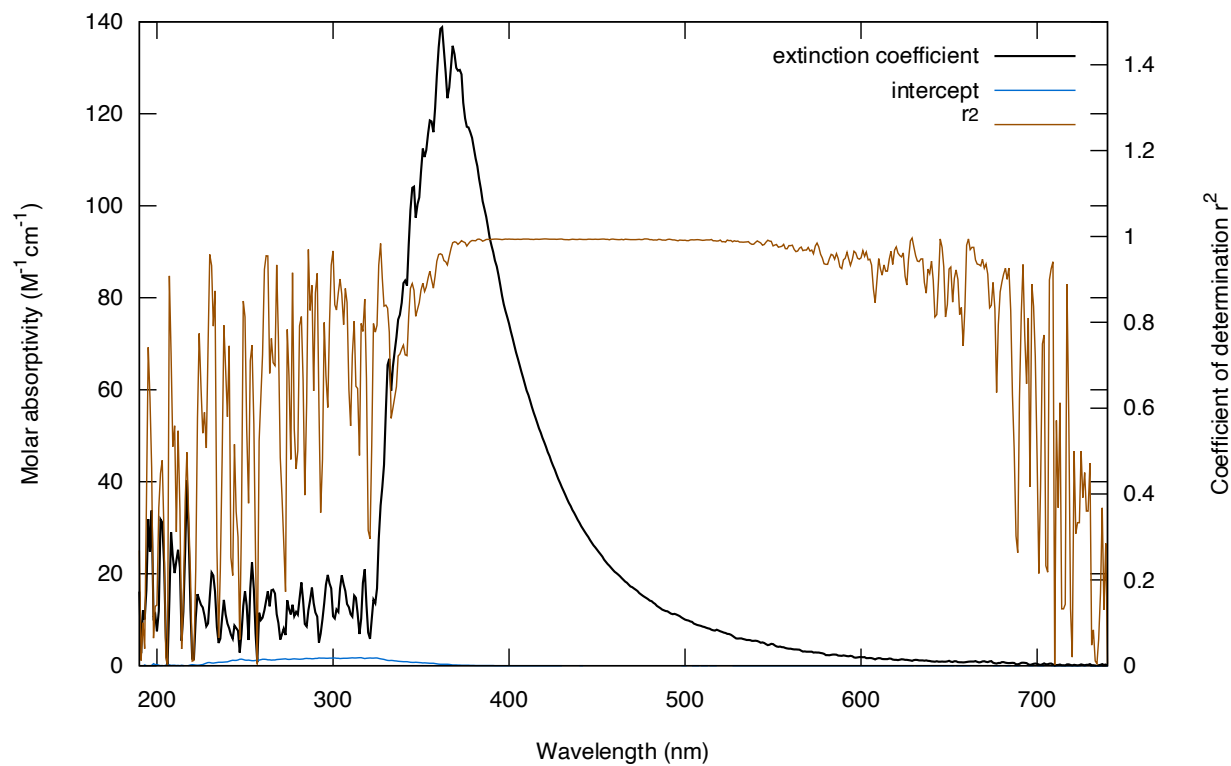
UV absorption linearity of **4c** at pH 3.8UV absorption linearity of **4c** at pH 7.4

UV absorption linearity of 5a at pH 3.8



UV absorption linearity of 5a at pH 7.4



UV absorption linearity of **5b** at pH 3.8UV absorption linearity of **5b** at pH 7.4

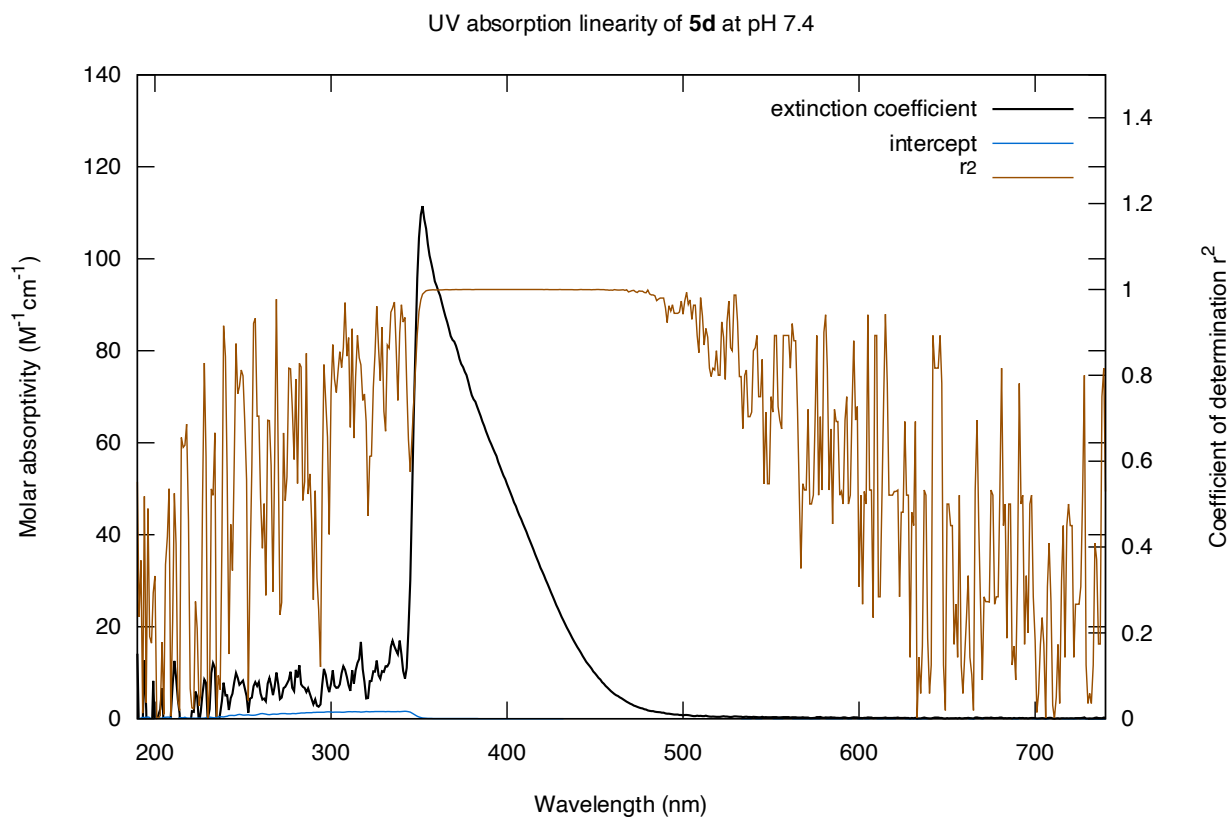
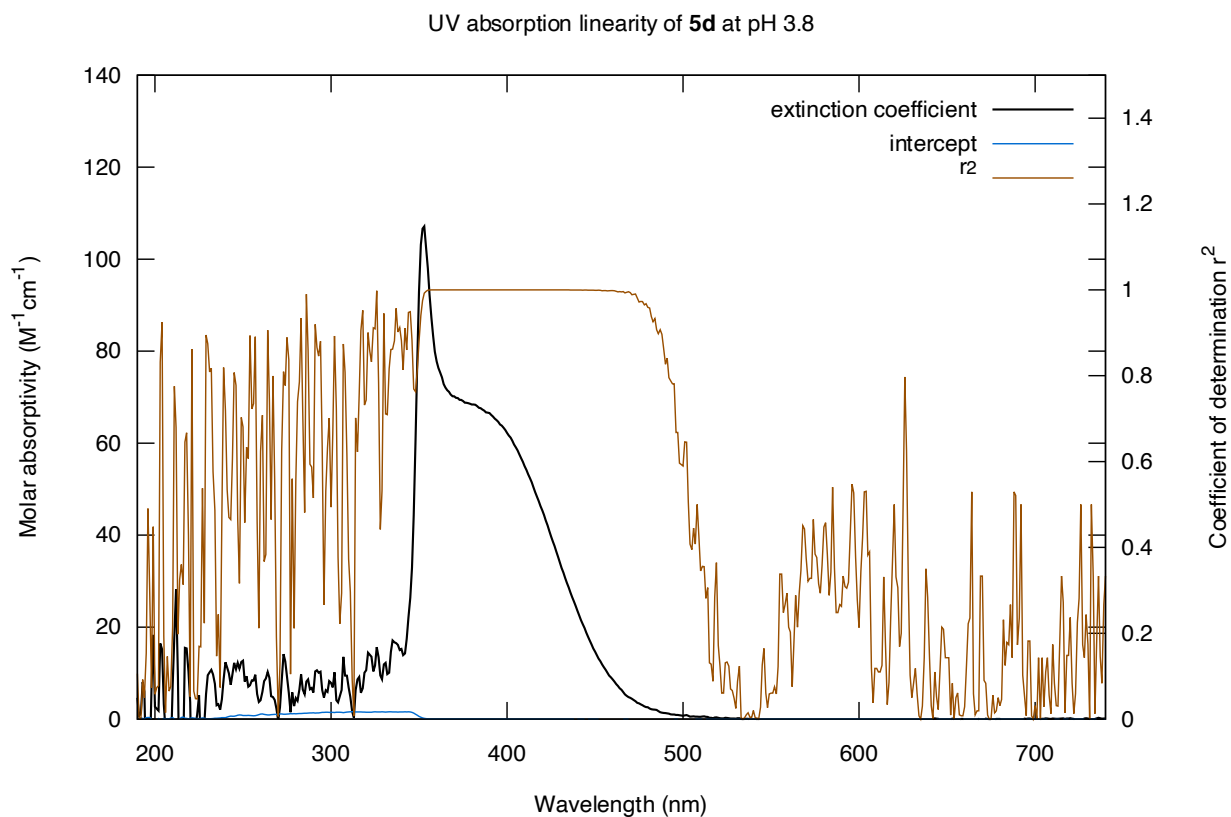


Figure 2. Molar extinction coefficients, r^2 , and residual intercepts 3, 4 and 5 plotted against wavelength.

	pH 3.8		pH 7.4	
	λ_{\max} [nm]	ϵ [$M^{-1}cm^{-1}$]	λ_{\max} [nm]	ϵ [$M^{-1}cm^{-1}$]
3a	380	42.13	380	45.67
3b	380	41.47	380	41.77
3c	385	39.90	385	39.33
4a	392	39.30	392	44.27
4b	400	32.87	392	33.17
4c	397	39.53	397	38.50
5a	380	60.63	380	62.70
5b	415	67.30	415	53.93
5d	392	65.80	385	65.80

Table 1. Summary of determined extinction coefficients of KATs at pH 3.8 and pH 7.4.

UV-Vis measurement of KAT ligation rate

Sample preparation and kinetic measurement procedure

A 15 mM solution of **KAT** in CH₃CN-buffer cosolvent (1:1 v/v) and a 15 mM solution of the hydroxylamine **6** in the same cosolvent were prepared. 1 mL of the hydroxylamine solution was added into a quartz cuvette containing 1 mL of the KAT solution and well mixed before beginning the time course measurement on NanoDrop. The mixing time was not more than 5 seconds. A triplicate of each reaction was measured for all KATs, excepts for **5c**, which did not have sufficient solubility (> 1.5 mM) in the buffer-solvent mixture to provide a good signal-to-noise ratio in the UV concentration measurement. KAT **5d** was synthesized and used instead.

NanoDrop acquisition method and raw data processing

Wavelengths from 190-840 nm were recorded at each timepoint. After beginning of the measurement a timepoint will be collected every 3 seconds between 0-204 s, every 10 seconds between 204 - 354 s, and every 15 seconds between 357 - 1002 s from time zero.

The data were recorded in the Thermo workbook format (.twbk), which was converted by a customized script (see appendix) to a tab-separated value (.tsv) text format before used to derive the rate constants.

Noise analysis of the Nanodrop kinetic measurement

A blank measurement was performed to observe the scale and temporal-spectral pattern of noise in the Thermo Scientific NanoDrop™ kinetic measurements. An example was shown below.

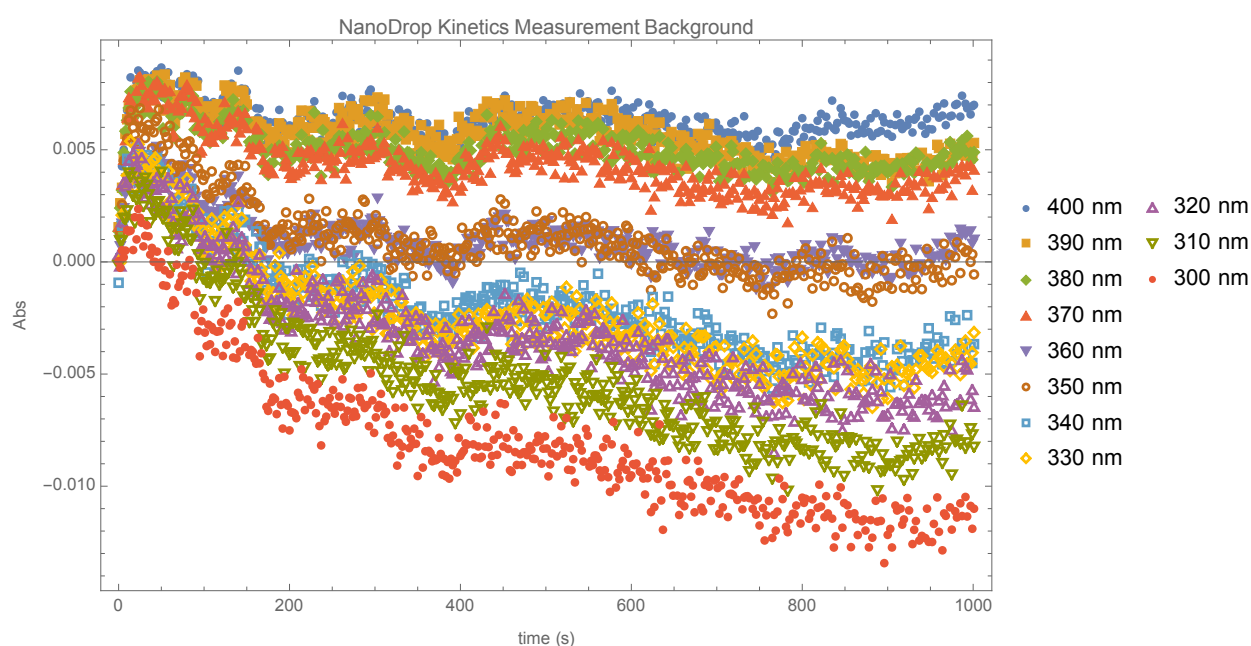


Figure 3. Noise pattern of NanoDrop from blank measurement.

This measurement was done in pure acetonitrile. Stability of signal over time was acceptable for wavelengths longer than 350 nm without immediate need of correction. All wavelengths suffered from a jump in absorbance (decrease of light intensity) in the first 20 seconds, possibly from ignition pattern of the xenon lamp. For wavelengths chosen for kinetic profiling (>380 nm) the precision of absorbance was excellent (± 0.002 absorbance units), apart from a non-zero background due to the initial jump.

Data fitting workflow

After the absorbance data was collected over the reaction course, a wavelength was chosen for a specific KAT under specific pH value, to have minimal overlap with the reaction product. Such wavelengths will decrease more over the reaction (see Fig. 4) and were therefore suitable to derive the remaining KAT concentration in the reaction system.

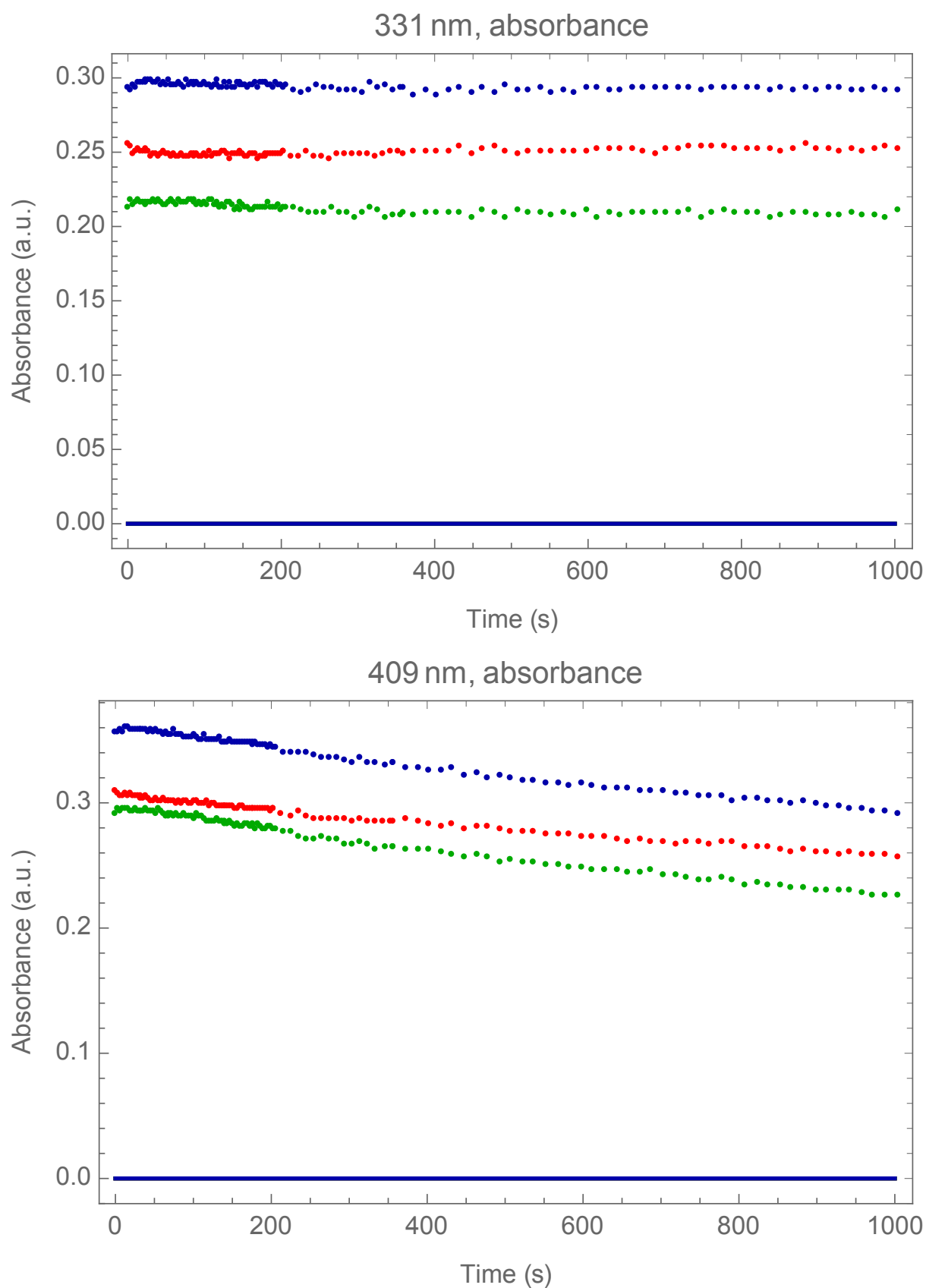


Figure 4. Absorbance time course from measurement of **4a** at pH 7.4. The wavelength picked at 331 nm did not decrease with time because the same absorption is also present in the product. The absorption at 409 nm was specific to KATs and provides a suitable dataset for kinetic analysis. The colors red, green and blue represent the 1st, 2nd and 3rd replicate of the same measurement.

The absorbance was subtracted with the instrument background before being divided with the extinction coefficient to obtain the concentration of the KAT. The reciprocal concentrations were plotted over time to give a plot.

In a second order reaction with the two reactants having equal initial concentrations, the integrated rate law will be $\frac{1}{[A]} = kt + \frac{1}{[A_0]}$, where $[A]$ is the concentration of the species of interest, $[A_0]$ is initial concentration, and k is the second order rate constant.

Linear regression was then performed to each of the data series in the triplicate. Assuming the reaction to be second order, the slope will correspond to the rate constant and intercept the initial reciprocal concentration.

The instrument background was fitted by a script from the dataset upon two constraints: first by maximizing the linearity of the reciprocal concentration plot, and then minimizing the spread of the derived initial concentration among the triplicates. The following example demonstrates the effect of an off-fit instrument background value:

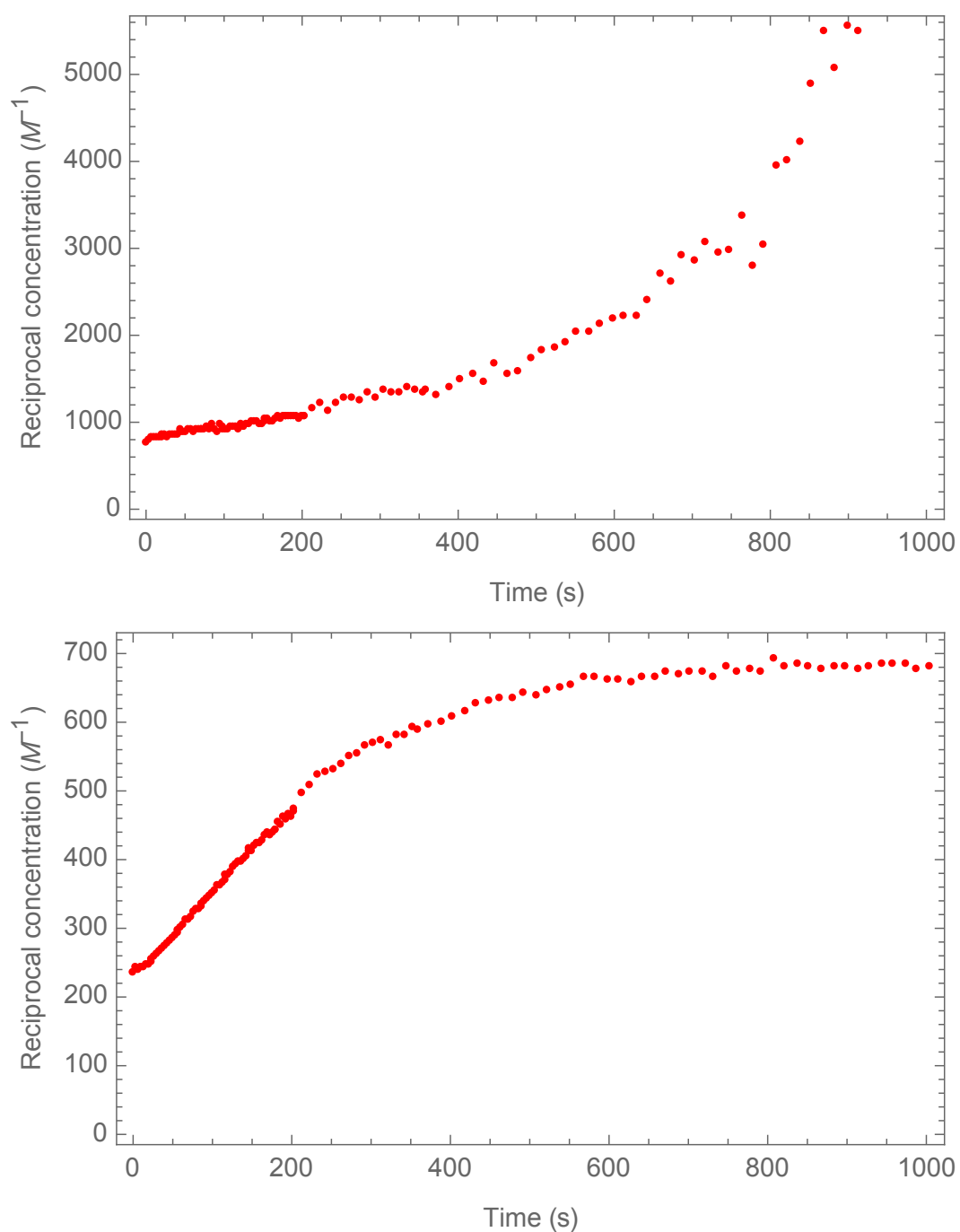
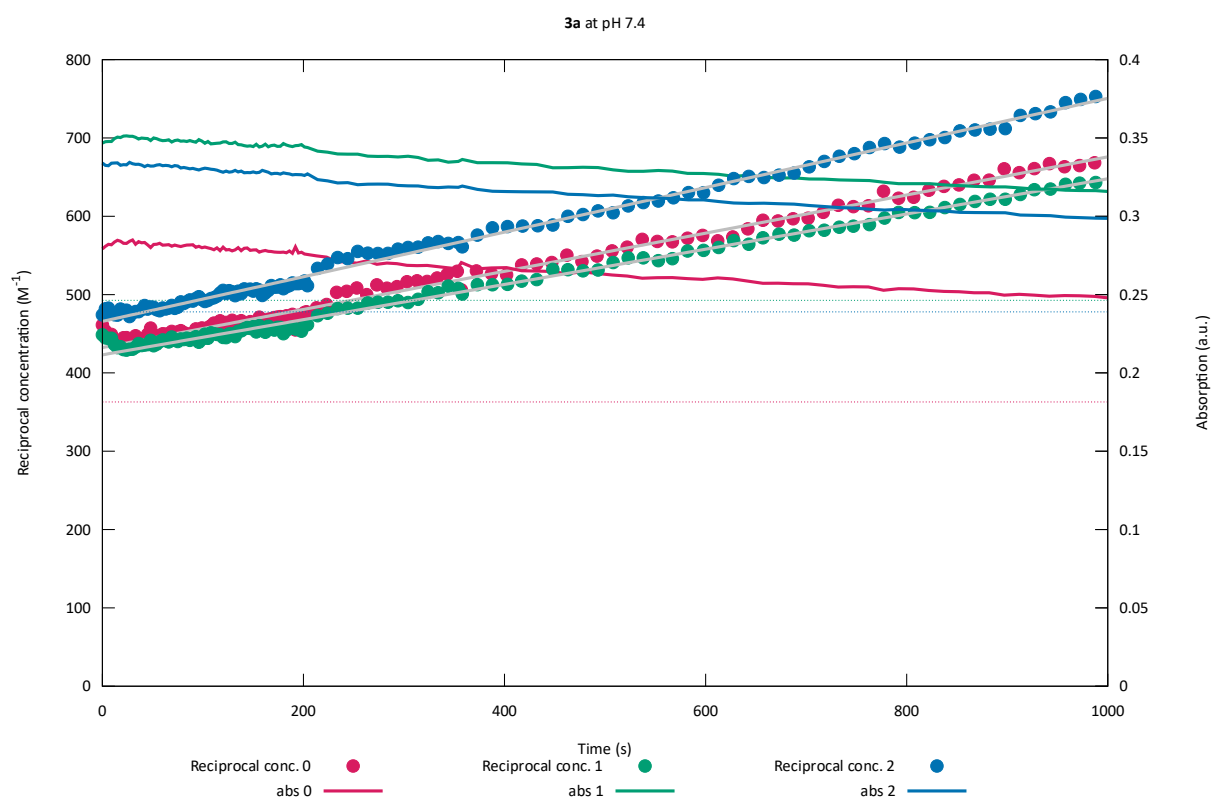
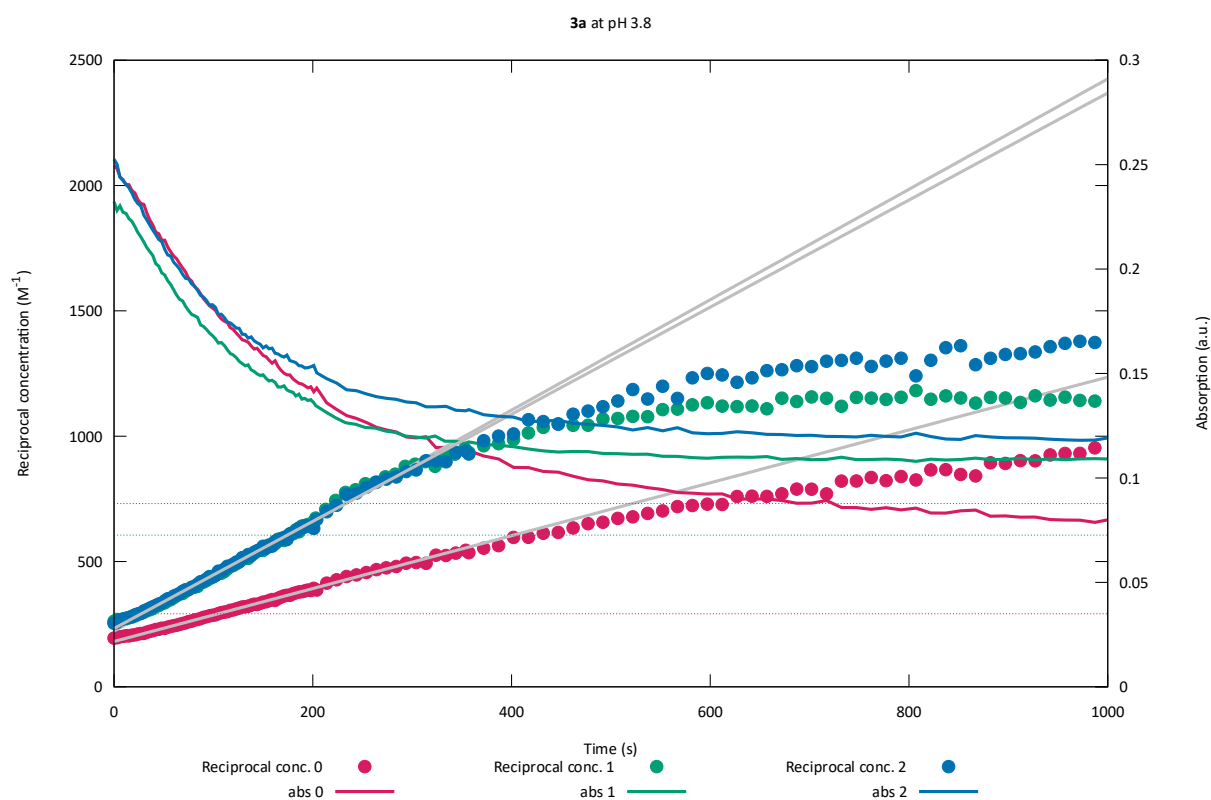
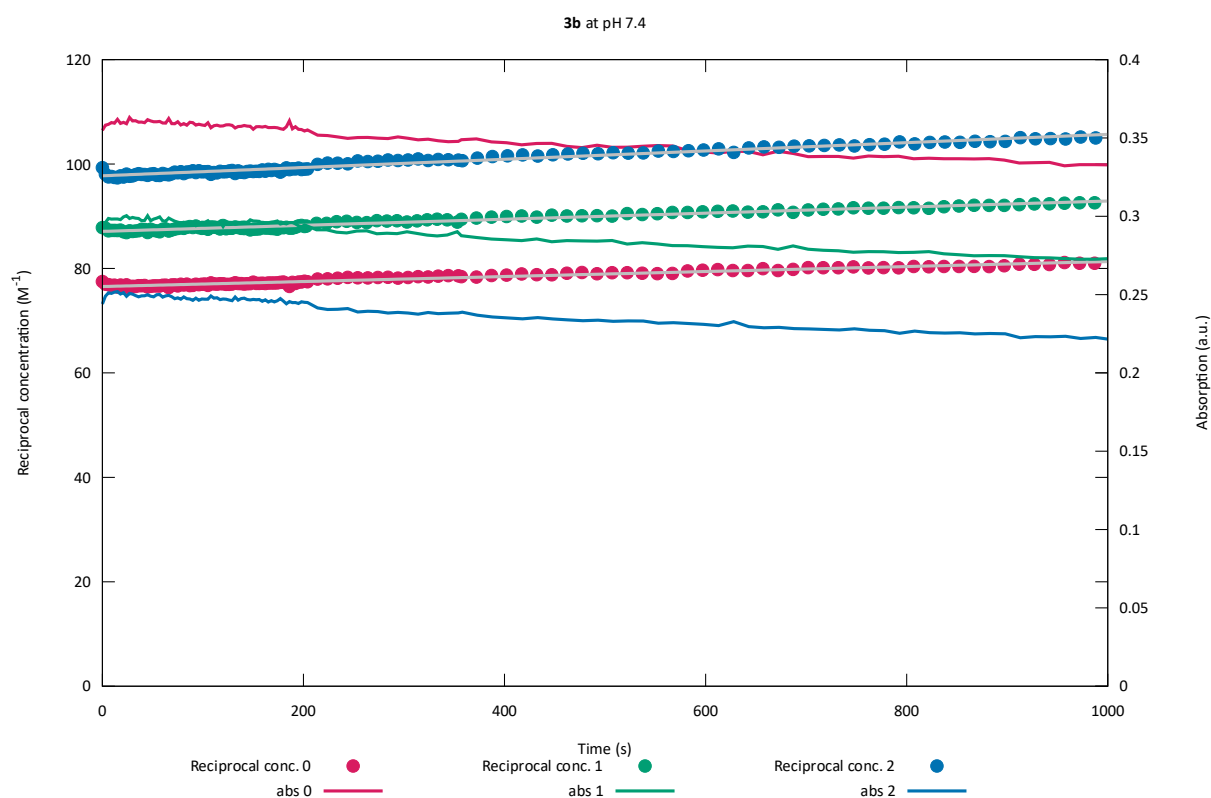
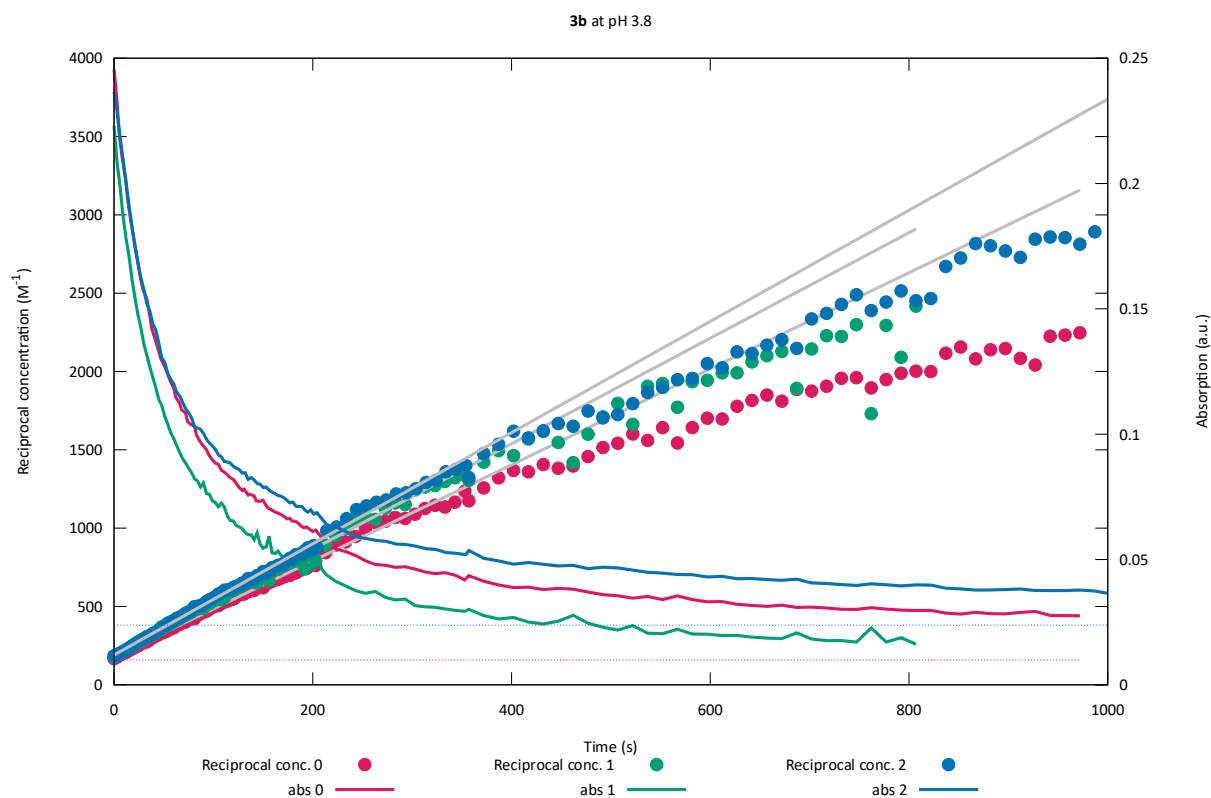


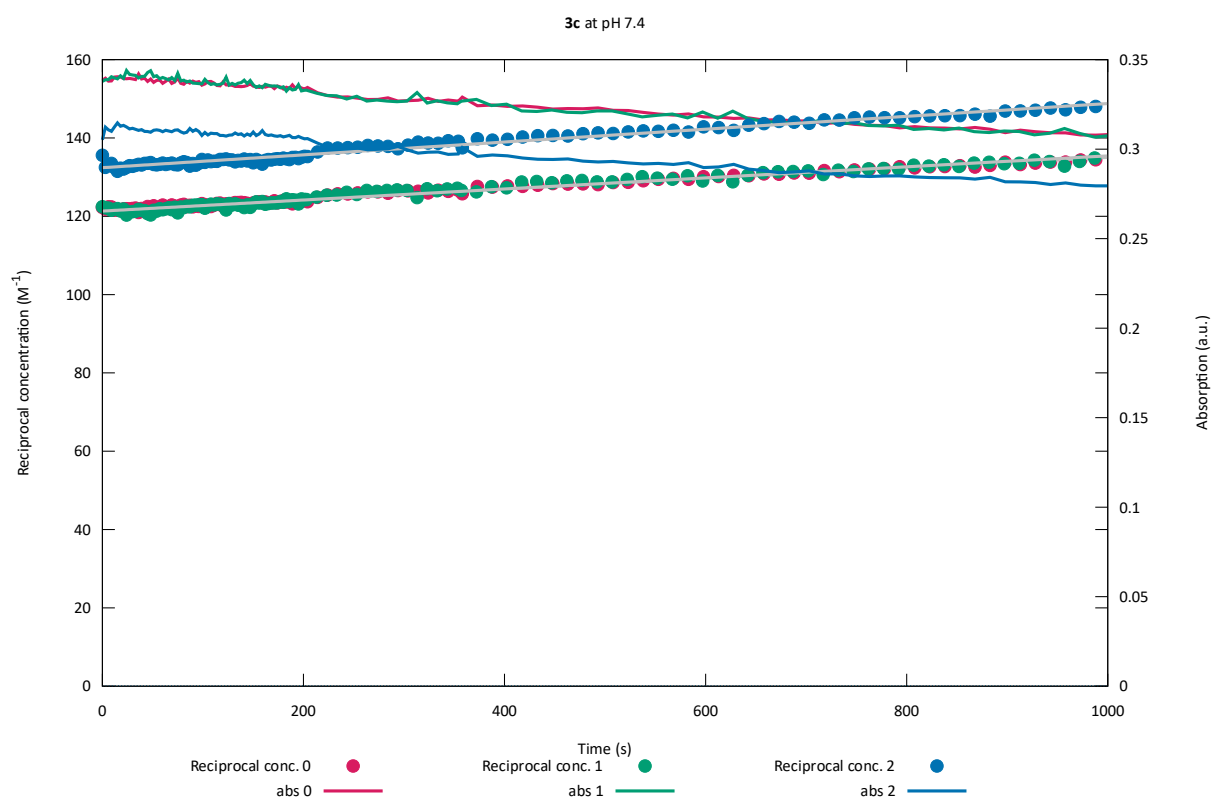
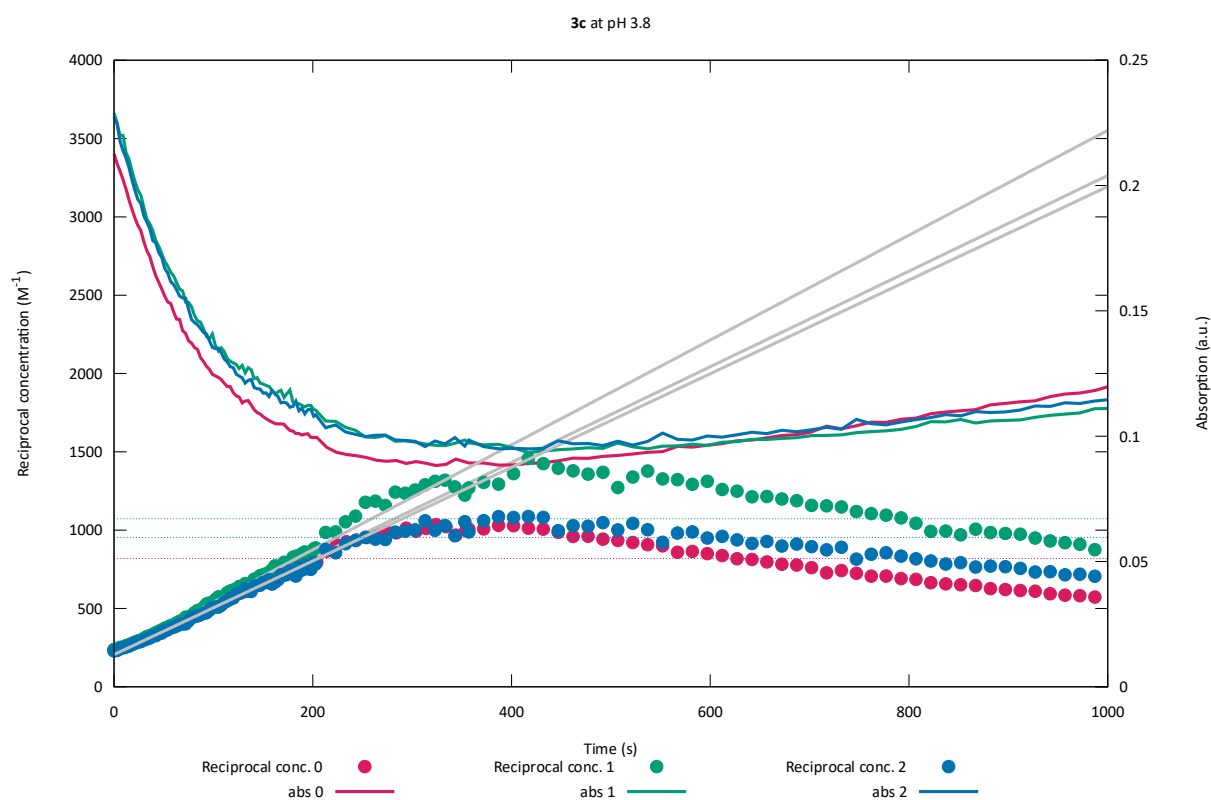
Figure 5. Effect of wrongly determined instrument background. The background was taken too high in the graph on the left, causing a concave curvature in the reciprocal concentration plotted over time. Insufficient subtraction of the absorption background, in the contrary, causes a convex curvature, as shown on the right.

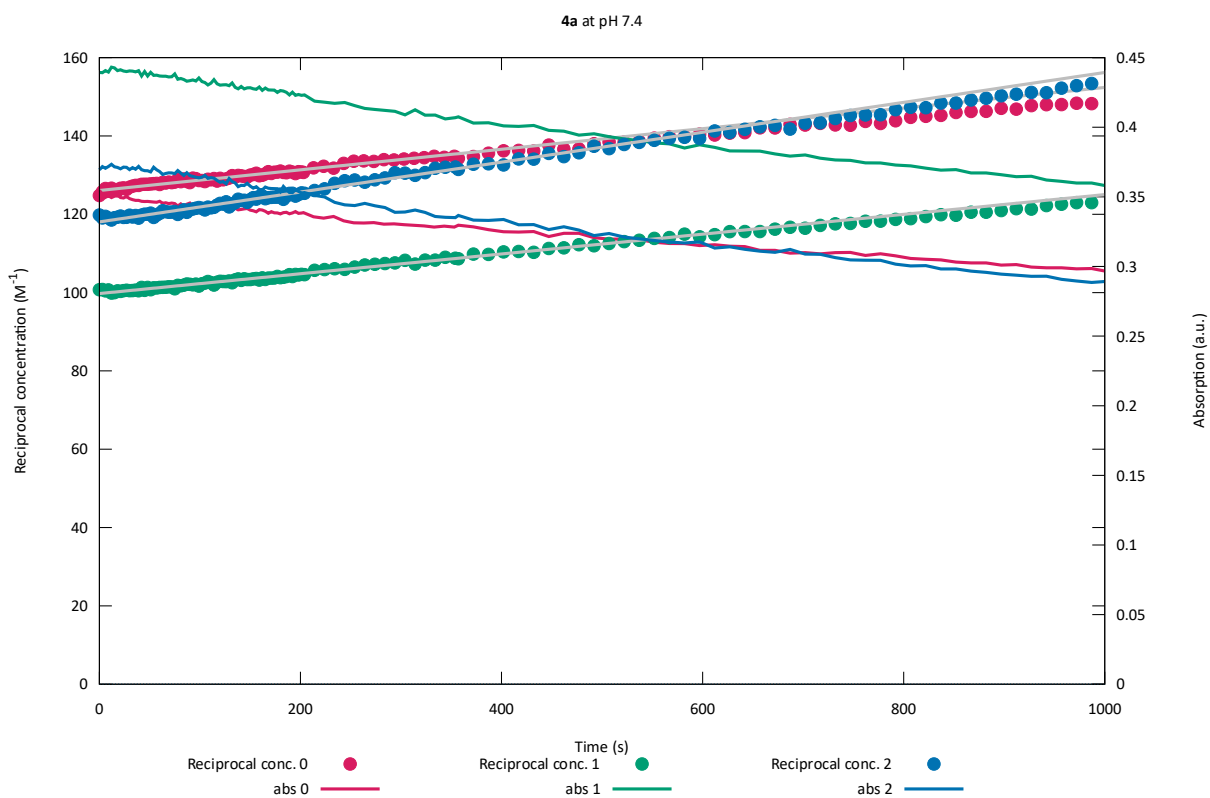
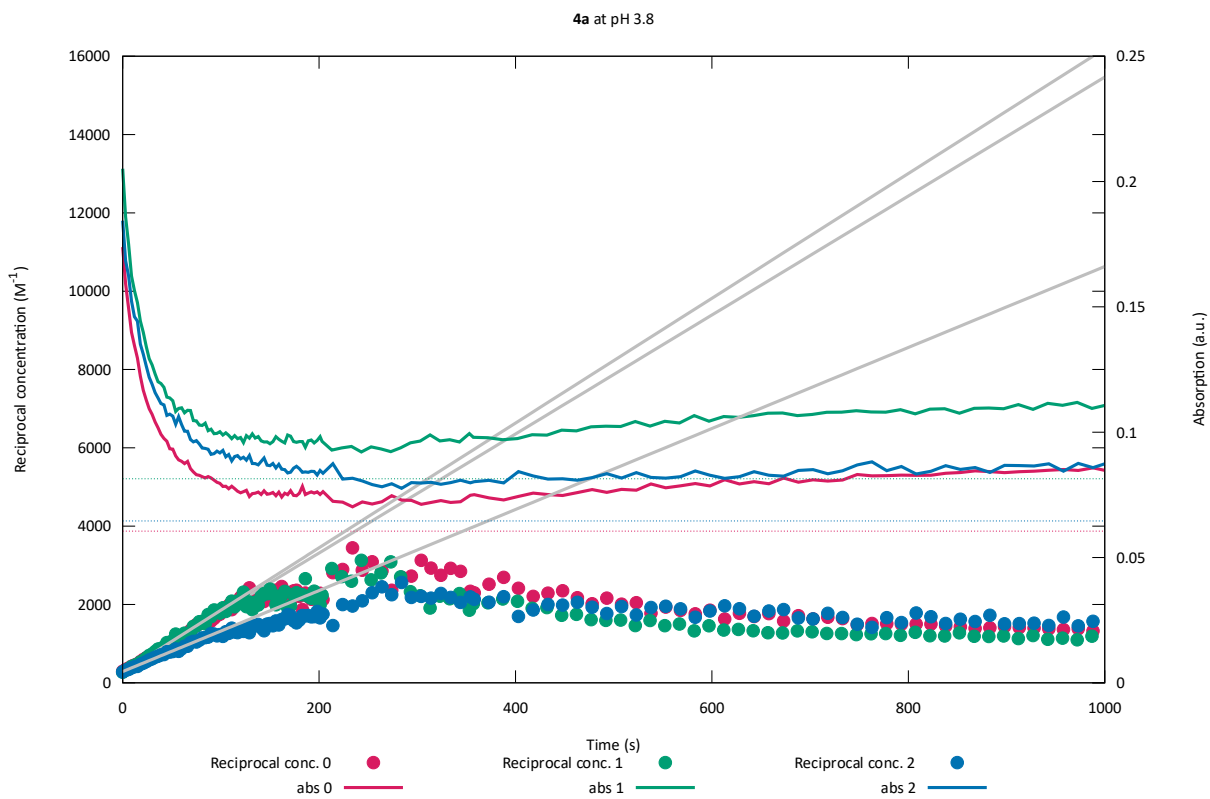
Kinetic plots

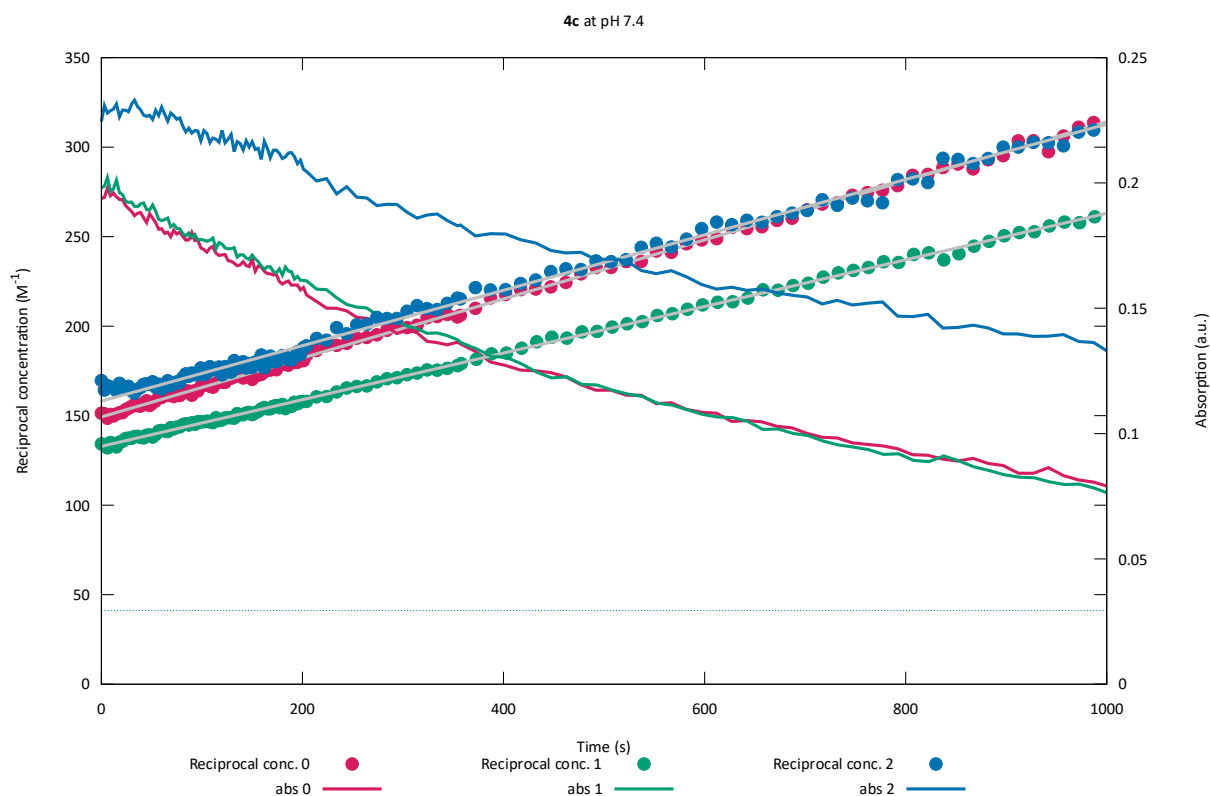
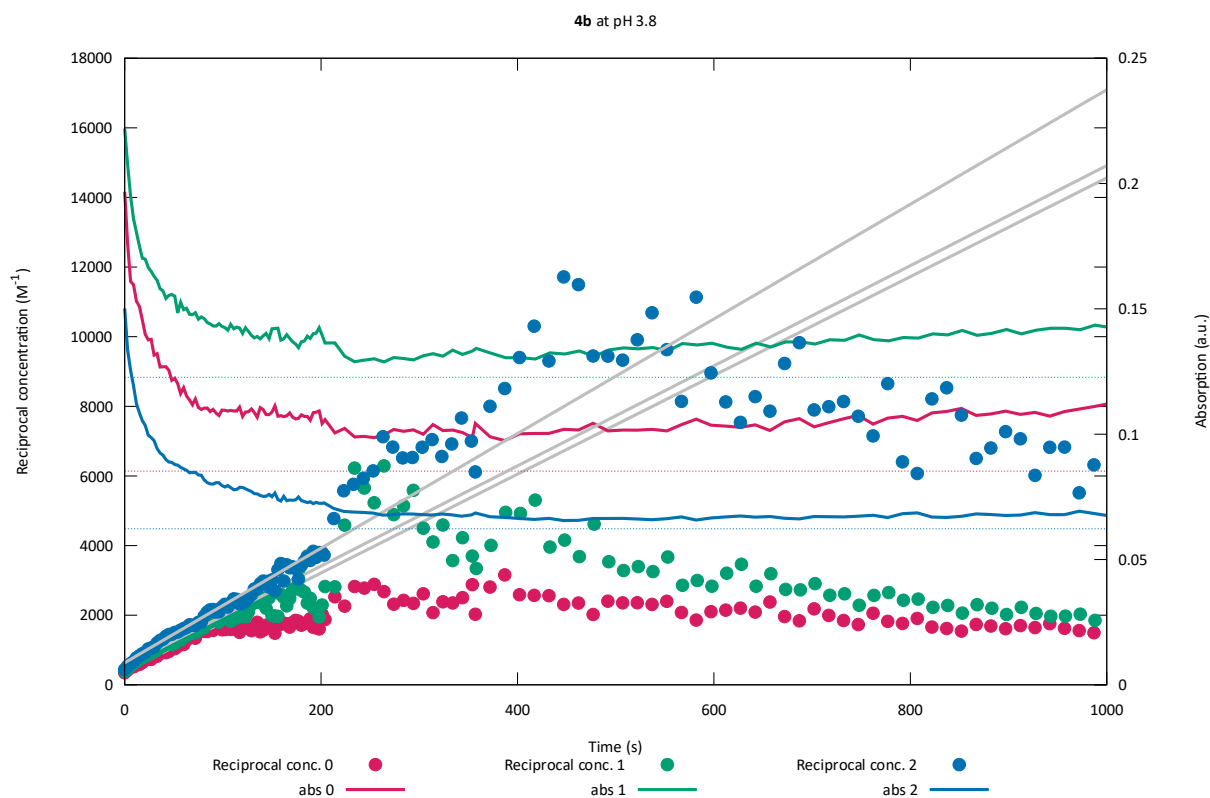
Absorption time courses (solid curves), reciprocal concentration plots (colored dots), determined instrument background (lightly colored dotted horizontal lines), and linear fits (grey lines) used to calculate rate constants were plotted below:

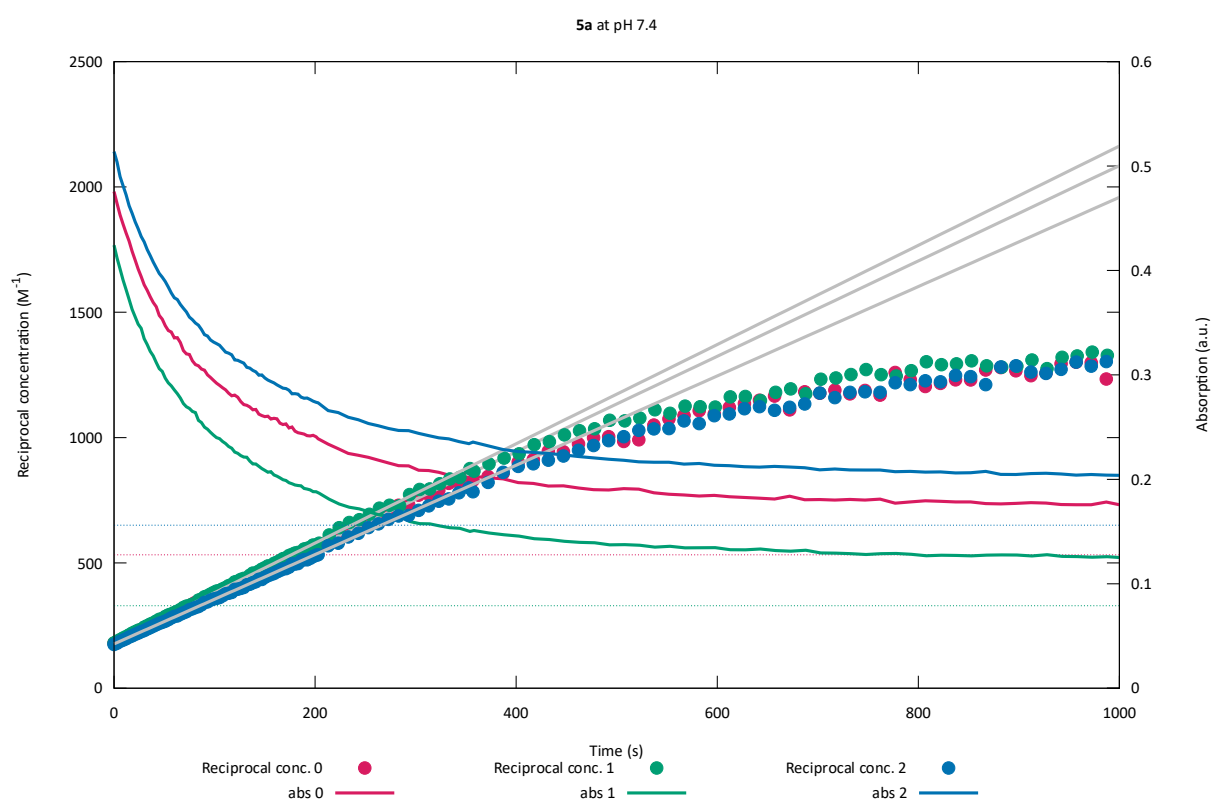
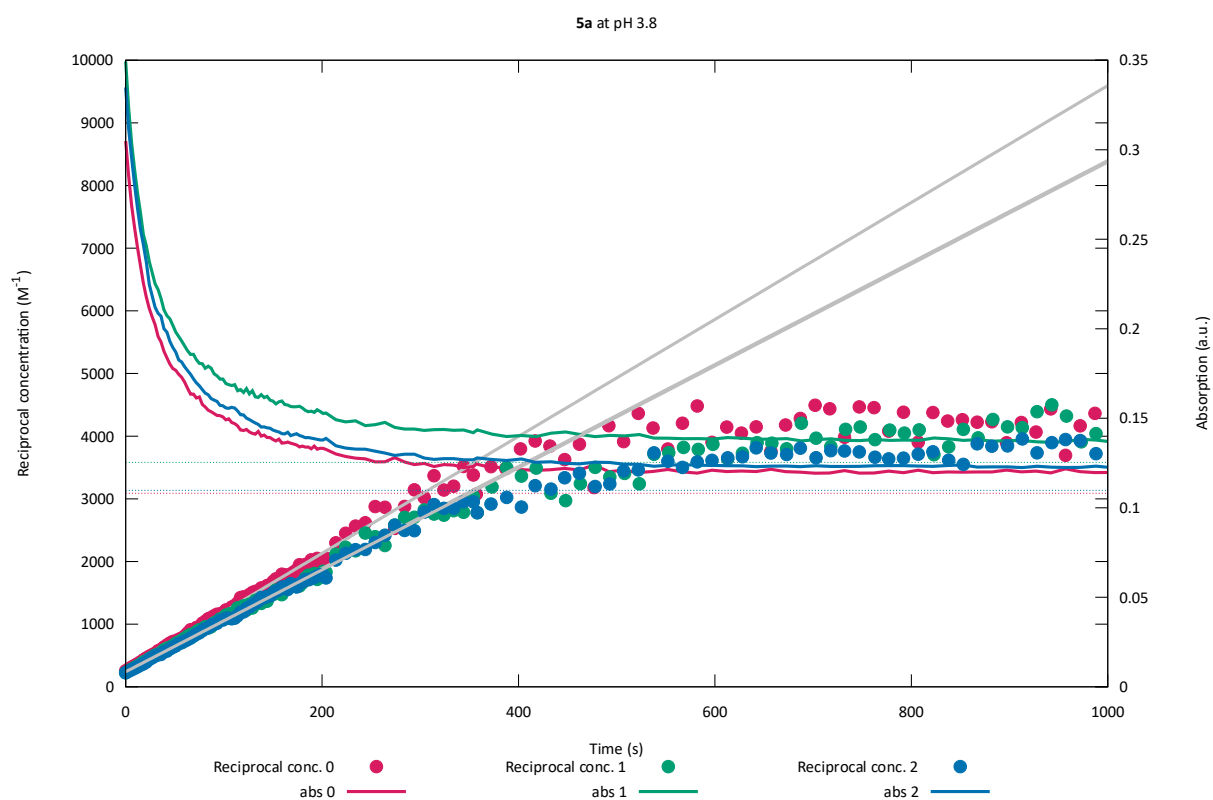


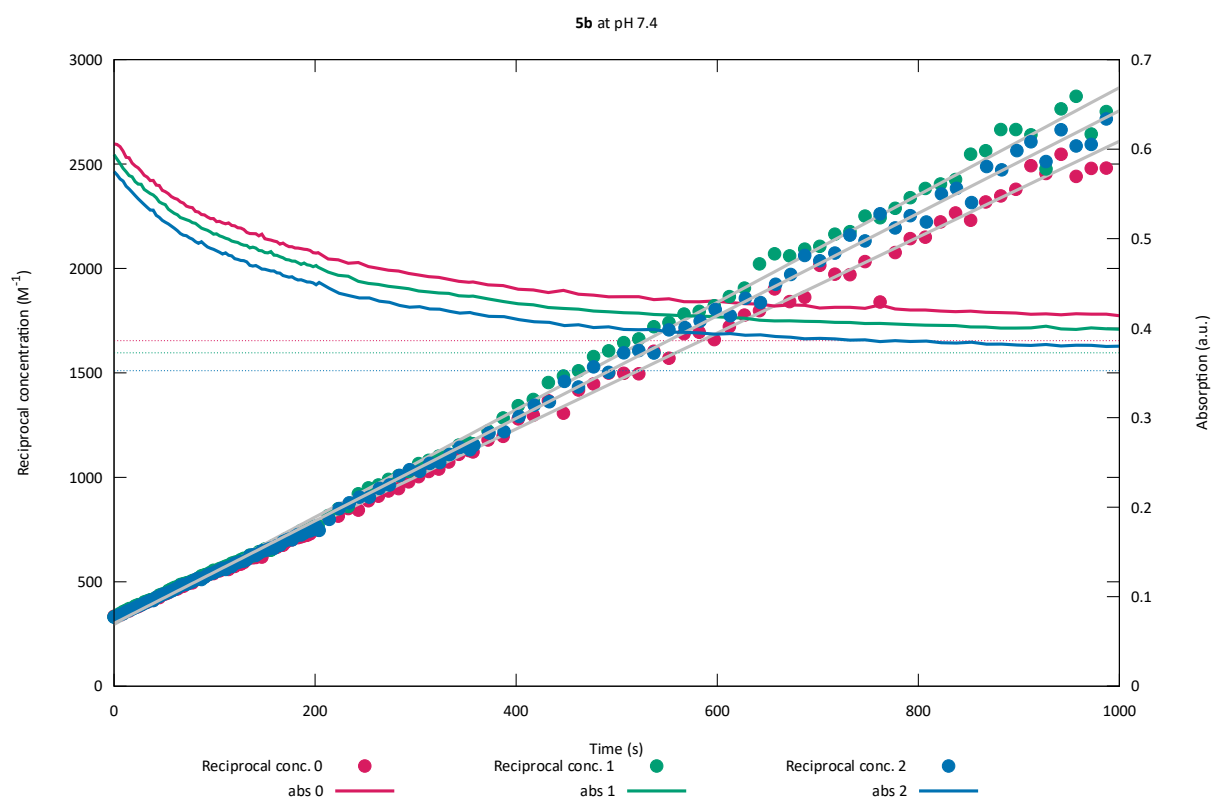
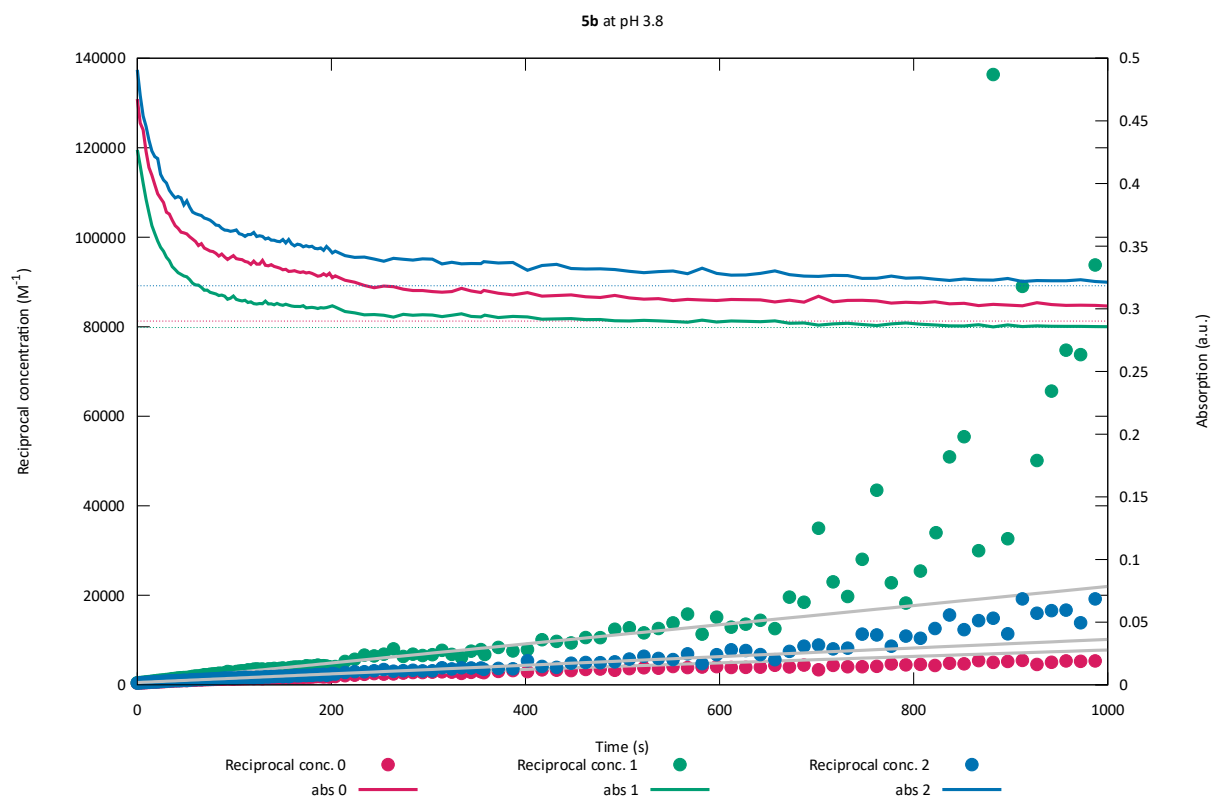












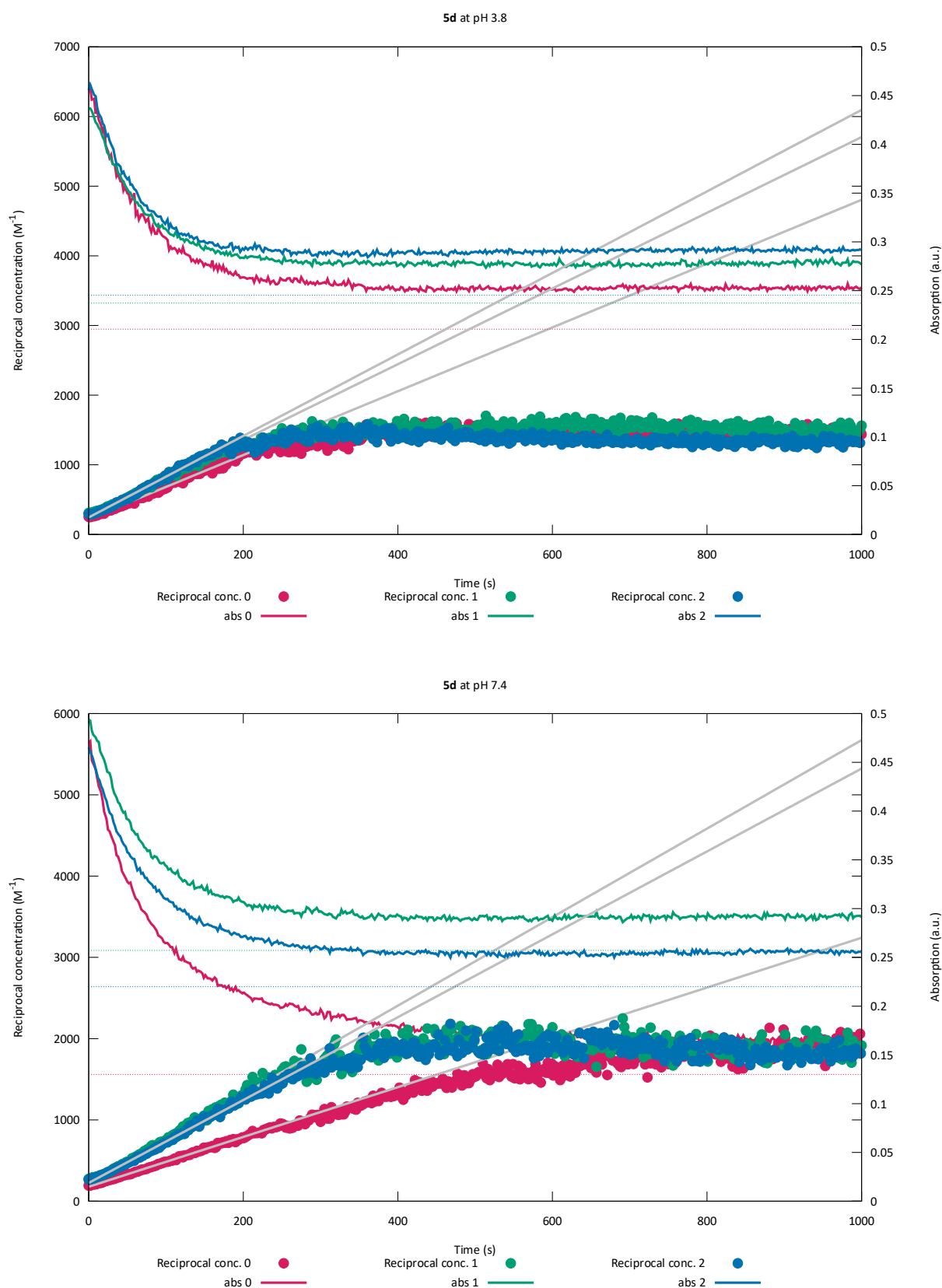


Figure 6. UV time course of KAT ligation and reciprocal concentration plot, and its linear fit used to calculate the rate constants. The colors red, green and blue denote the 1st, 2nd and 3rd triplicate of the same reaction.

Buffer Preparation

Potassium phosphate buffer : acetonitrile (1:1 v/v)

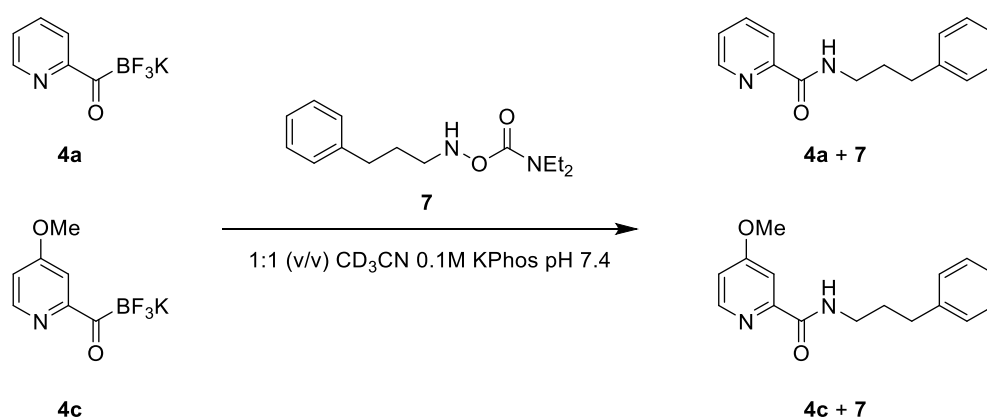
250 mM stock solutions of KH_2PO_4 (**A**) and K_2HPO_4 (**B**) were prepared. 16 mL of **A** and 64 mL of **B** were mixed in a Schott flask. 100 mL of CH_3CN (HPLC grade) was added to the flask and the pH was adjusted with HCl (2 M) or KOH (2 M) to 7.4 using a HI2210 pH Meter. The Schott flask was filled up to 200 mL with Millipore water.

Potassium acetate buffer : acetonitrile (1:1 v/v)

250 mM stock solutions of acetic acid (**C**) and potassium acetate (**D**) were prepared. 70.4 mL of **C** and 9.6 mL of **D** were mixed in a Schott flask. 100 mL of CH_3CN (HPLC grade) was added to the flask and the pH was adjusted with HCl (2 M) or KOH (2 M) to 3.8 using a HI2210 pH Meter. The Schott flask was filled up to 200 mL with Millipore water.

NMR Competition Experiments

To investigate the relative ligation rates of different substituted pyridine KATs (**4a-c**), and unsubstituted aryl KATs (**3a**, **4a**, and **5a**) at pH 7.4, pairwise competition ligation experiments were performed. NMR samples containing two KATs in CD₃CN-pH 7.4 potassium phosphate buffer (1:1 v/v) were prepared so that both KATs were roughly 10 mM in concentration. The precise concentrations were determined against the pre-quantified residual proton signal of CHD₂CN as an internal standard (vide infra). Relative to total amount of KATs, 0.2 equivalences of hydroxylamine **7** were added as a solution in CD₃CN (73.7 mM) and the mixture was thoroughly mixed. After around 40000 s, the concentration of two KATs and two ligation products were determined with ¹H NMR by the integration of the 3-H proton peak on the pyridyl ring.



Scheme 1. Example of a competition ligation experiment, between **4a** and **4c**.

Calibration of solvent residual proton peak as concentration internal standard

Solutions of 26.42 mM, 20.12 mM and 9.49 mM mesitylene in CD₃CN (determined by gravimetric measurements) were prepared from the same bottle of CD₃CN which was used throughout the competition study. ¹H-NMR spectra of the solutions were measured and the integration values of the aryl proton were set to 79.26 (3 x 26.42 mM), 60.36 (3 x 20.12 mM) and 28.46 (3 x 9.49 mM), respectively. The integration values of the pentet at δ 1.94 ppm will then correspond to the mM concentration of residual monoprotinated solvent, CHCD₂CN. These integration values from the three samples were 62.51, 62.69 and 62.57 respectively, giving an average of 62.59 and sample standard deviation of 0.0917. In the

following NMR samples prepared from this bottle of CD₃CN, the concentration of chemically distinct protons can then be determined by setting the CHD₂CN pentet peak area to 62.59. For CD₃CN-aqueous buffer solutions with 1:1 v/v ratio, the CHD₂CN pentet peak areas were set to 31.30 (62.59 x 0.5) instead.

Phasing and backgrounding

Manual phasing and multipoint background correction through cubic spline fitting of the chosen points with no target signal (CHD₂CN and KAT pyridyls) were performed to reduce the influence of the huge H₂O peak at δ 4.23 ppm. Normal aqueous buffer was preferred over deuterated buffer to avoid the complication from pH/pD discrepancy.

Competition results

Concentration of ligation products (e.g. **7** + **4a**) were plotted below and compared with modeling results (see next section):

		7	4a	4c
4a vs 4c	Initial concentration	3.68	11.7	9.43
			7+4a	7+4c
	Final concentration	N.D.	1.17	2.48
	Model prediction		0.82	2.86
		7	4a	4b
4a vs 4b	Initial concentration	4.49	11.96	10.5
			7+4b	7+4b
	Final concentration		1.92	2.71
	Model prediction		1.50	2.99
		7	4b	4c
4b vs 4c	Initial concentration	4.1	7.0	7.84
			7+4b	7+4c
	Final concentration		1.45	2.9
	Model prediction		1.36	2.74

Table 2. Competition results across **4a**, **4b**, and **4c** with comparison to model prediction. All concentration values are in mM. A clear trend can be seen that $k_{rel}(\mathbf{4c}) > k_{rel}(\mathbf{4b}) > k_{rel}(\mathbf{4c})$.

		7	3a	4a
3a vs 4a	Initial concentration	4.44	10.58	11.07
			7+3a	7+4a
	Final concentration	N.D.	1.74	2.71
	Model prediction		1.1	3.4
		7	3a	5a
3a vs 5a	Initial concentration	4.25	10.11	9.95
			7+3a	7+5a
	Final concentration		N.D.	4.10
	Model prediction		0	4.22
		7	4a	5a
4a vs 5a	Initial concentration	4.11	9.71	9.69
			7+4a	7+5a
	Final concentration		N.D.	4.05
	Model prediction		0	4.03

Table 3. Competition results across **3a**, **4a**, and **5a** with comparison to model prediction.

Reaction outcome and model prediction

The outcome of competing ligation between two KATs (termed “KAT a” and “KAT b”) and a hydroxylamine (“HA”) to form two products (“Amide a” and “Amide b”) can be described by the following system of differential equations and boundary conditions:

$$\begin{aligned}
 -[KAT a]' &= [Amide a]' = k_a [KAT a][HA] \\
 -[KAT b]' &= [Amide b]' = k_b [KAT b][HA] \\
 [HA]' &= [KAT a]' + [KAT b]' \\
 [HA]_0, [KAT a]_0, [KAT b]_0 &: \text{obtained from NMR measurement,} \\
 [Amide a]_0 &= [Amide b]_0 = 0
 \end{aligned}$$

Which was solved numerically with Mathematica using the DSolve function over 0~40000 s.

The modeling results were plotted below:

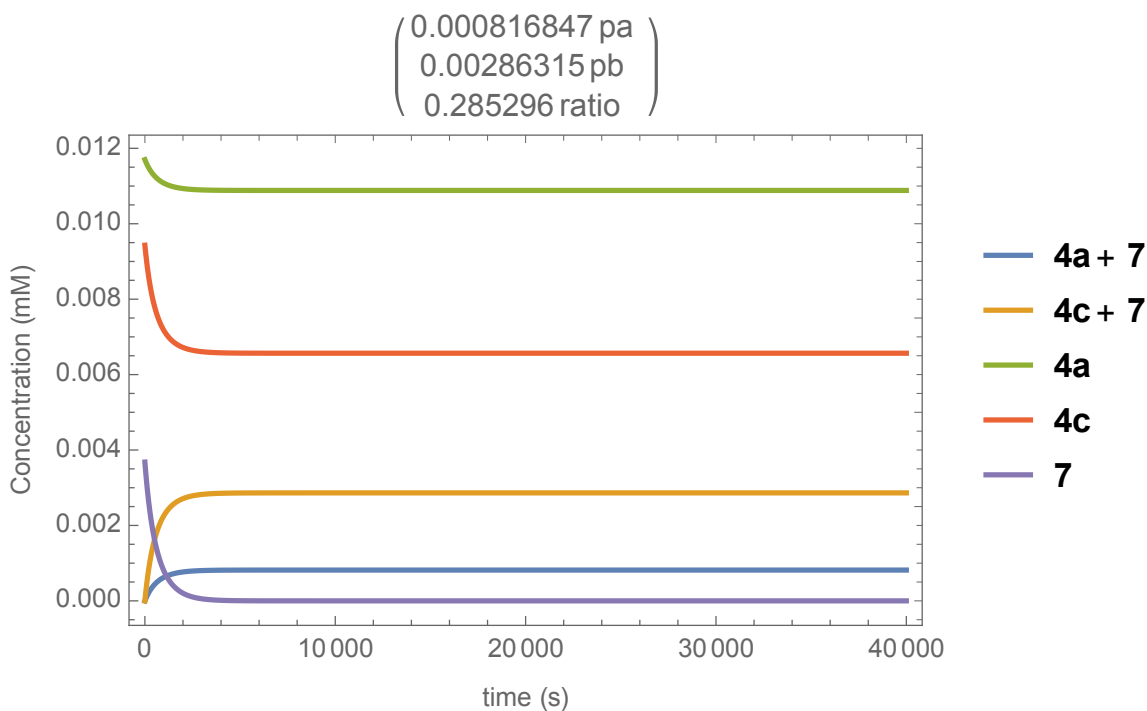


Figure 7. Modelling result for competition of **4a** vs **4c**.

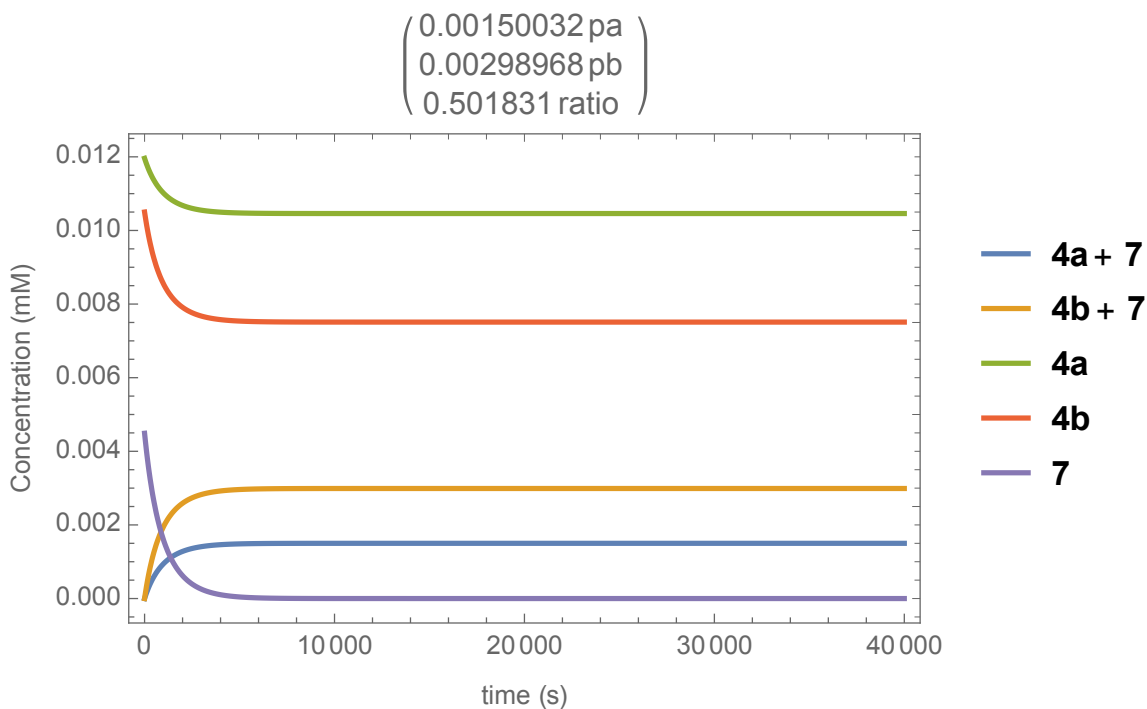


Figure 8. Modelling result for competition of **4a** vs **4b**.

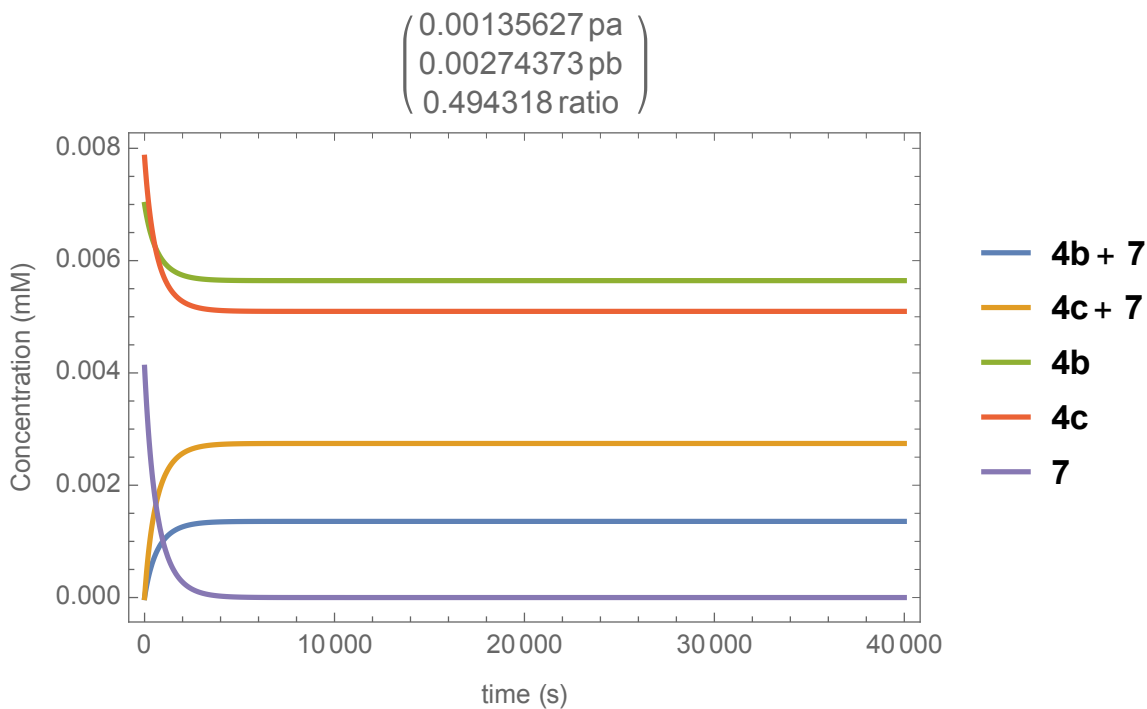


Figure 9. Modelling result for competition of **4b** vs **4c**.

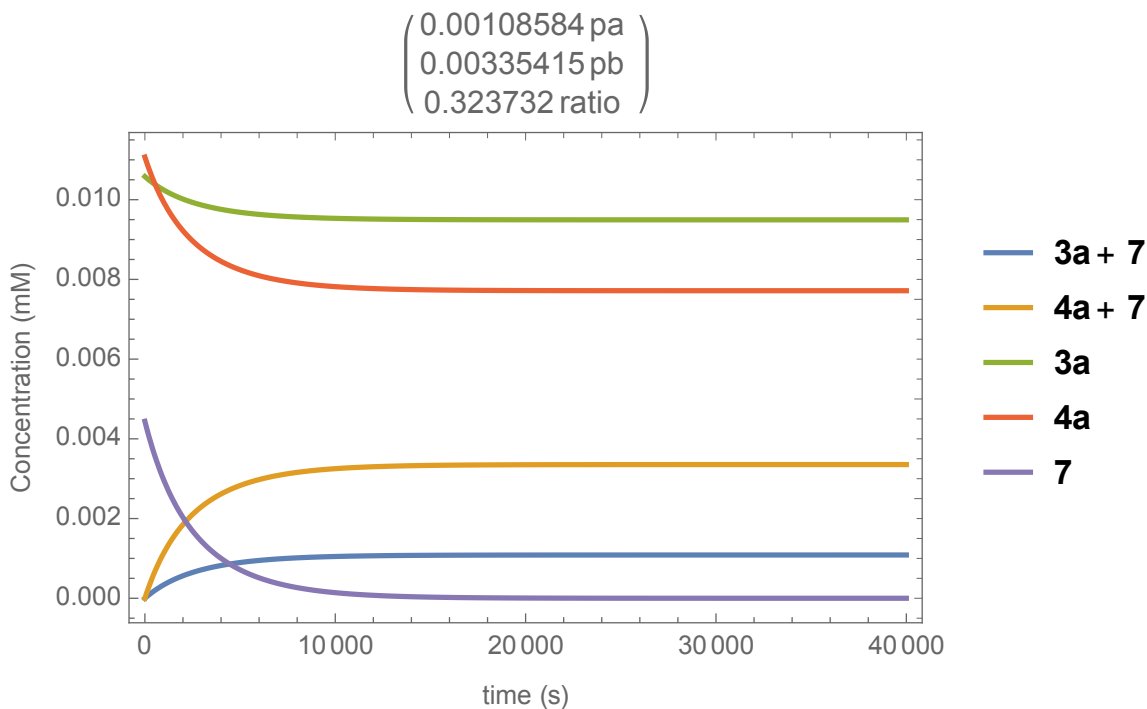


Figure 10. Modelling result for competition of **3a** vs **4a**.

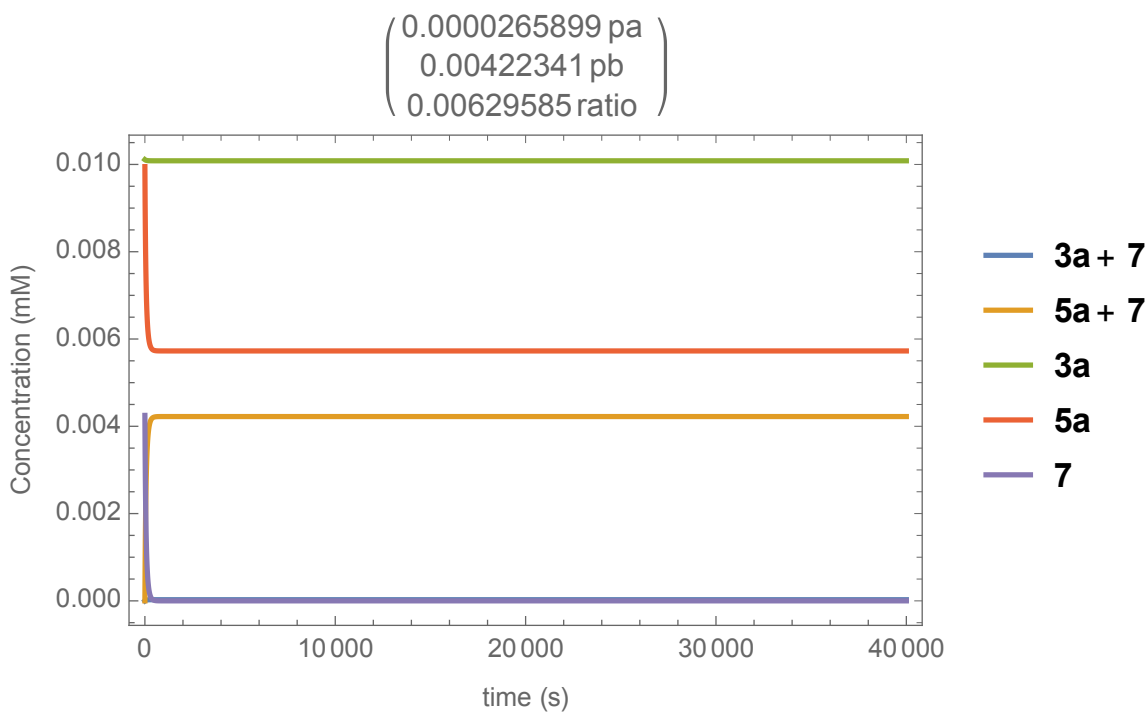


Figure 11. Modelling result for competition of **3a** vs **5a**.

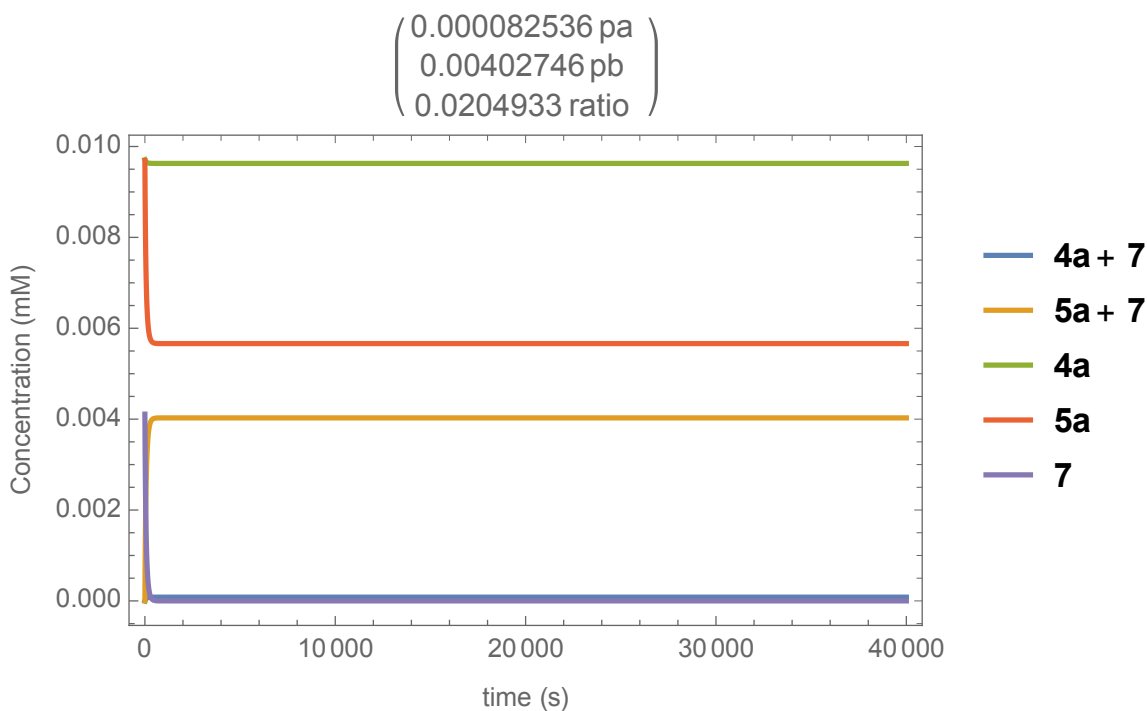


Figure 12. Modelling result for competition of **4a** vs **5a**.

X-ray - Crystallographic Data

Experimental

All crystals were measured on either a XtaLAB Synergy, Dualflex, Pilatus 300K diffractometer or on a Bruker APEX-II Duo (Mo) diffractometer. The crystals were kept at 100.0 K during data collection. Using Olex2⁵, the structure was solved with the SHELXT⁶ structure solution program using Intrinsic Phasing and refined with the SHELXL⁷ refinement package using Least Squares minimization. All crystals were grown from potassium phosphate buffer:CH₃CN (1:1 v/v, pH 7.4) at 4°C.

Crystal data for 4b

CCDC Deposition Number: 2077022

Crystal Data for C₆H₃BClF₃KNO (*M* = 247.45 g/mol): monoclinic, space group C2/c, *a* = 34.02(3) Å, *b* = 7.073(7) Å, *c* = 7.323(7) Å, β = 90.209(15)°, *V* = 1762(3) Å³, *Z* = 8, *T* = 100.0(1) K, μ (MoK α) = 0.913 mm⁻¹, *D*_{calc} = 1.866 g/cm³, 7115 reflections measured (4.79° ≤ 2 θ ≤ 55.108°), 2029 unique (*R*_{int} = 0.0999, *R*_{sigma} = 0.0931) which were used in all calculations. The final *R*₁ was 0.0545 (*I* > 2 σ (*I*)) and *wR*₂ was 0.1268 (all data).

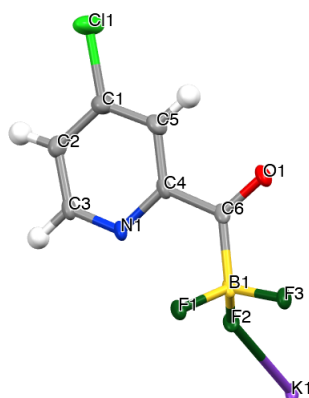


Figure 13. Asymmetric unit of the crystal structure **4b**.

⁵ Dolomanov, O. V.; Bourhis, L. J.; Gildea, R. J.; Howard, J. A. K.; Puschmann, H., OLEX2: a complete structure solution, refinement and analysis program. *Journal of Applied Crystallography* **2009**, *42* (2), 339-341.

⁶ Sheldrick, G., SHELXT - Integrated space-group and crystal-structure determination. *Acta Crystallographica Section A* **2015**, *71* (1), 3-8.

⁷ Sheldrick, G., Crystal structure refinement with SHELXL. *Acta Crystallographica Section C* **2015**, *71* (1), 3-8.

Crystal data for 4c

CCDC Deposition Number: 2077021

Crystal Data for $C_7H_6BF_3KNO_2$ ($M=243.04$ g/mol): monoclinic, space group $P2_1/c$, $a = 17.517(13)$ Å, $b = 6.924(5)$ Å, $c = 7.458(6)$ Å, $\beta = 97.957(16)^\circ$, $V = 895.9(11)$ Å³, $Z = 4$, $T = 100.0(1)$ K, $\mu(\text{MoK}\alpha) = 0.616$ mm⁻¹, $D_{\text{calc}} = 1.802$ g/cm³, 7041 reflections measured ($4.696^\circ \leq 2\theta \leq 55.078^\circ$), 2053 unique ($R_{\text{int}} = 0.0969$, $R_{\text{sigma}} = 0.1060$) which were used in all calculations. The final R_1 was 0.0565 ($I > 2\sigma(I)$) and wR_2 was 0.1284 (all data).

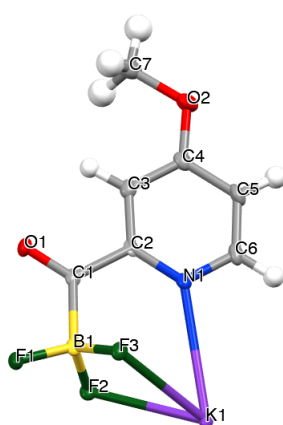


Figure 14. Asymmetric unit of the crystal structure **4c**.

Crystal data for 5a

CCDC Deposition Number: 2077023

Crystal Data for $C_{10}H_7BF_3NO$ ($M=224.98$ g/mol): monoclinic, space group $P2_1/c$, $a = 8.8884(2)$ Å, $b = 5.65110(10)$ Å, $c = 18.6358(4)$ Å, $\beta = 101.702(2)^\circ$, $V = 916.61(3)$ Å³, $Z = 4$, $T = 100.0(1)$ K, $\mu(\text{Cu K}\alpha) = 1.273$ mm⁻¹, $D_{\text{calc}} = 1.630$ g/cm³, 7772 reflections measured ($9.694^\circ \leq 2\theta \leq 159.614^\circ$), 1929 unique ($R_{\text{int}} = 0.0327$, $R_{\text{sigma}} = 0.0280$) which were used in all calculations. The final R_1 was 0.0338 ($I > 2\sigma(I)$) and wR_2 was 0.0931 (all data).

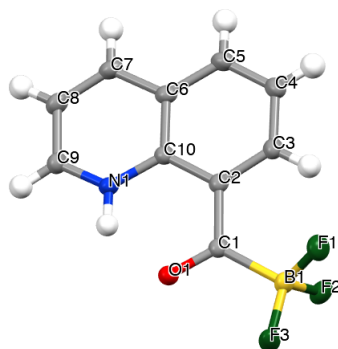


Figure 15. Asymmetric unit of the crystal structure **5a**.

Crystal data for 5b

CCDC Deposition Number: 2077024

Crystal Data for $C_{10}H_5BClF_3KNO$ ($M = 297.51$ g/mol): monoclinic, space group $P2_1/c$, $a = 18.2357(4)$ Å, $b = 7.2075(2)$ Å, $c = 8.4490(2)$ Å, $\beta = 90.372(2)^\circ$, $V = 1110.46(5)$ Å³, $Z = 4$, $T = 100.0(1)$ K, $\mu(\text{Cu K}\alpha) = 6.684$ mm⁻¹, $D_{\text{calc}} = 1.780$ g/cm³, 26706 reflections measured ($4.846^\circ \leq 2\theta \leq 159.8^\circ$), 2406 unique ($R_{\text{int}} = 0.0698$, $R_{\text{sigma}} = 0.0282$) which were used in all calculations. The final R_1 was 0.0875 ($I > 2\sigma(I)$) and wR_2 was 0.2575 (all data).

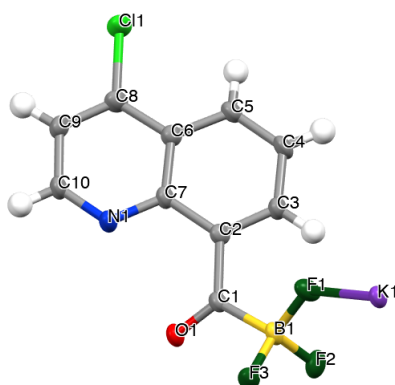


Figure 16. Asymmetric unit of the crystal structure **5b**.

Crystal data for 5d

CCDC Deposition Number: 2077025

Crystal Data for $C_{13}H_{13}BF_3NO_3$ ($M=299.05$ g/mol): triclinic, space group P-1, $a = 7.6684(2)$ Å, $b = 9.2792(2)$ Å, $c = 18.6002(6)$ Å, $\alpha = 85.335(2)$, $\beta = 87.229(2)^\circ$, $\gamma = 84.797(2)$, $V = 1312.62(6)$ Å³, $Z = 4$, $T = 100.0(1)$ K, $\mu(\text{Cu K}\alpha) = 1.157$ mm⁻¹, $D_{\text{calc}} = 1.513$ g/cm³, 6292 reflections measured ($4.77^\circ \leq 2\theta \leq 159.746^\circ$), 6292 unique ($R_{\text{int}} = 0.0310$, $R_{\text{sigma}} = 0.0229$) which were used in all calculations. The final R_1 was 0.0740 ($I > 2\sigma(I)$) and wR_2 was 0.2352 (all data).

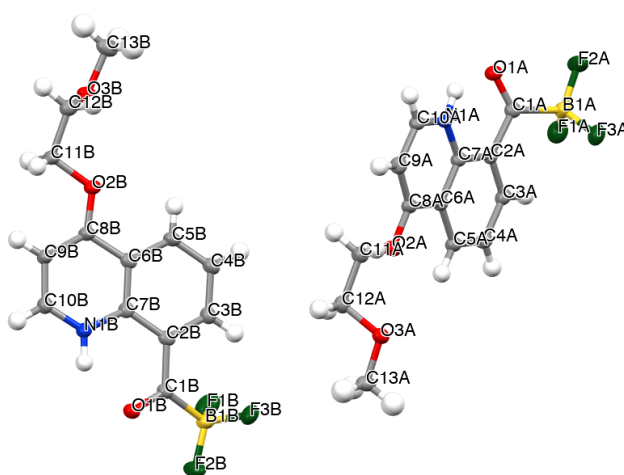
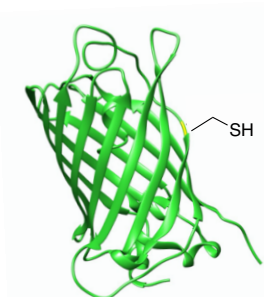


Figure 17. Asymmetric unit of the crystal structure **5d**.

Protein Experiments

Expression and purification of sfGFP(S147C)



The pET28b plasmid encoding for sfGFP-S147C with a C-terminal His6-tag (GSSHHHHHSSGAENLYFQG, first Met processed during expression) was kindly provided by Raphael Hofmann (ETH Zurich). The His6-tagged sfGFP-S147C was expressed in *E. coli* according to previous reports with slight modifications.⁸ Chemically competent BL21 (DE3) cells were heat-shock transformed with the plasmids and used to inoculate overnight precultures in lysogeny broth (LB) Miller medium containing 50 $\mu\text{g/mL}$ Kanamycin. 5 mL of the preculture was diluted 1:100 with fresh selective LB miller medium. After the culture has reached approximately an OD_{600} of 0.6 protein expression was induced by adding isopropyl β -D-1-thiogalactopyranoside (IPTG) to a final concentration of 0.5 mM. Following protein expression at 18 $^{\circ}\text{C}$ and 120 rpm for 18h, cells were harvested by centrifugation (5,000 \times g, 30 min, 4 $^{\circ}\text{C}$). After removing the supernatant the cell pellet was resuspended in 10 mL binding buffer (20 mM HEPES, 350 mM NaCl, 20 mM imidazole, pH 7.4) and stored at -80 $^{\circ}\text{C}$ until purification. The cell suspension was thawed at rt, placed on ice and treated with a spatula tip of lysozyme and DNase I and nutated at 4 $^{\circ}\text{C}$ for 1 h. The cells were lysed by sonication (4 \times 1 min) at 0 $^{\circ}\text{C}$ and the lysate was centrifuged (12,000 \times g, 30 min, 4 $^{\circ}\text{C}$) and filtered (0.2 μm). According to the manufacturer's protocol, the supernatant was purified by Ni^{II}-NTA affinity purification at 4 $^{\circ}\text{C}$ using binding buffer and the protein was eluted using the same buffer containing 400 mM imidazole instead. The protein was collected and dialyzed against 20 mM Tris HCl, 1 mM DTT (pH 7.4) and purified at 4 $^{\circ}\text{C}$ on ion exchange Mono Q 5/50 GL column with buffer A (25 mM Tris-HCl pH 8.5) and a gradient of buffer B (buffer A with 1 M NaCl). sfGFP was obtained in >95% purity (SDS-PAGE) with an yield of 104 mg/1.0 L culture.

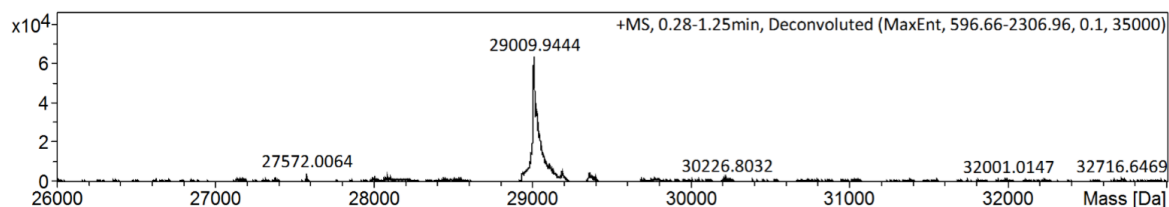
Prior to **ESI-MS** determination, the protein was desalted using a PD MiniTrap (GE Healthcare) eluting with MilliQ water containing 0.1% formic acid.

⁸ Pédelacq, J.-D.; Cabantous, S.; Tran, T.; Terwilliger, T. C.; Waldo, G. S., Engineering and characterization of a superfolder green fluorescent protein. *Nature Biotechnology* **2006**, *24* (1), 79-88.

ESI-MS:

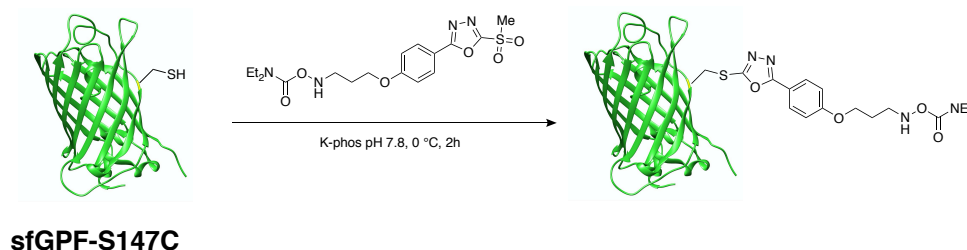
Calculated mass: 29009.4163 Da (-20.03 Da for GFP chromophore formation)

Observed mass: 29009.9444 Da

**Figure 18.** Deconvoluted mass spectrum (ESI) of sfGFP(S147C).

Protein sequence (His6-tag underlined, first Met processed during expression):

GSSHHHHHSSGAENLYFQMRKGEELFTGVVPIVLVDGDVNGHKFSVRGEGEGDATNGKLTCLKF
 ICTTGKLPVPWPTLVTTLTYGVCFARYPDHMKQHDFFKSAMPEGYVQERTISFKDDGTYKTRAEV
 KFEGDTLVNRIELKGI~~DF~~KEDGNILGHKLEYNFNCHNVYITADKQKNGIKANFKIRHNVEDGSQL
 ADHYQQNTPIGDGPVLLPDNHYLSTQSVLSKDPNEKRDHMLLEFVTAAGITHGMDELYK*

sfGFP(S147C)-hydroxylamine bioconjugate

The synthesis of sfGFP-S147C-hydroxylamine was performed according to a procedure previously reported in literature.⁹ An aliquot of sfGFP-S147C (1mL, 70 μ M, 1.0 equiv) was supplemented with 500 equiv of DTT (0.5 M in MilliQ H₂O), inverted and incubated for 1h at rt. DTT was removed through repetitive (5x) spin diafiltration (Amicon® Ultra – 4, 10 kDa MWCO) with degassed potassium phosphate buffer (0.1M, 1 mM EDTA, pH 7.8) at 4 °C. The reduced sfGFP-S147C was further added to a solution of hydroxylamine **x** (10 mM in DMF, 138 μ l, 10.0 equiv), inverted and incubated for 2 h on ice. Excess hydroxylamine was

⁹ White, C. J.; Bode, J. W., PEGylation and Dimerization of Expressed Proteins under Near Equimolar Conditions with Potassium 2-Pyridyl Acyltrifluoroborates. *ACS Central Science* **2018**, 4 (2), 197-206.

removed through a PD MidiTrap G-25 desalting column (GE Healthcare) and eluted in MilliQ water containing 0.1% formic acid for mass analysis.

ESI-MS:

Calculated mass: 29342.0653 Da (-20.03 Da for GFP chromophore formation)

Observed mass: 29342.2650 Da

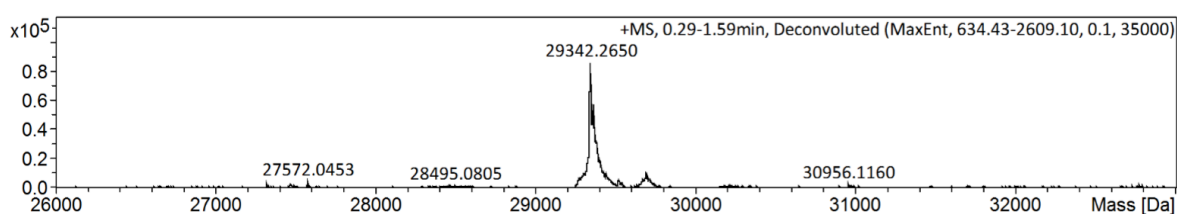
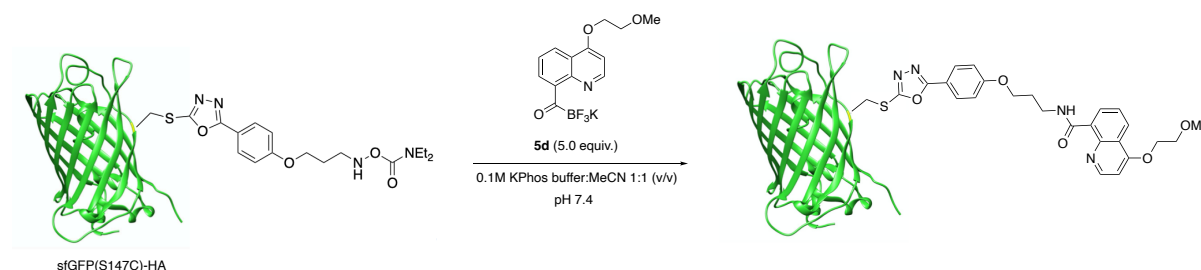


Figure 19. Deconvoluted mass spectrum (ESI) of sfGFP-S147C-hydroxylamine bioconjugate.

KAT ligation with sfGFP(S147C)-hydroxylamine bioconjugate 9

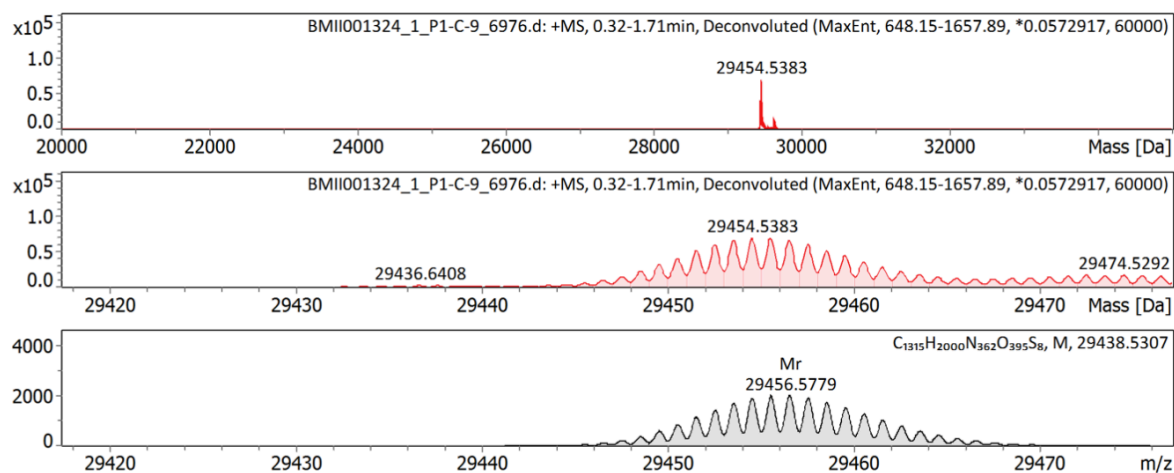


An aliquot of sfGFP(S147C)-hydroxylamine bioconjugate (1.0 mL, 70 μ M, 1.0 equiv) in degassed potassium phosphate buffer (0.1M, 1 mM EDTA, pH 7.8) was passed through a PD midiTrap G-25 desalting column (GE Healthcare) for buffer exchange eluting with potassium phosphate buffer:CH₃CN 1:1 v/v (0.1 M, pH 7.4) and concentrated to 1.0 mL via spin diafiltration (Amicon® Ultra – 4, 10 kDa MWCO). 200 μ L of the resulting sfGFP-hydroxylamine bioconjugate solution (14 nmol) was treated with a solution (7.0 μ L, 10 mM, 5.0 equiv) containing **5d** in the same buffer. The mixture was vortexed and incubated for 90 min at rt. The reaction was passed through a PD MiniTrap G-25 desalting column (GE Healthcare) eluting with MilliQ H₂O. ESI-MS indicated full conversion of sfGFP(S147C)-hydroxylamine conjugate to the ligated amide-bioconjugate.

ESI-MS:

Calculated mass: 29456.5779 Da (-20.03 Da for GFP chromophore formation)

Observed mass: 29454.5383 Da

**Figure 20.** Deconvoluted mass spectrum (ESI) of sfGFP(S147C)-amide-bioconjugate **9**.**Acid-Base titration**

4a or **5a** were dissolved in 1:1 CH₃CN-H₂O (2 mL) to form a solution with concentration approximately 0.02 M. The solution was stirred while HCl (400 μ L, 0.1 M) was added slowly. pH was measured by HANNA HI 2210 pH Meter, and volume of titrant was controlled by a syringe pump. The data was extracted from a video of the titration process. Image frames were captured using ffmpeg, Optical Character Recognition (OCR) were performed with tesseract for the syringe pump screen, and ssocr was used to read the pH meter seven segment display. The temporal resolution of data acquisition was around 1 second. A Ruby script was written to automate the process and is public available at: https://github.com/gnezd/ad_hoc_titrator

The 0.1 M HCl solution was calibrated with K₂CO₃, and the titration results (3 times repetition) were plotted below as pH versus equiv of acid. The pK_a was determined as the pH when 0.5 equiv acid was added.

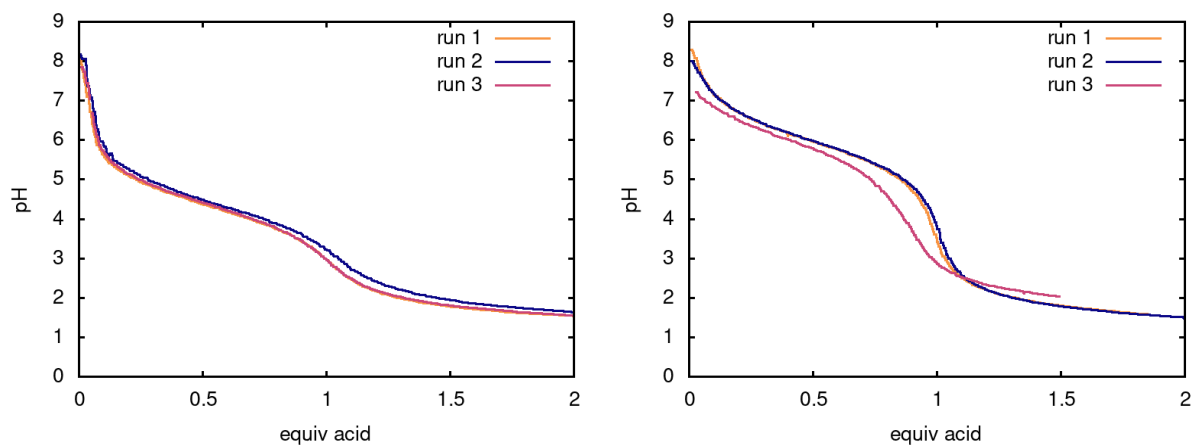


Figure 21. The titration curve of **4a** (left) and **5a** (right).

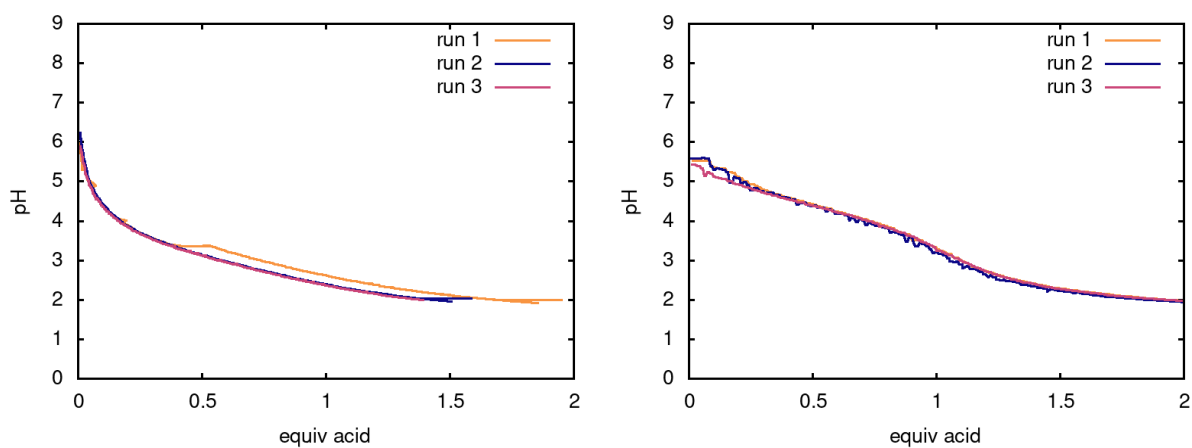


Figure 22. The titration curve of **4b** (left) and **5b** (right).

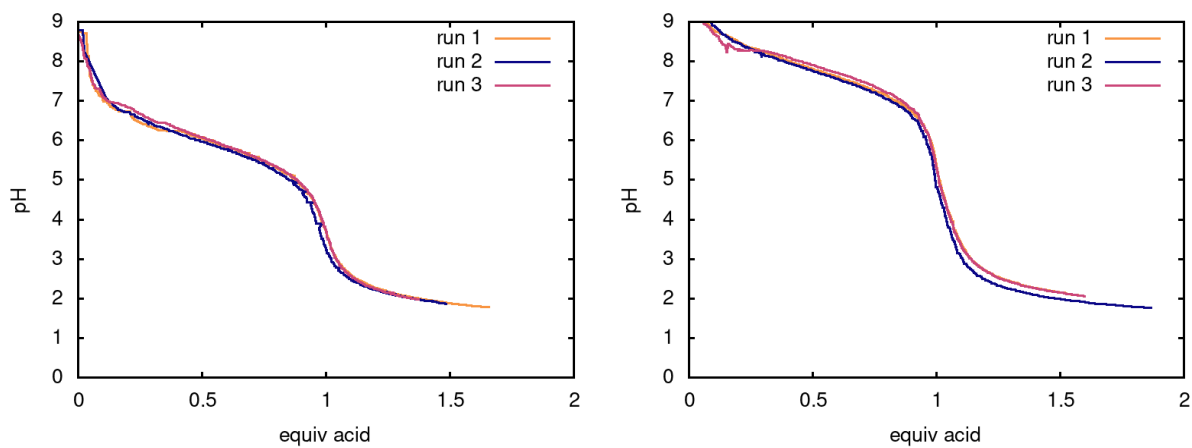
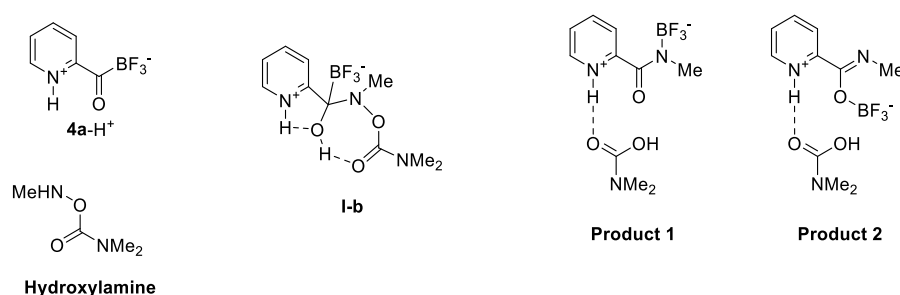


Figure 23. The titration curve of **4c** (left) and **5d** (right).

Computational model

All quantum chemical computations were performed with the ORCA package (version 4.2.1) using the B3LYP functional and a ma-def2-TZVP basis set.^{10,11} Dispersion effect was correct with the D3BJ method. The hydroxylamine *N*-substituent was changed to methyl to reduce computation costs. The transition states were located by performing a Nuged Elastic Band (NEB) computation from the optimized intermediate to optimized postulated products. An example is listed below in **Scheme 2**.



Scheme 2. The computed ligation of **4a** goes through an intermediate and leads to several possible products such as **Product 1** and **Product 2**, with the trifluoroborate group ending up on either the amide nitrogen or the amide oxygen. According to NEB computations, the reaction path leading to a nitrogen-trifluoroborate product gave a lower TS energy in all cases.

The free energy reference point of a reaction path was set at the sum of free energy of the KAT (protonated or non-protonated) and the hydroxylamine (-418.20175074 E_h). The structures of the tetrahedral adducts and their computed free energies were listed below in **Table 4-6**.

¹⁰ Neese, F., The ORCA program system. *WIREs Computational Molecular Science* **2012**, 2 (1), 73-78.

¹¹ Neese, F., Software update: the ORCA program system, version 4.0. *WIREs Computational Molecular Science* **2018**, 8 (1), e1327.

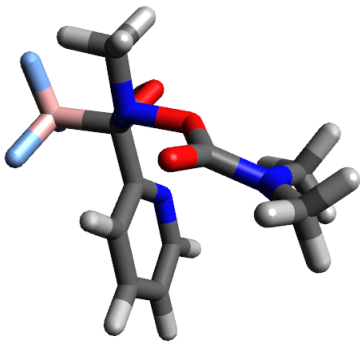
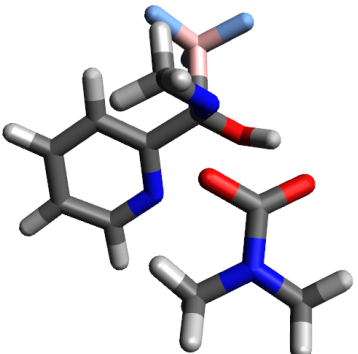
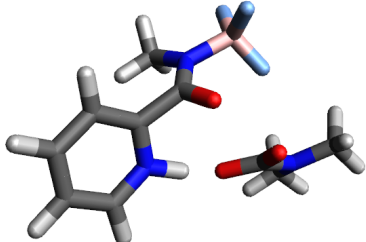
		
I-a -1103.76571266 E _h	TS-a -1103.7369724 E _h Imaginary frequency: -313.95 cm ⁻¹	Product-a -1103.88920661 E _h

Table 4. Intermediate and transition state for unprotonated **4a**. The computed free energy of **4a** was -685.56632577 E_h.

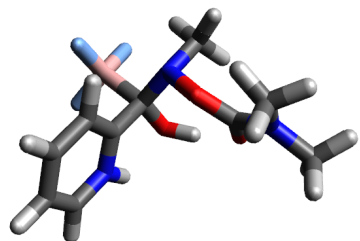
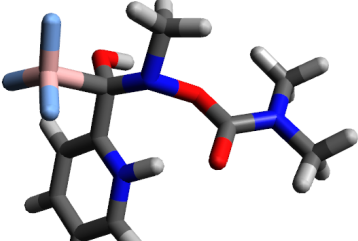
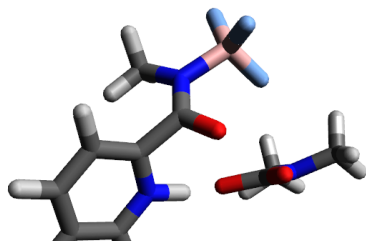
		
I-b -1104.27418833 E _h	TS-b -1103.77823795 E _h Imaginary frequency: -354.01 cm ⁻¹	Product-b -1104.38280409 E _h

Table 5. Intermediate and transition state for protonated **4a**. The computed free energy of **4a+H⁺** was -686.06380338 E_h.

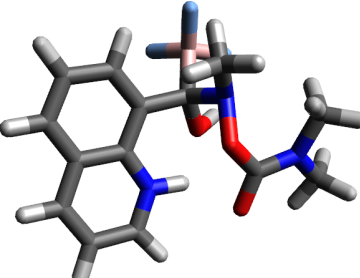
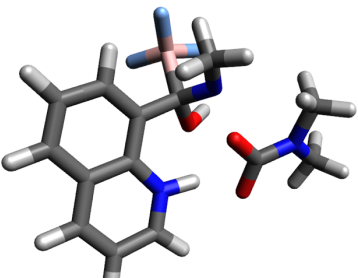
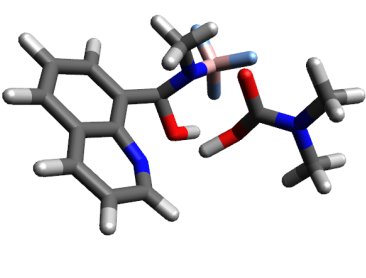
		
I-c -1257.83258157 E _h	TS-c -1257.8281185 E _h Imaginary frequency: -404.48 cm ⁻¹	Product-c -1257.96157213 E _h

Table 6. Intermediate and transition state for protonated **5a**. The computed free energy of **5a+H⁺** was -839.64126448 E_h.

The geometry of all structures can also be found in the supplemented archive file in .xyz format.

Computed reaction coordinate

In reaction coordinate C, where a protonated quinoline KAT underwent nucleophilic addition with a hydroxylamine, a transition state (**TS-add**) was identified in the computations. The relative energies of the transition states suggest that the formation of **TS-c** was the rate-limiting step throughout this reaction course.

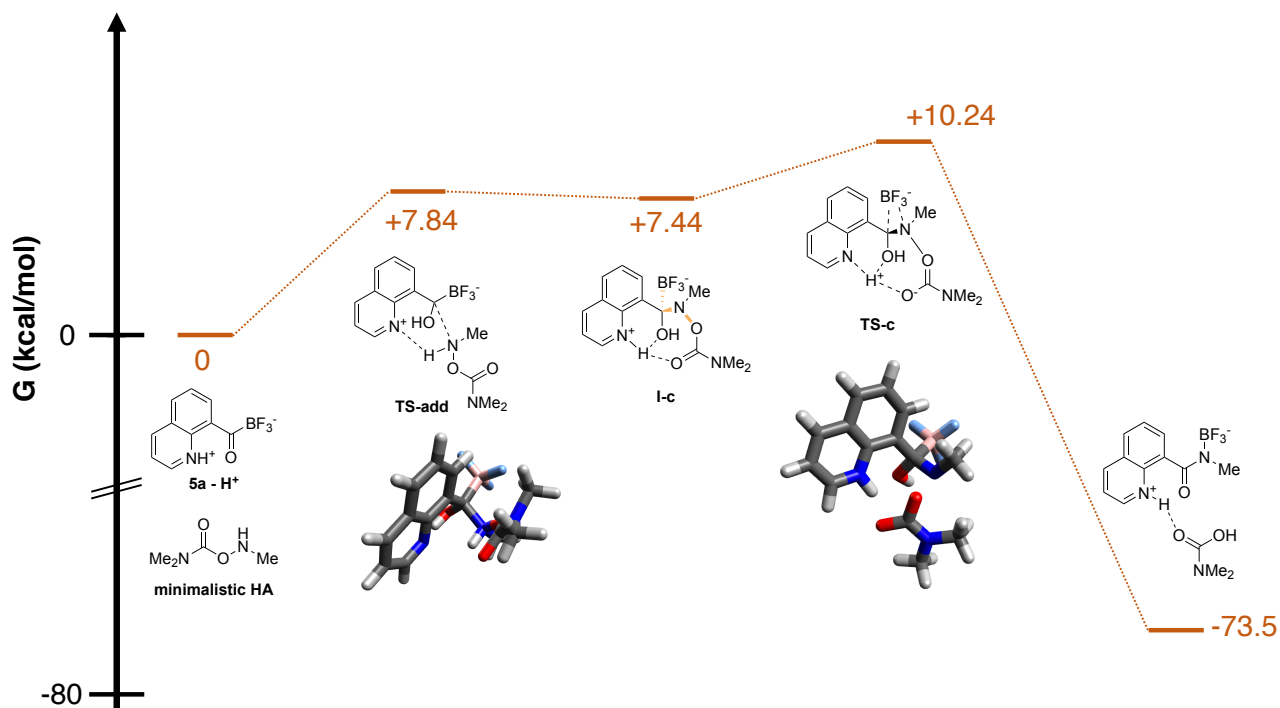


Figure 24. Computed reaction course of protonated KAT **5a** with hydroxylamine. The nucleophilic addition between the hydroxylamine and **5a-H⁺** leads to **TS-add** and then **I-c**, which further undergoes an elimination through **TS-c**, which is the highest transition state across the path. The relevance of **TS-c** in connecting **I-c** and the ligation product was further supported by performing the Intrinsic reaction coordinate (IRC) computation.

Realtime mass spectrometry analysis of the ligation reaction mixture

The ligation reaction mixture of KAT **4a** was analyzed with ESI-MS in situ and the mass corresponding to the borylated amide was found in the negative ion mode as the major peak.

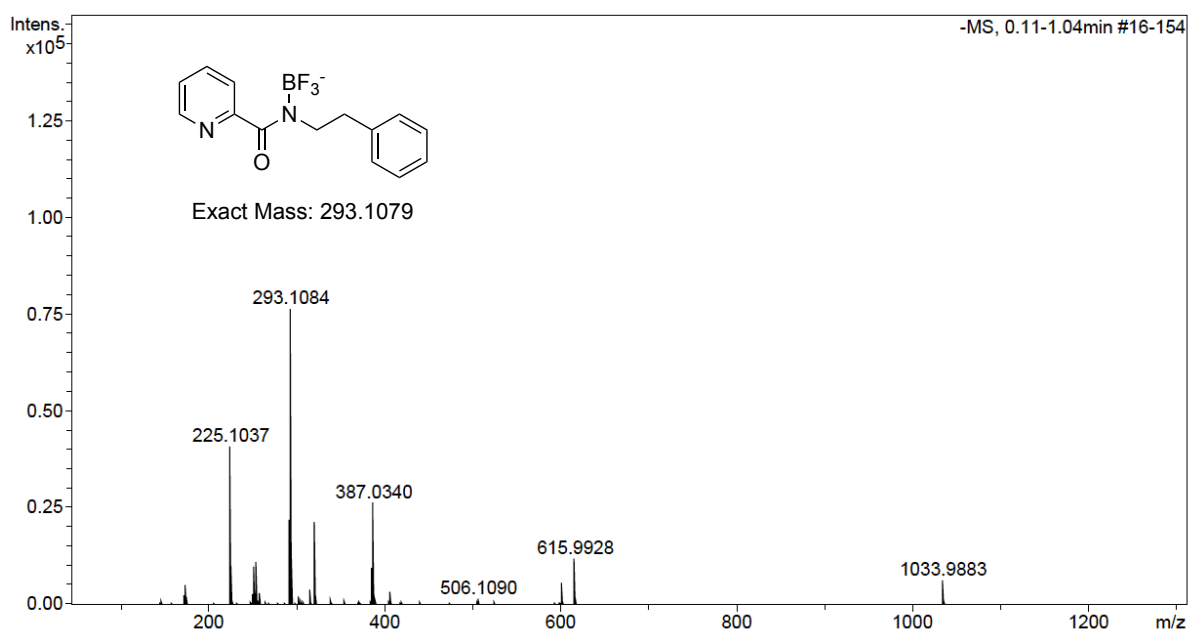
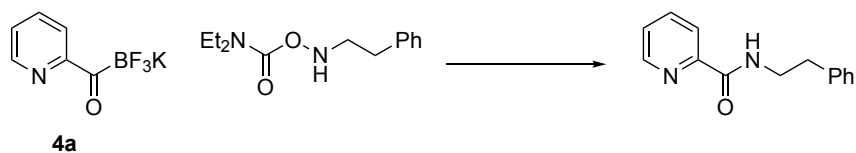
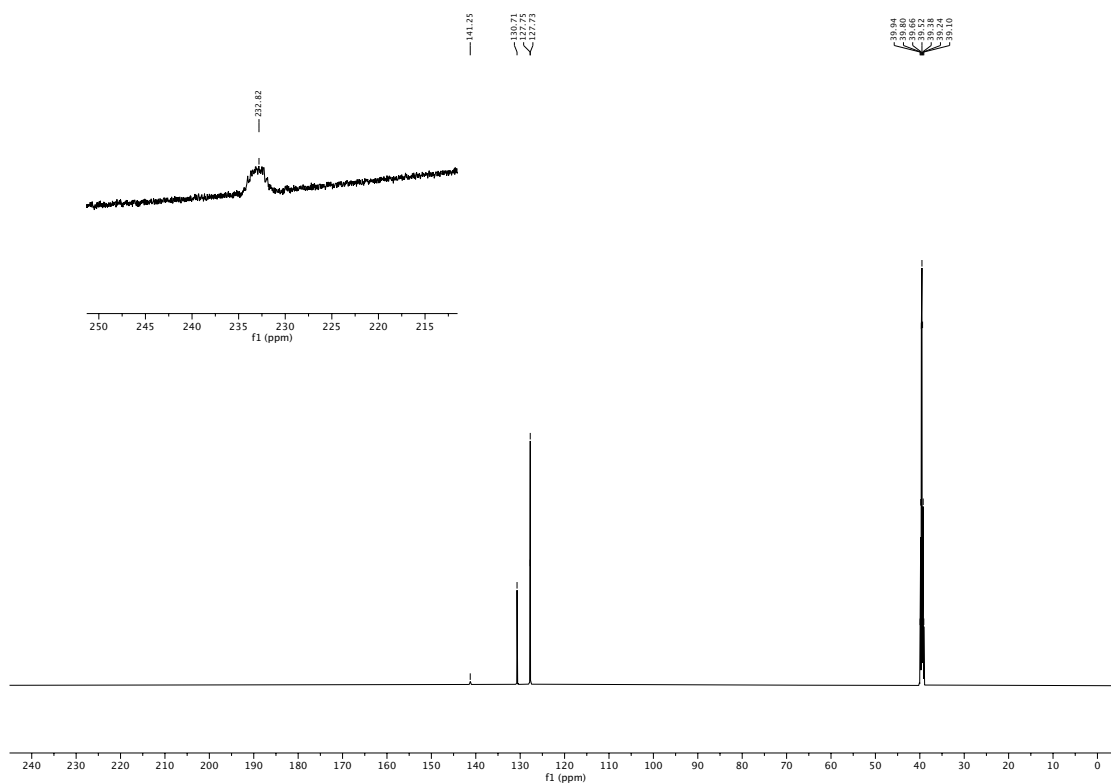
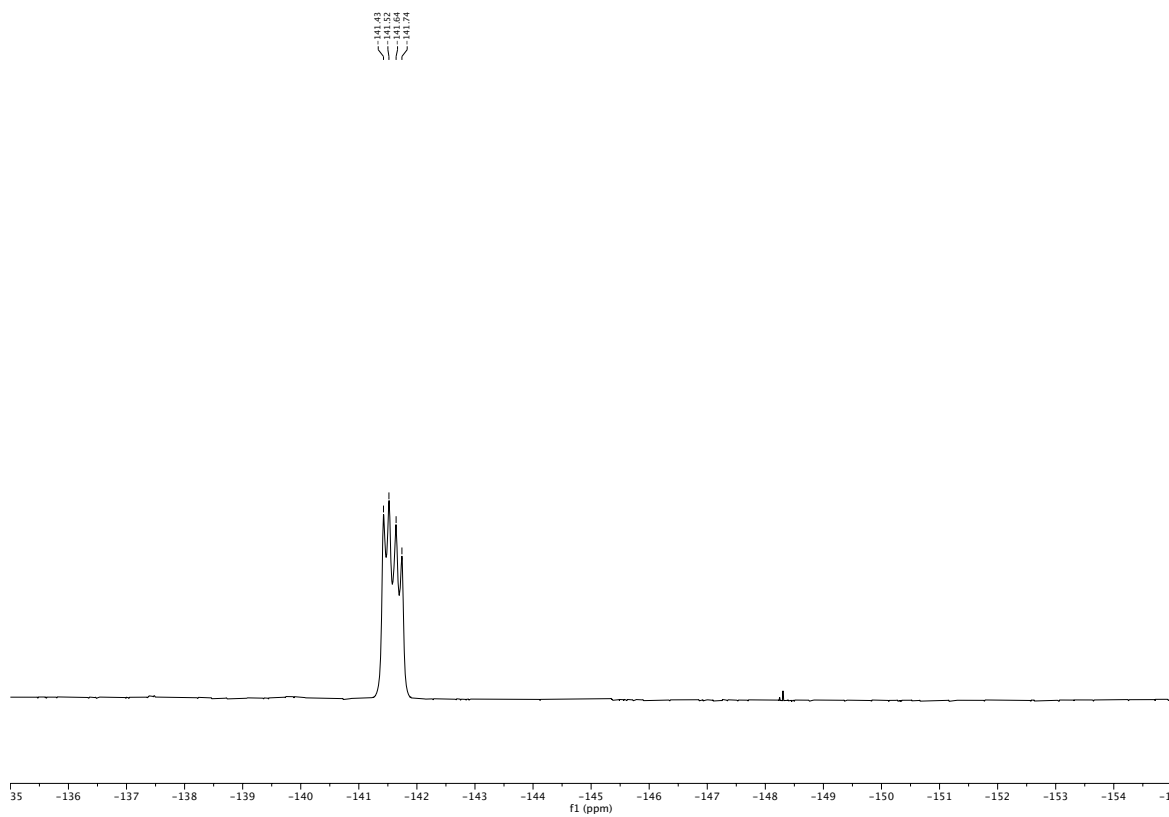
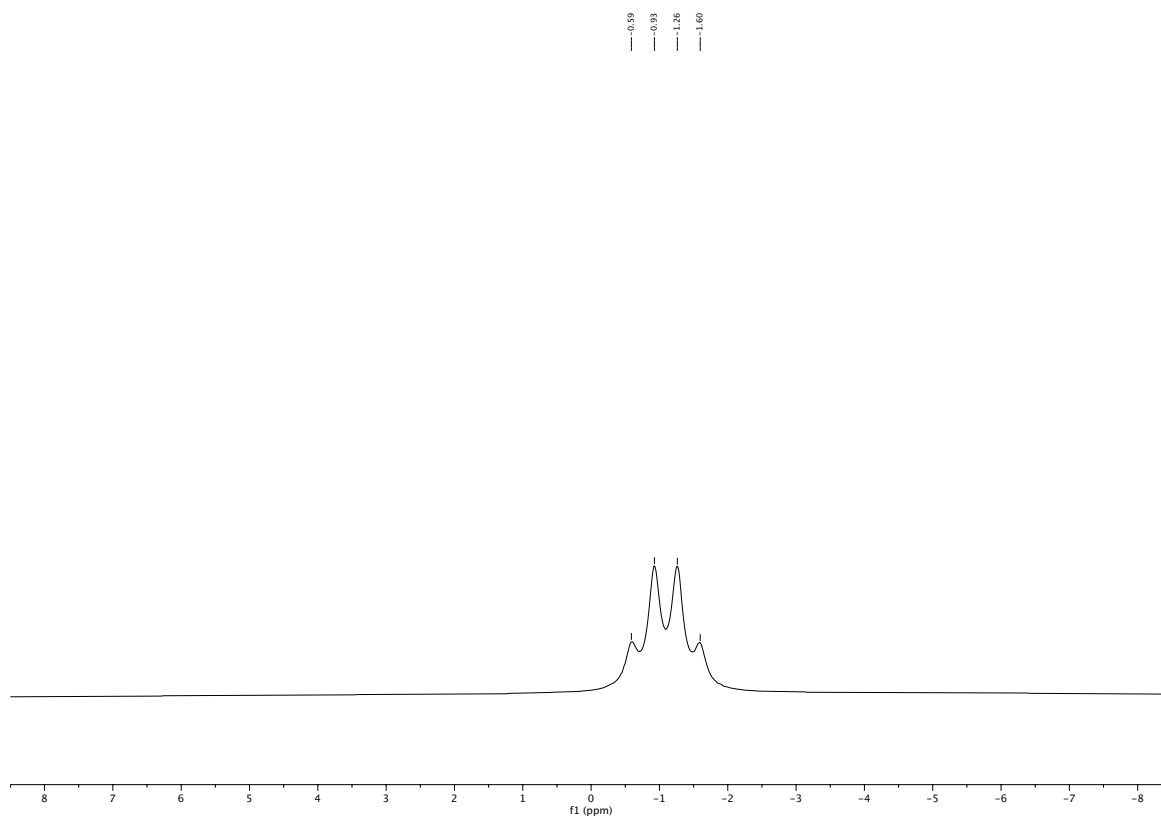
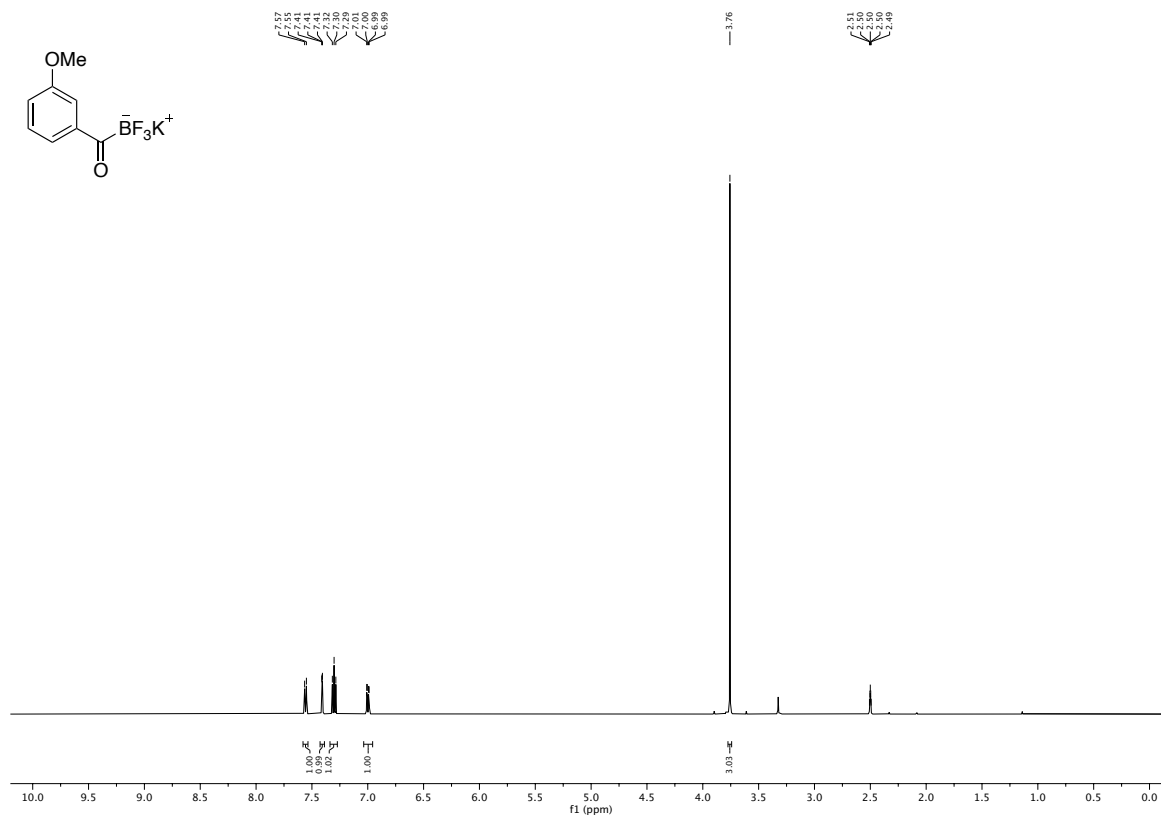
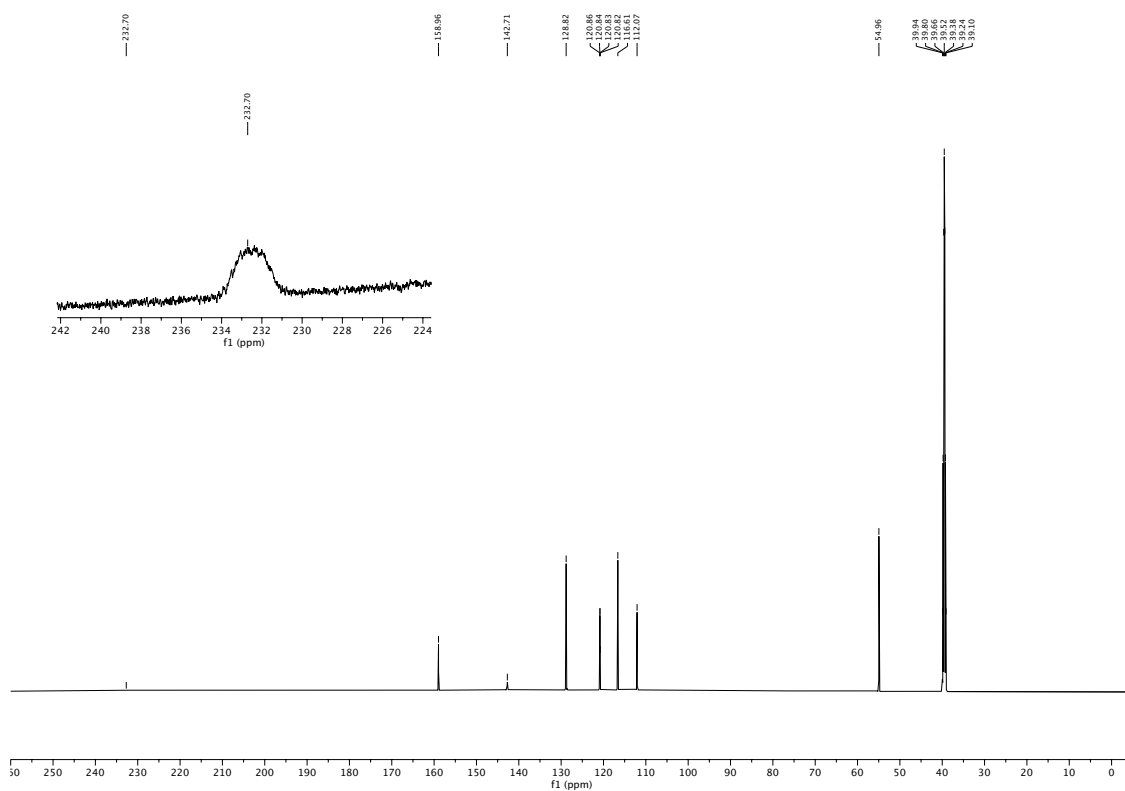
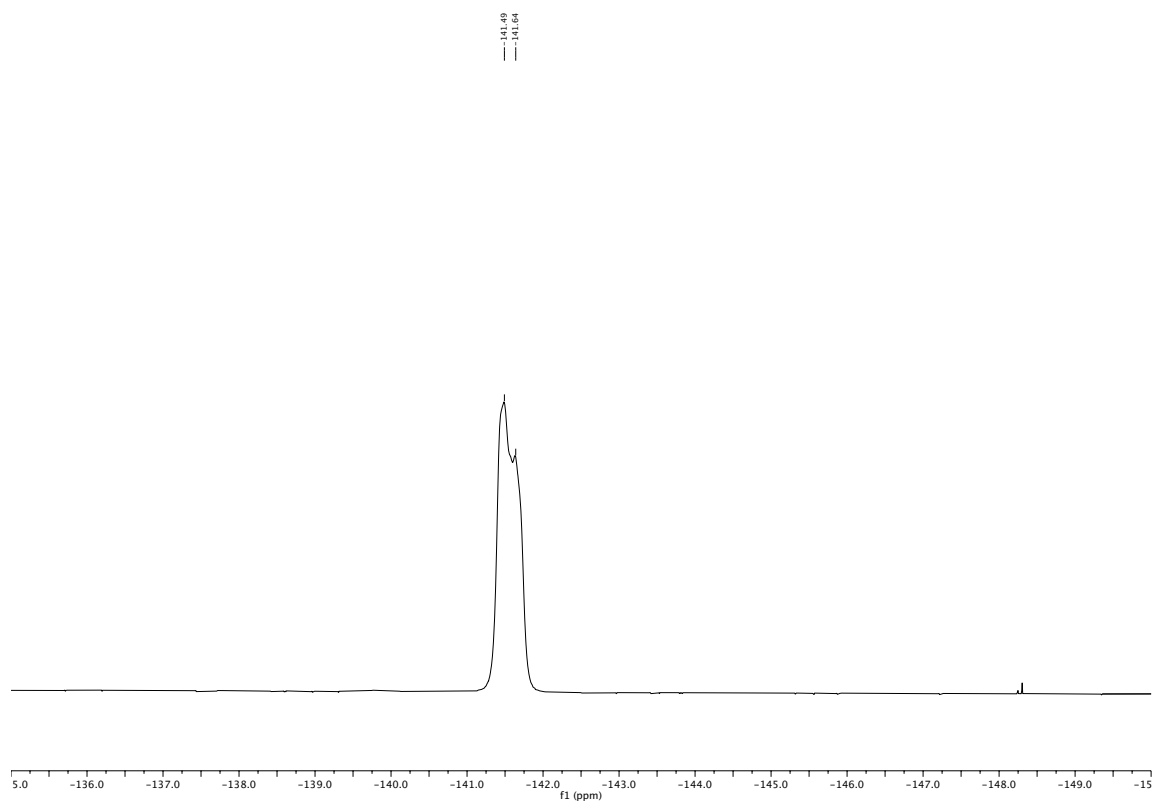
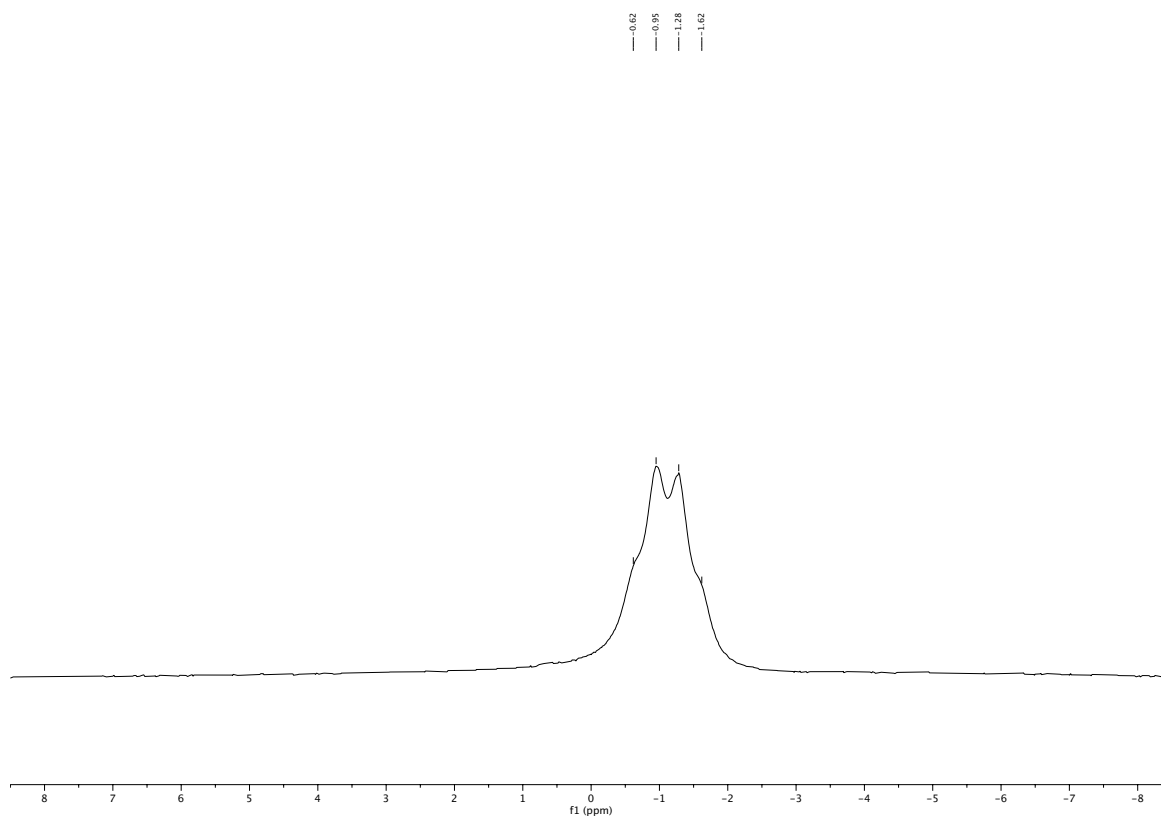
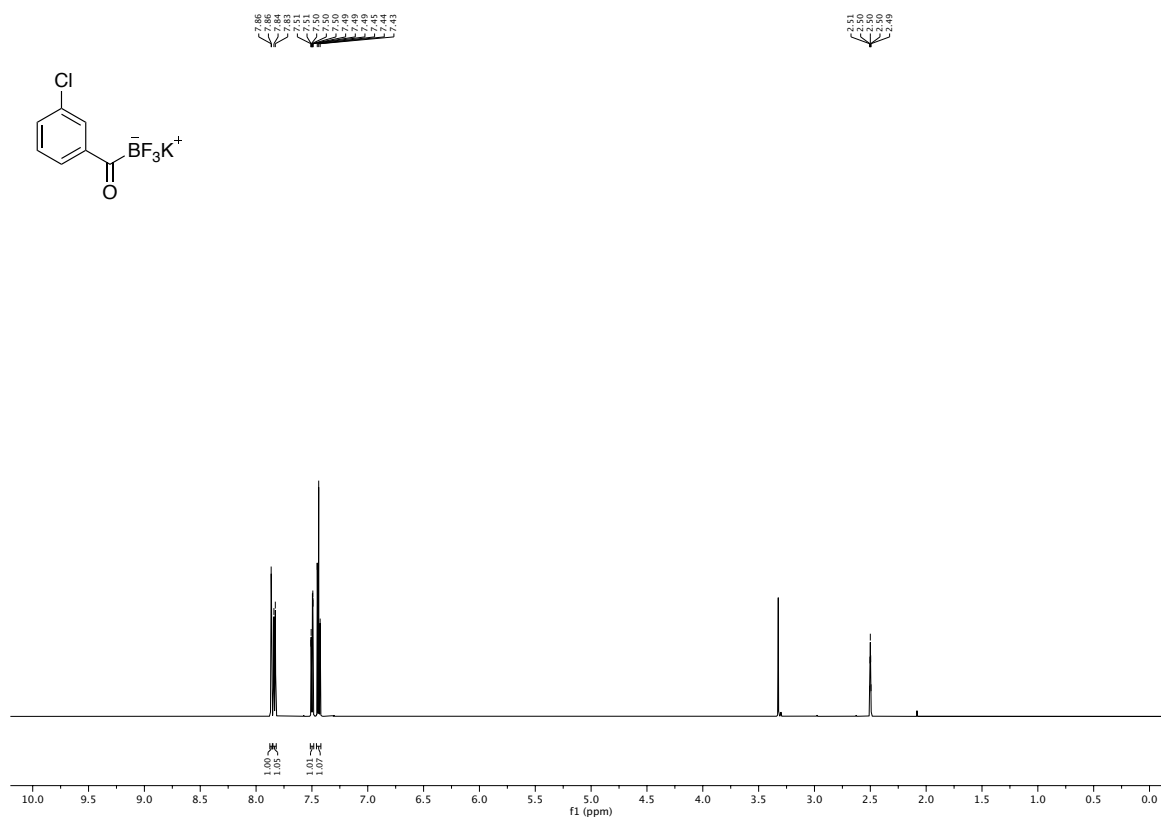


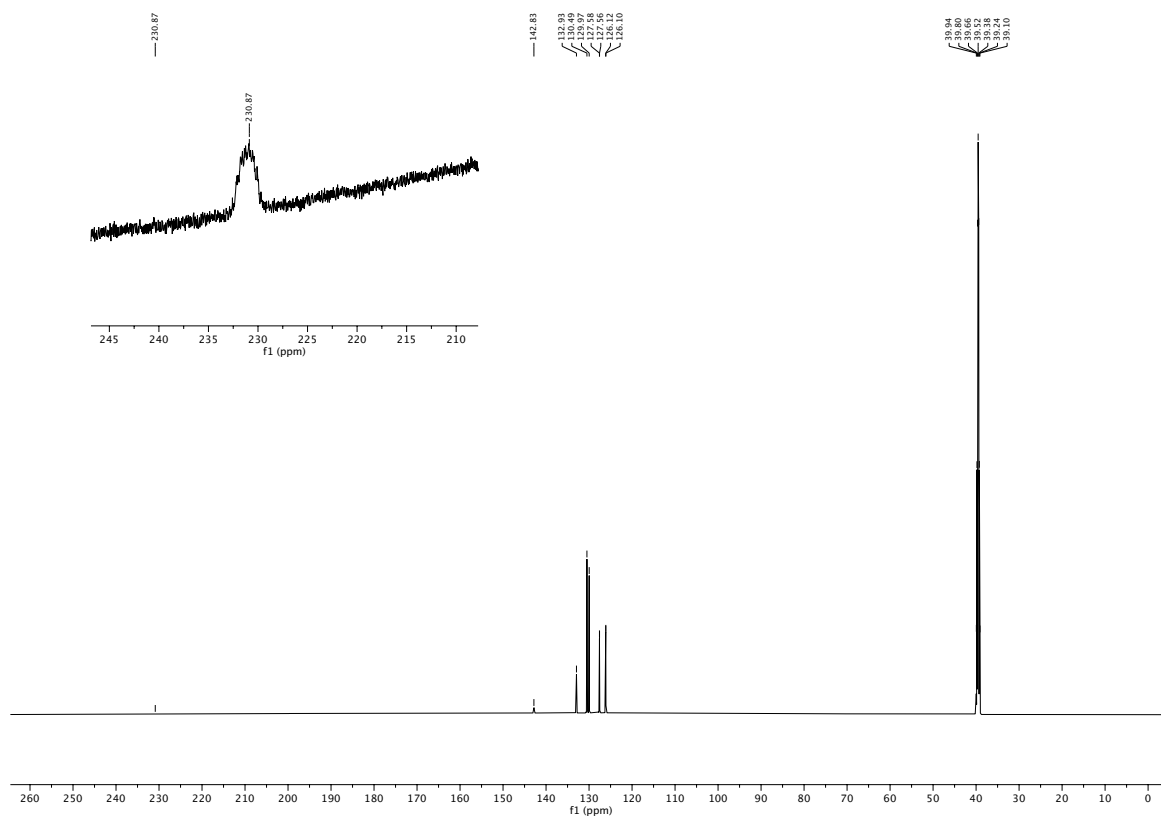
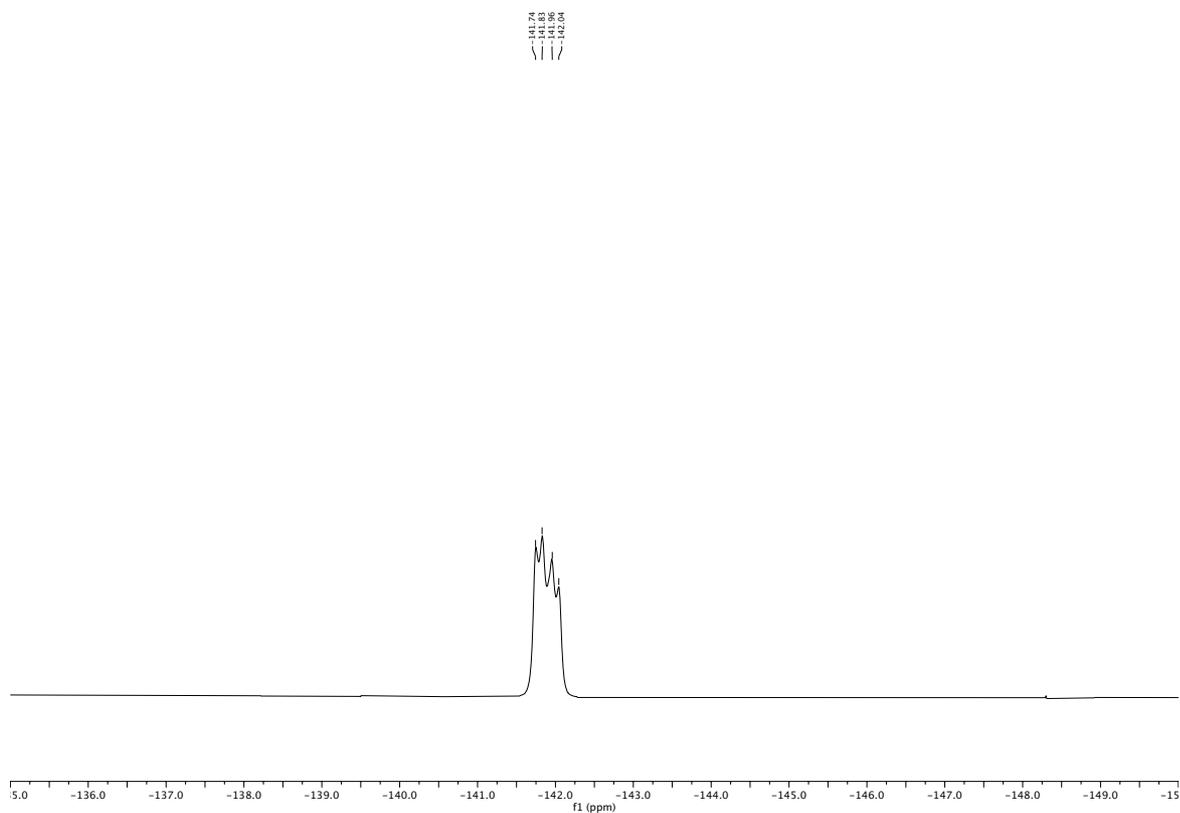
Figure 25. Mass spectrum of the real-time analysis of the ligation between KAT **4a** and *N*-phenethyl-*O*-diethylcarbamoyl hydroxylamine.

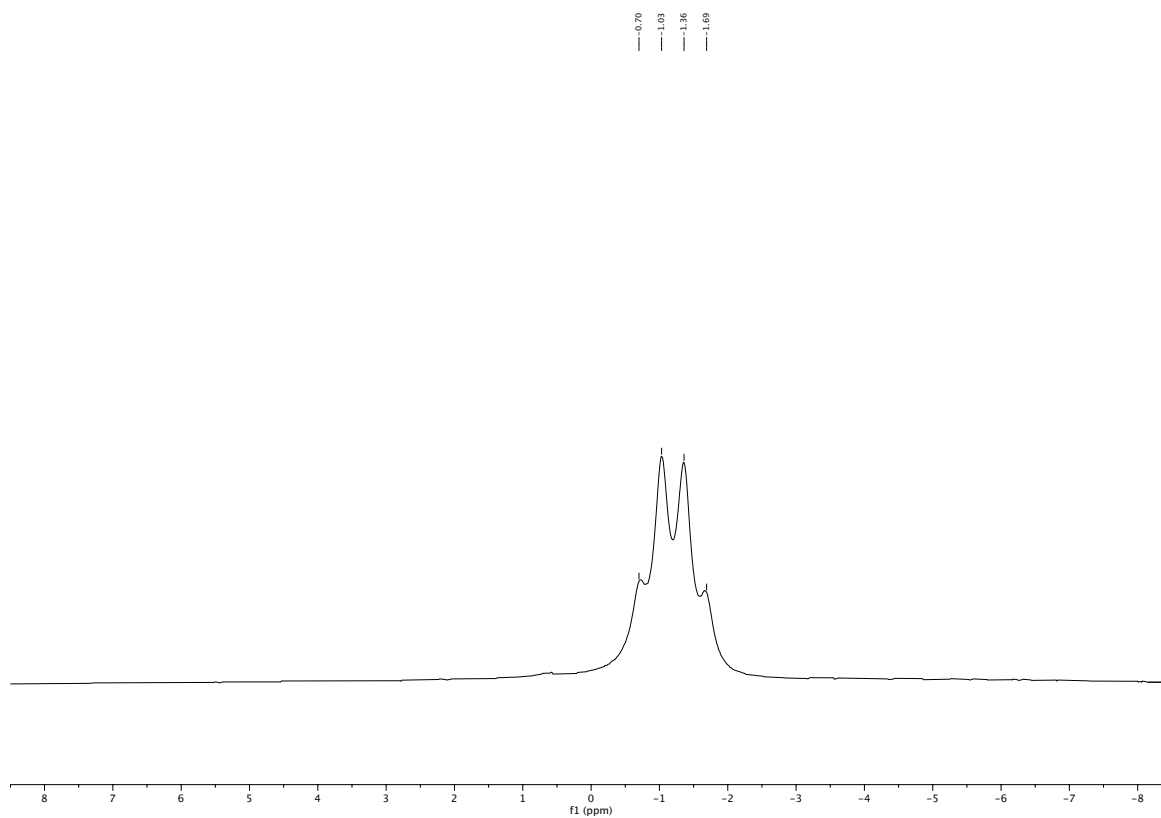
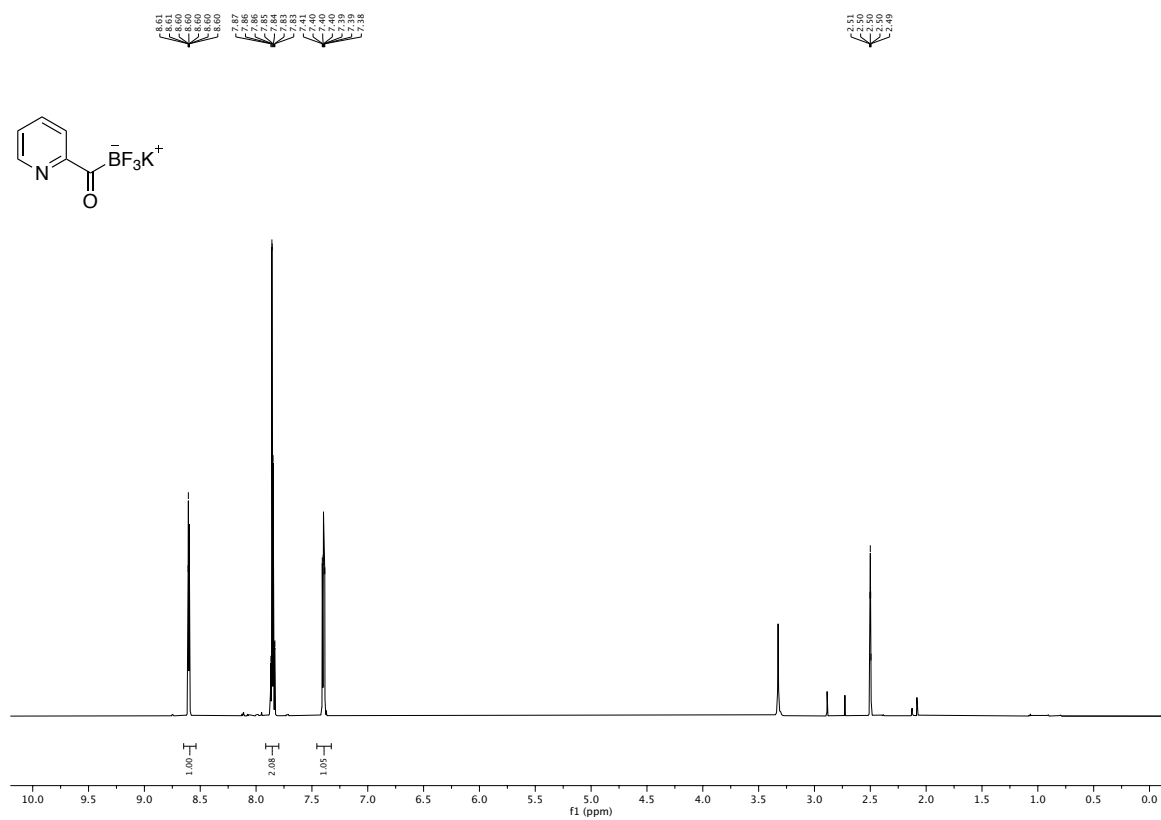
^{13}C -NMR spectrum (151 MHz, DMSO- d_6) **^{19}F -NMR spectrum (470 MHz, DMSO- d_6)**

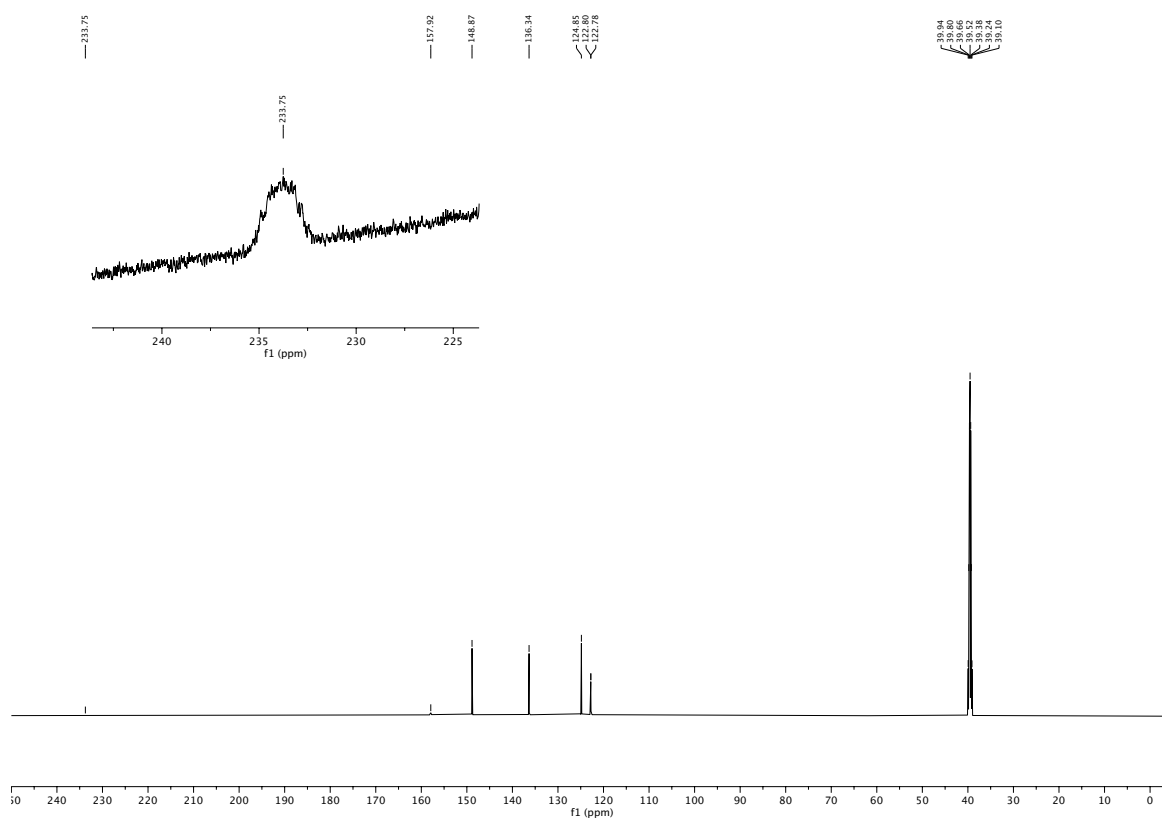
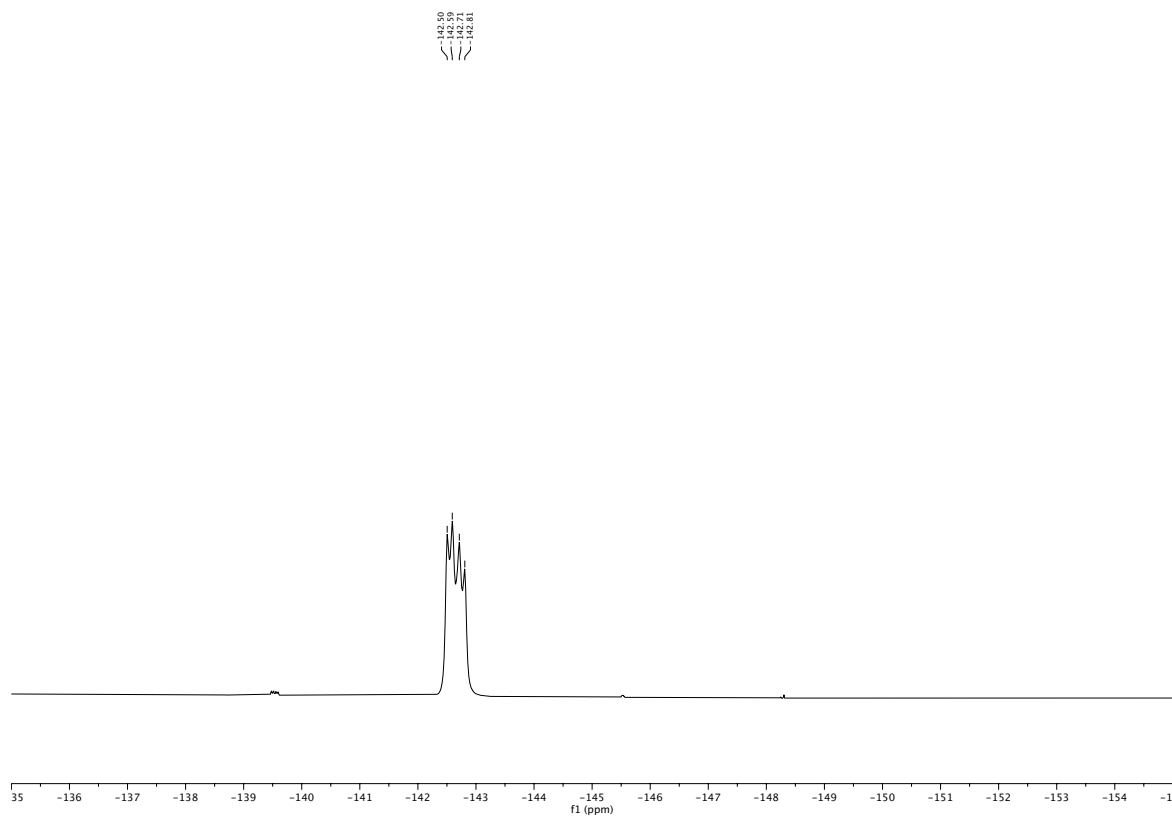
^{11}B -NMR spectrum (160 MHz, DMSO- d_6) **^1H -NMR spectrum (500 MHz DMSO- d_6)**

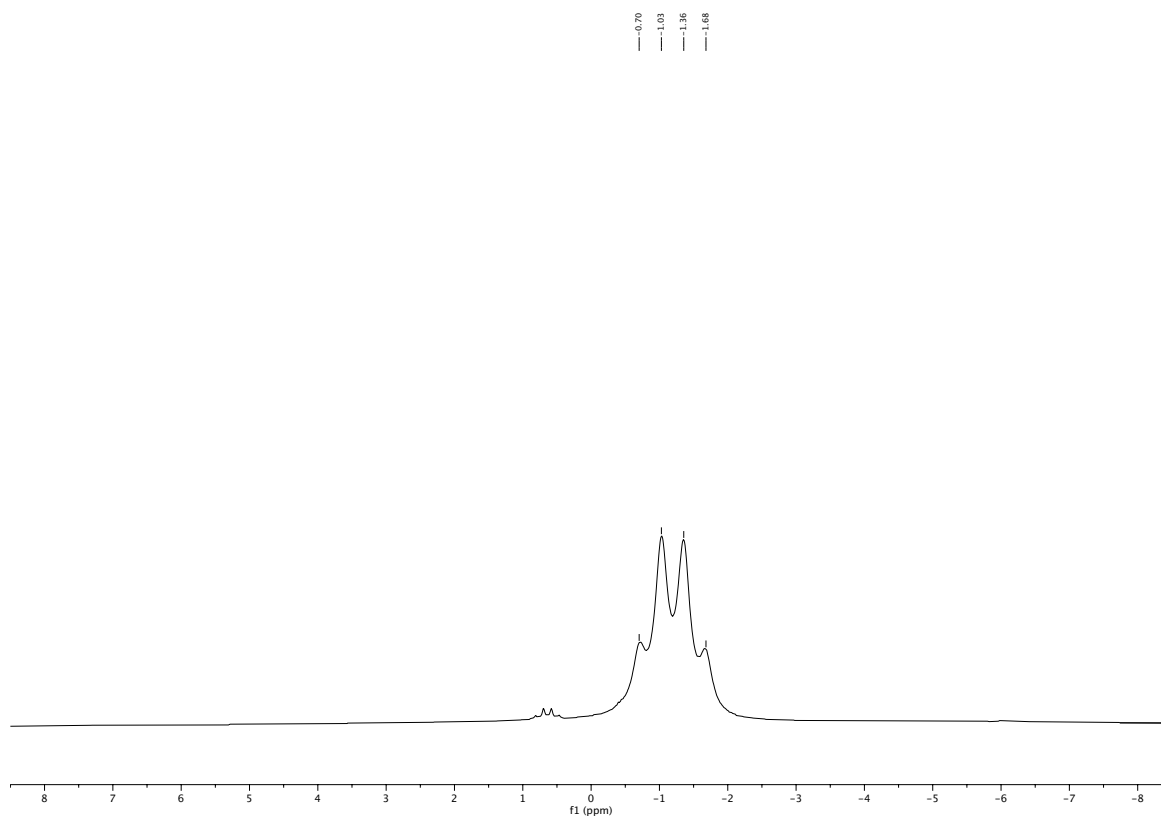
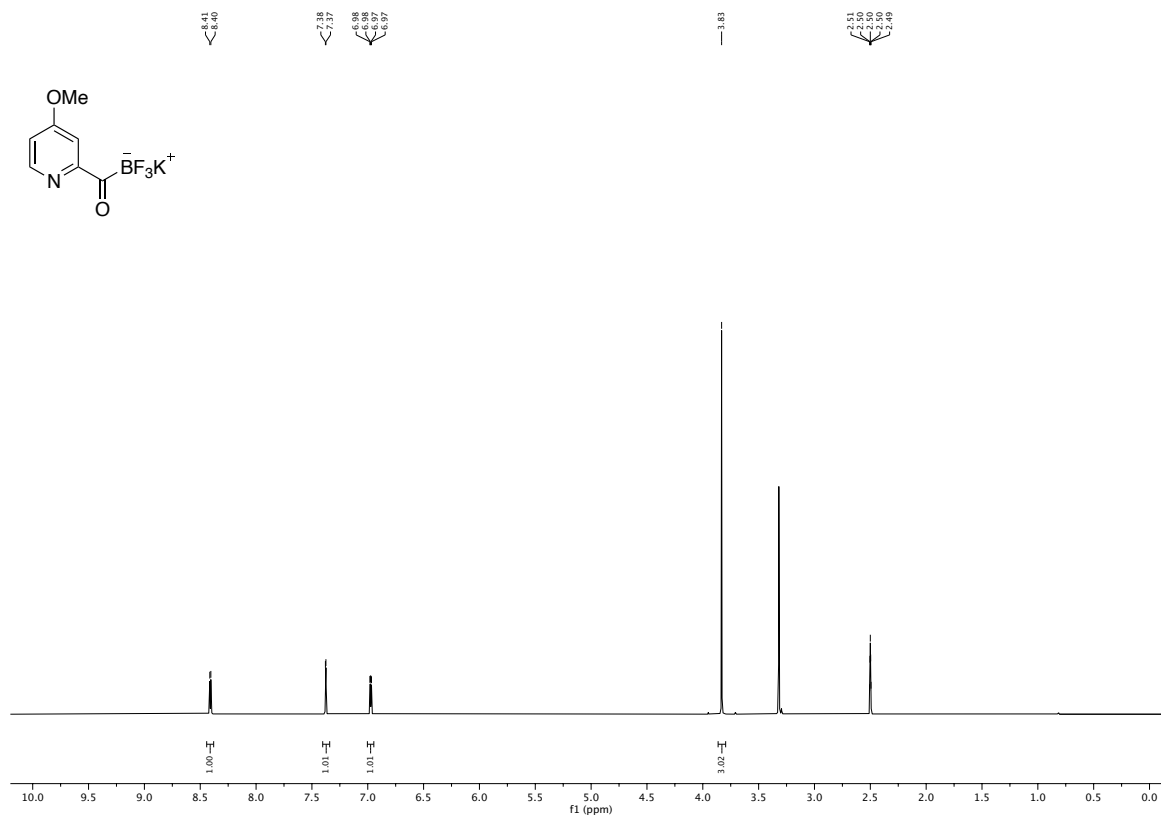
¹³C-NMR spectrum (151 MHz, DMSO-d₆)**¹⁹F-NMR spectrum (470 MHz, DMSO-d₆)**

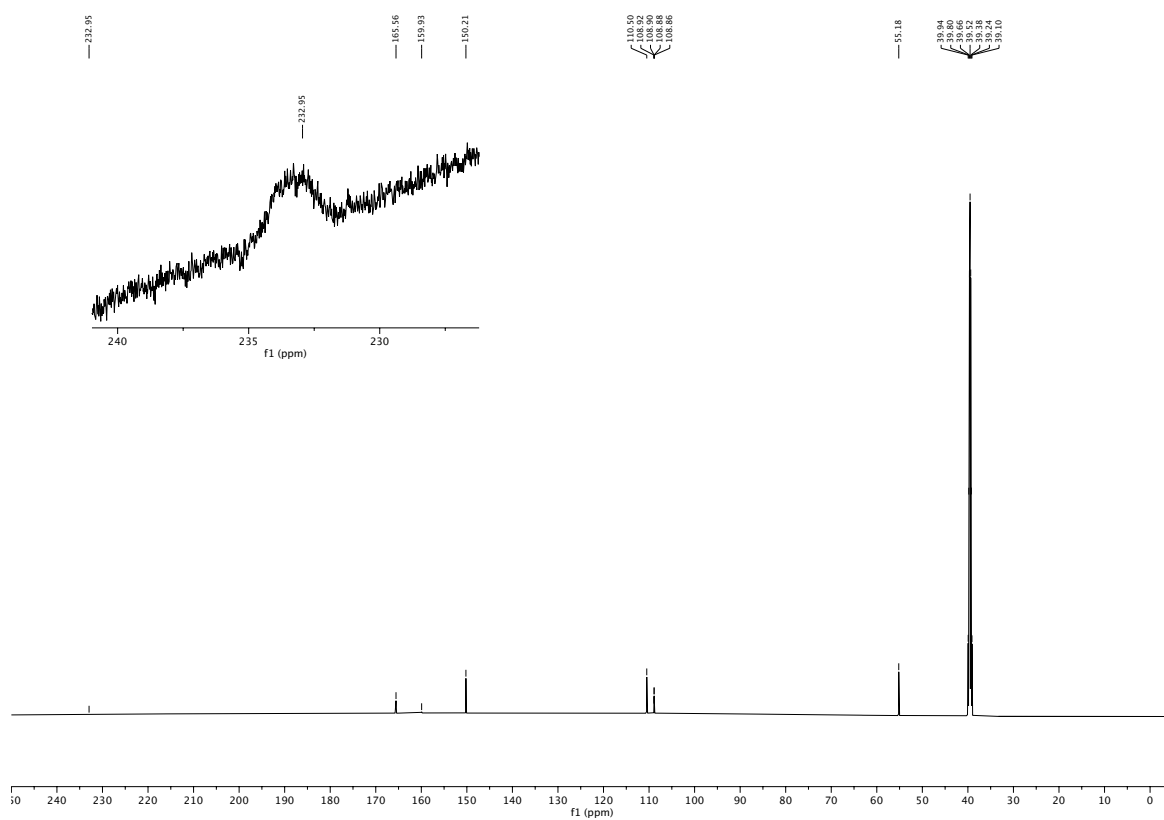
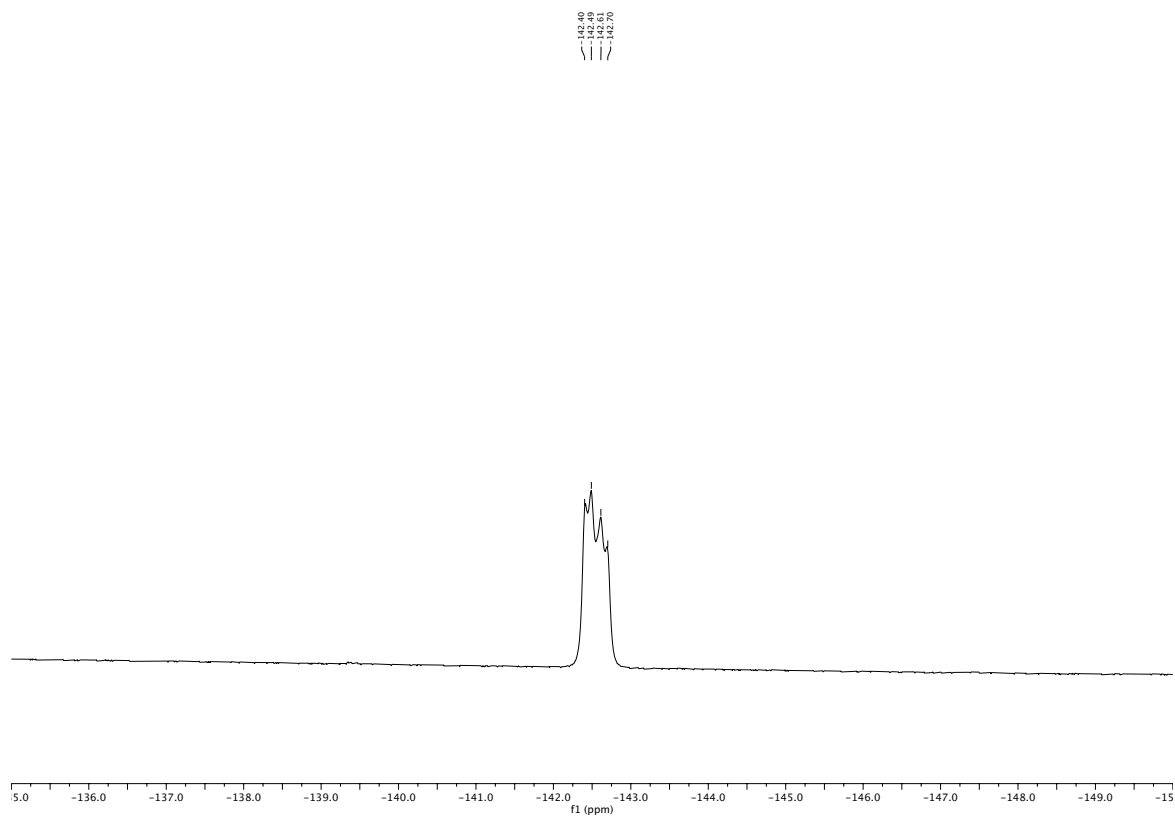
^{11}B -NMR spectrum (160 MHz, DMSO- d_6) **^1H -NMR spectrum (600 MHz DMSO- d_6)**

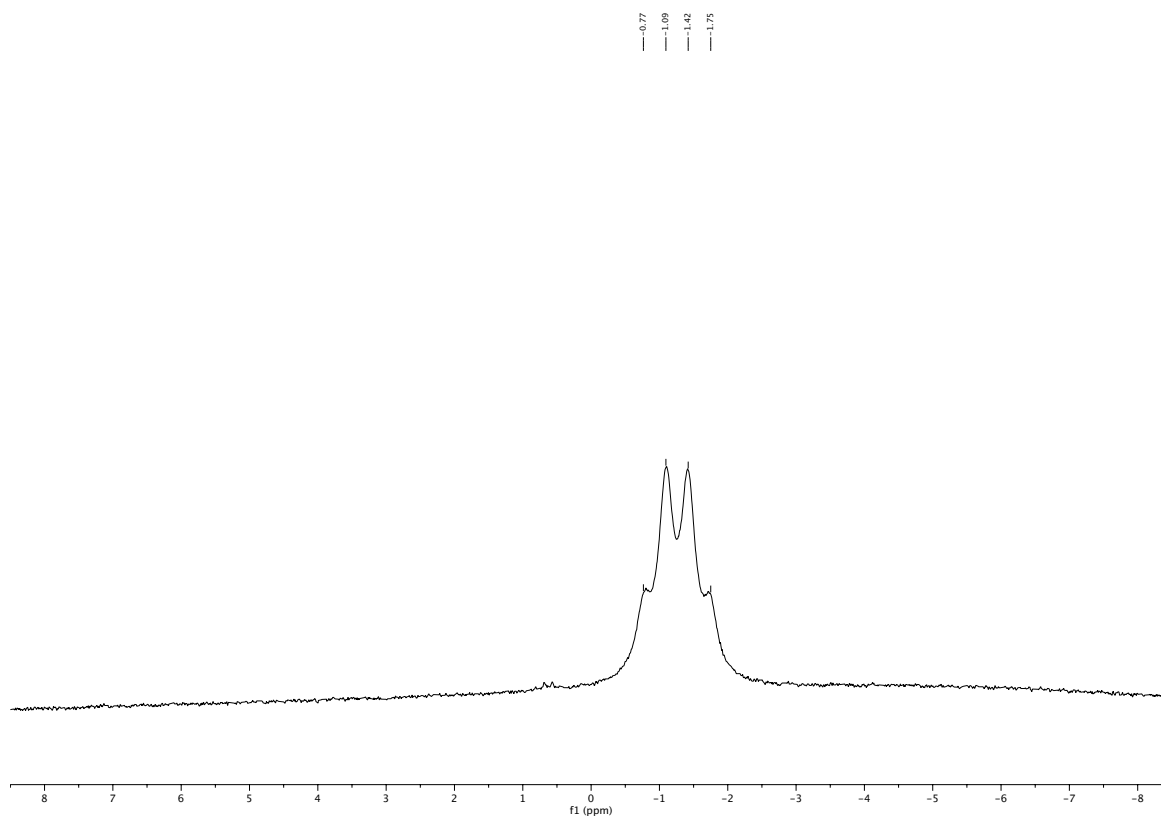
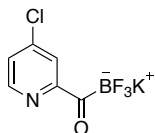
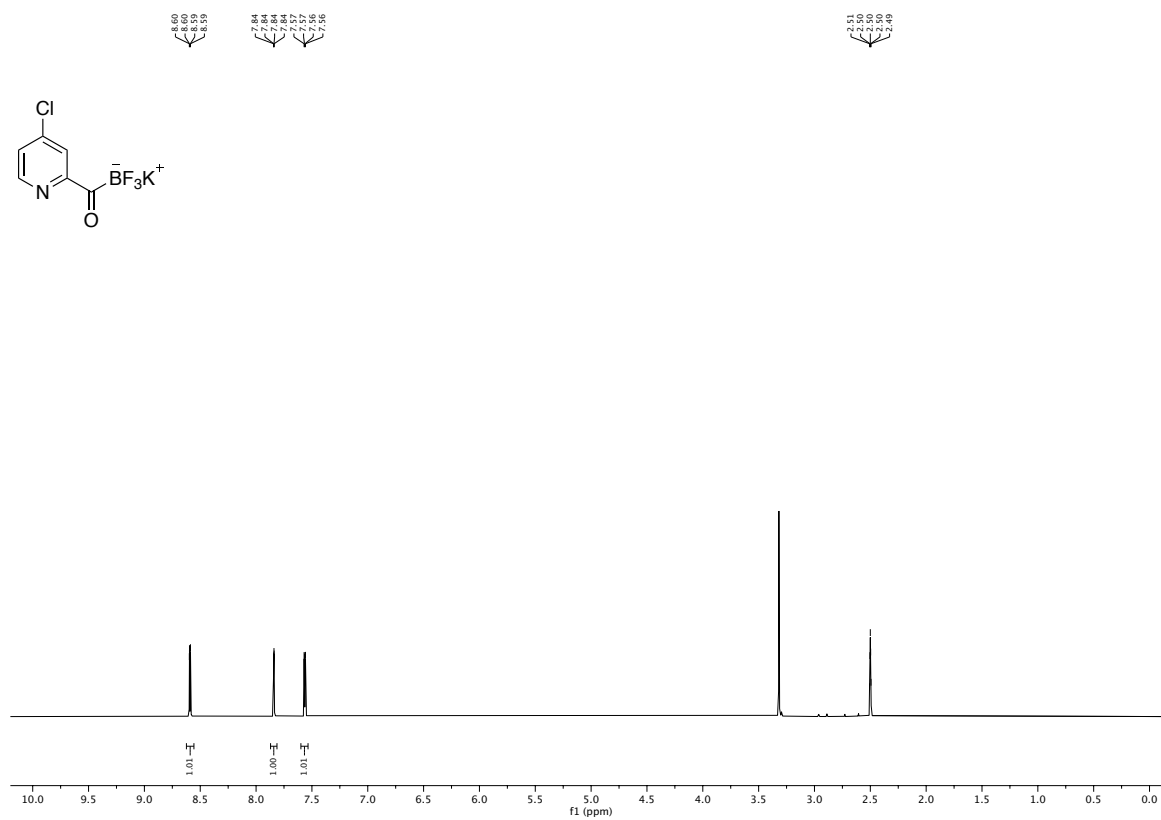
^{13}C -NMR spectrum (151 MHz, DMSO- d_6) **^{19}F -NMR spectrum (470 MHz, DMSO- d_6)**

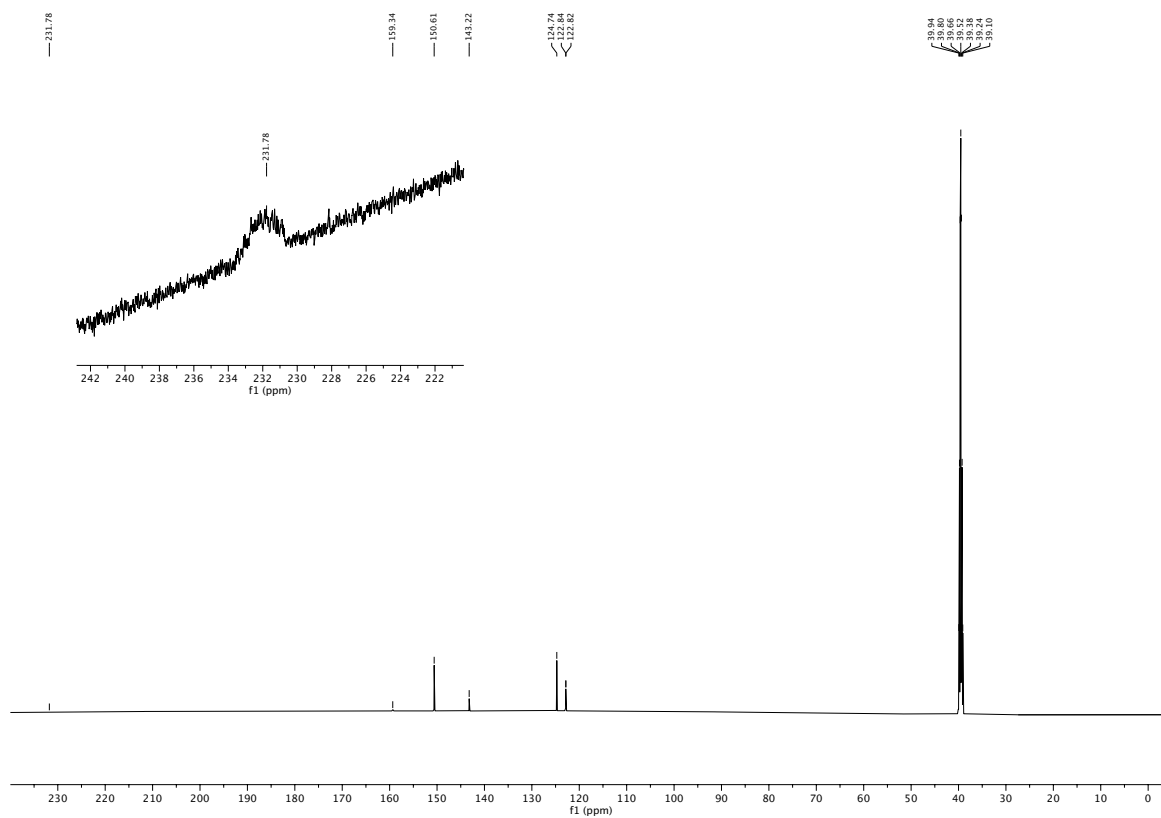
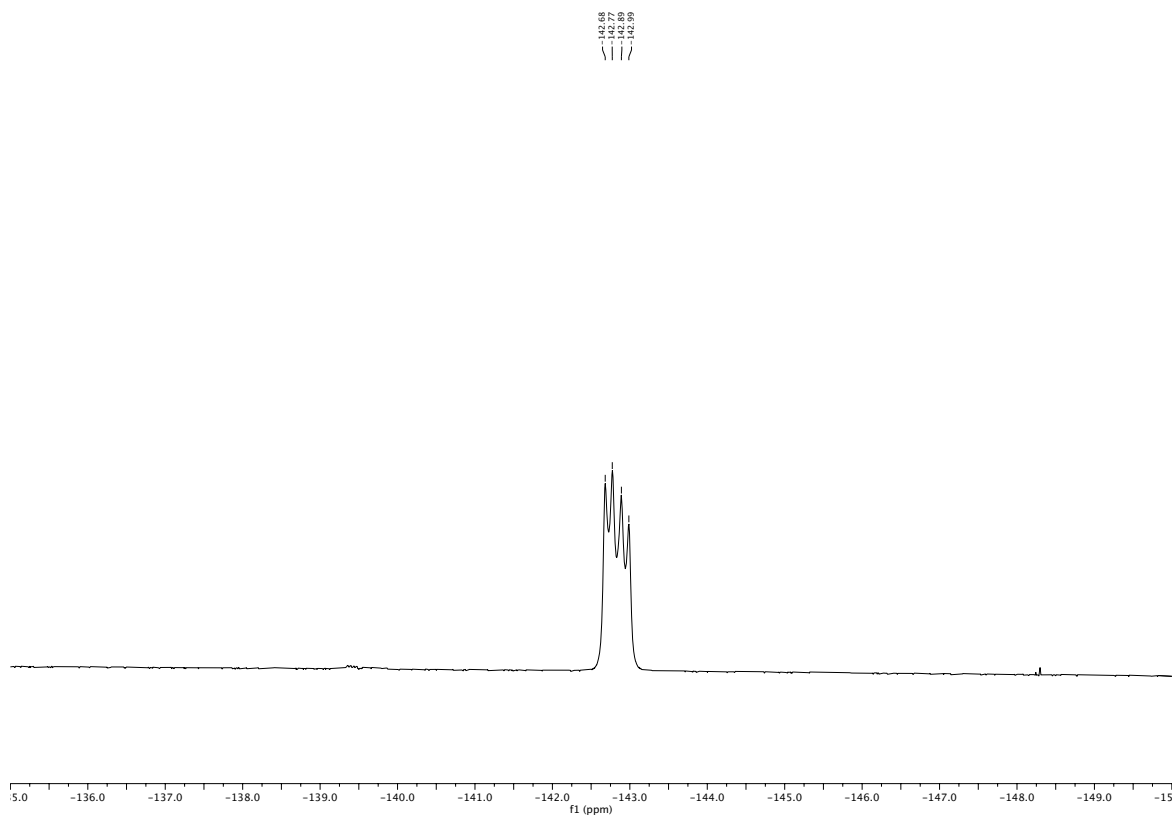
^{11}B -NMR spectrum (160 MHz, DMSO- d_6) **^1H -NMR spectrum (600 MHz DMSO- d_6)**

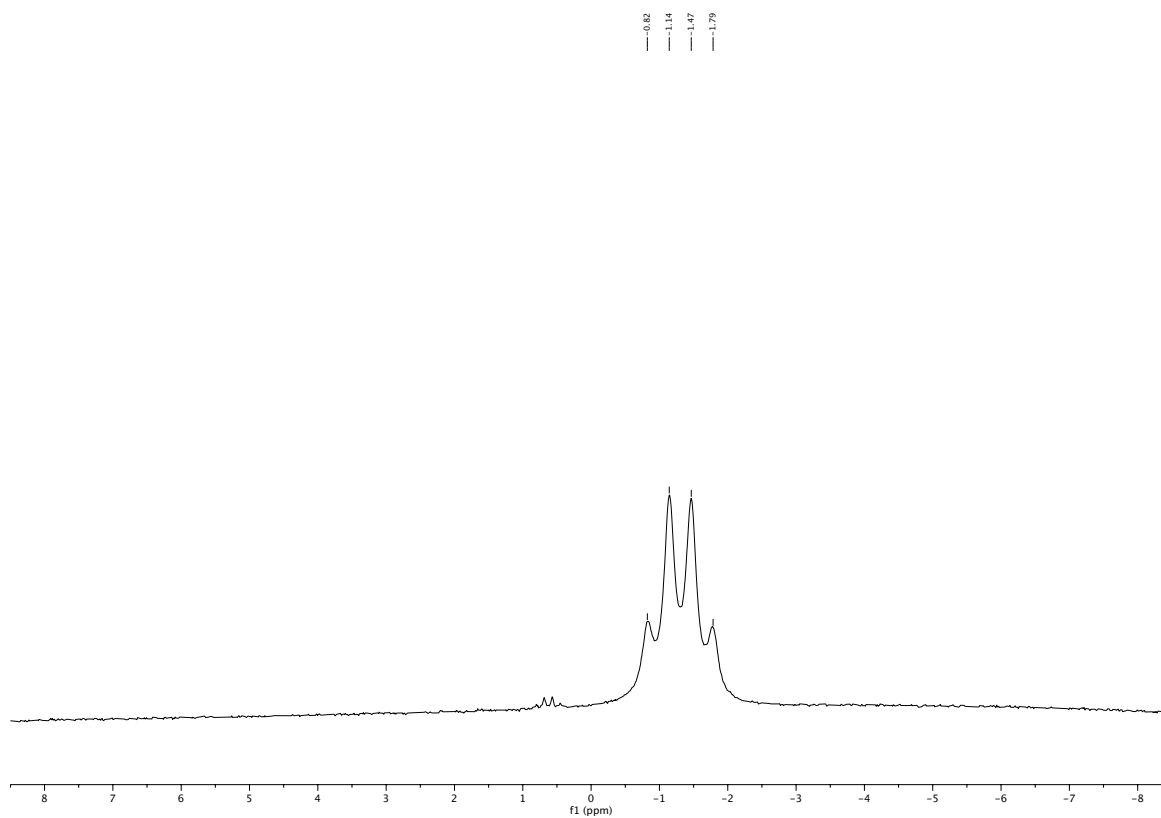
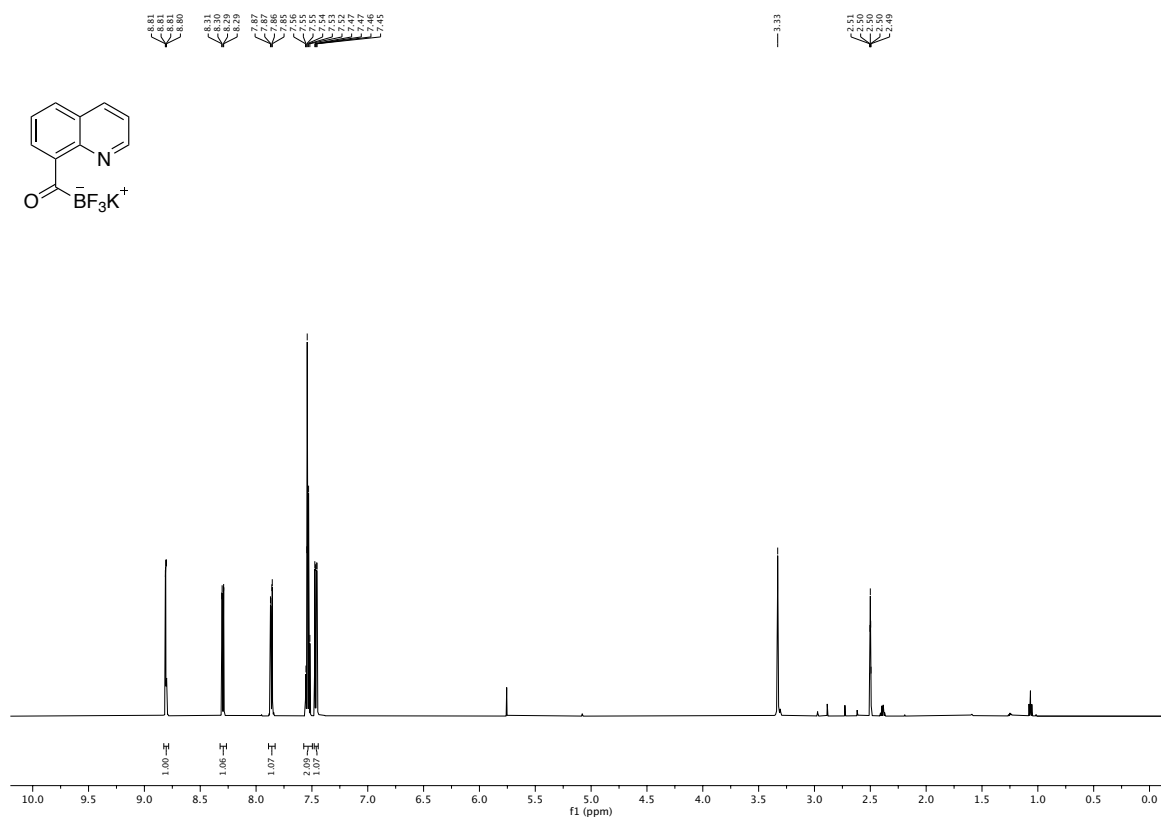
^{13}C -NMR spectrum (151 MHz, DMSO- d_6) **^{19}F -NMR spectrum (470 MHz, DMSO- d_6)**

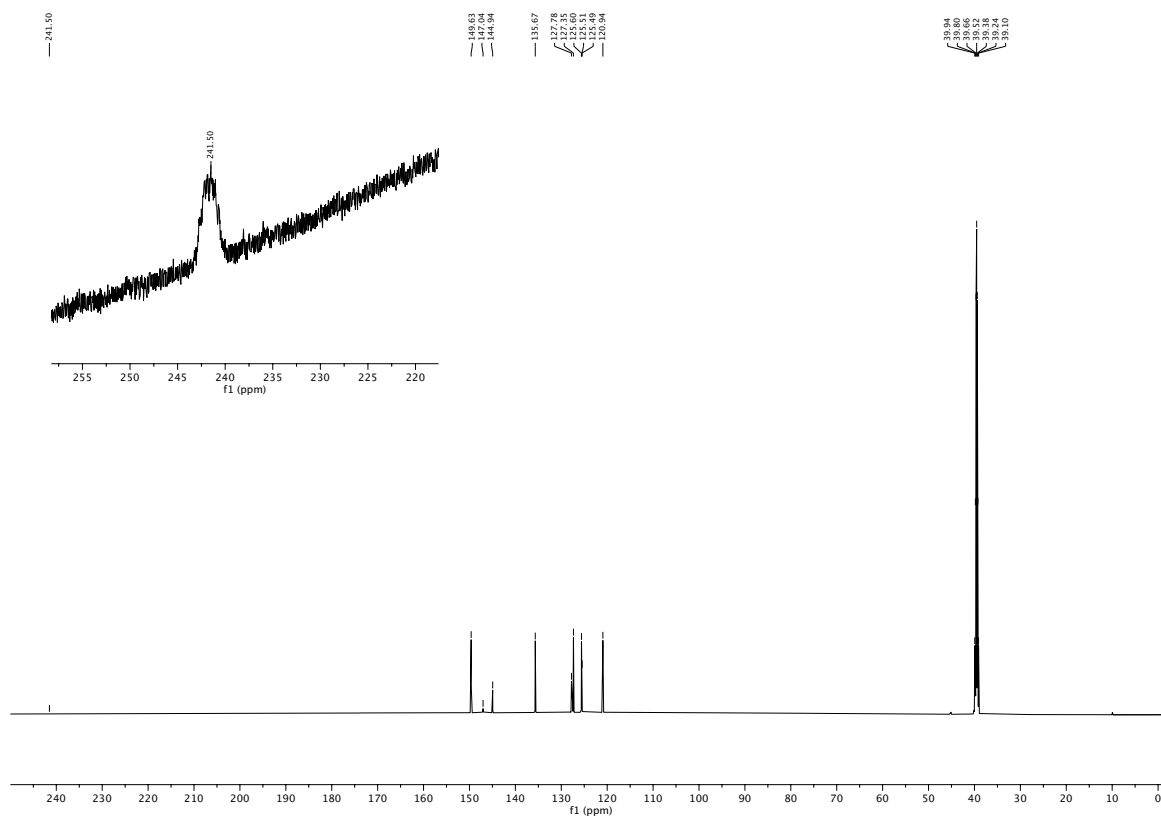
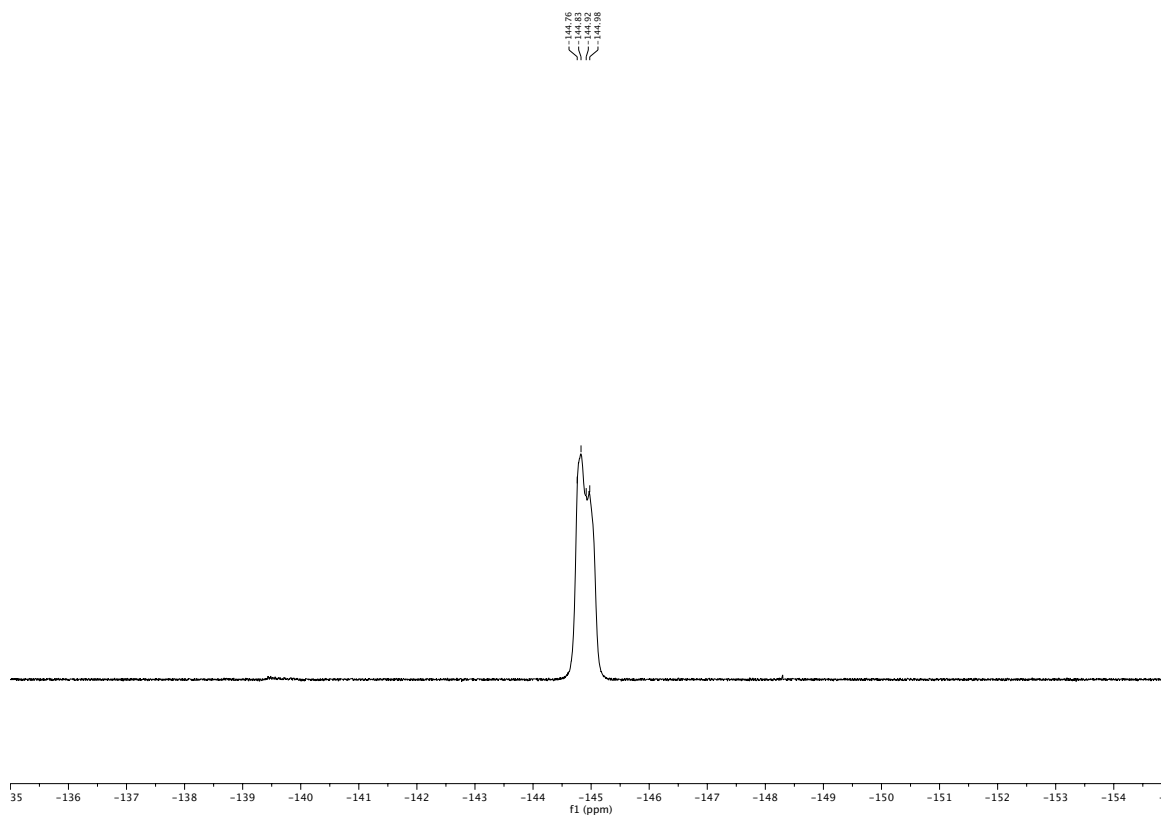
^{11}B -NMR spectrum (160 MHz, DMSO- d_6) **^1H -NMR spectrum (600 MHz DMSO- d_6)**

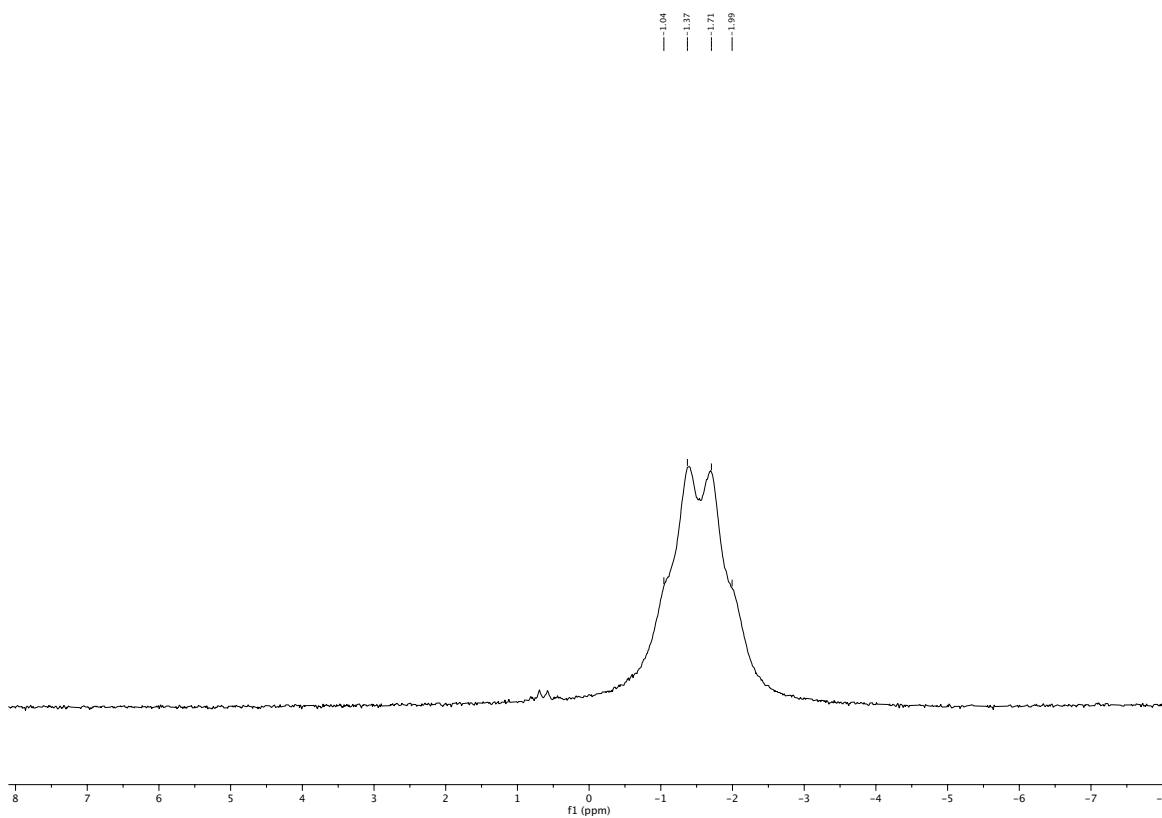
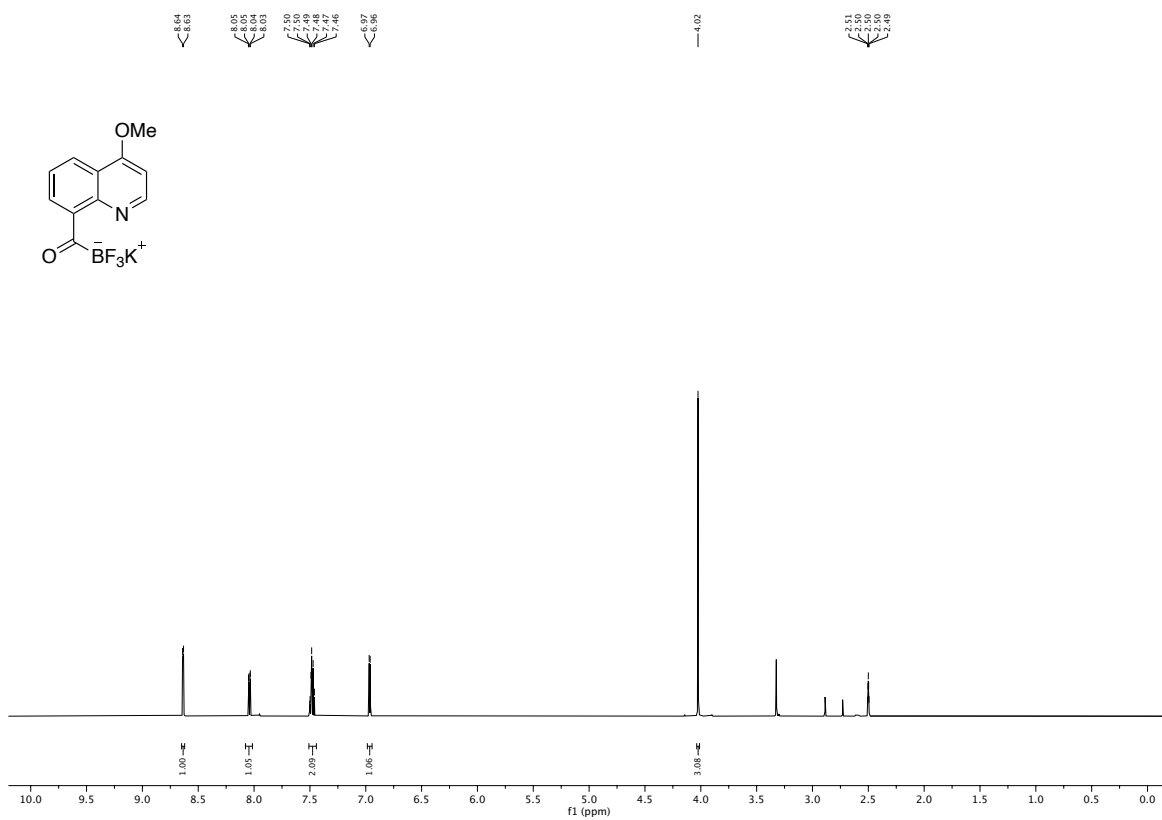
^{13}C -NMR spectrum (151 MHz, DMSO- d_6) **^{19}F -NMR spectrum (470 MHz, DMSO- d_6)**

^{11}B -NMR spectrum (160 MHz, DMSO- d_6) **^1H -NMR spectrum (600 MHz DMSO- d_6)**

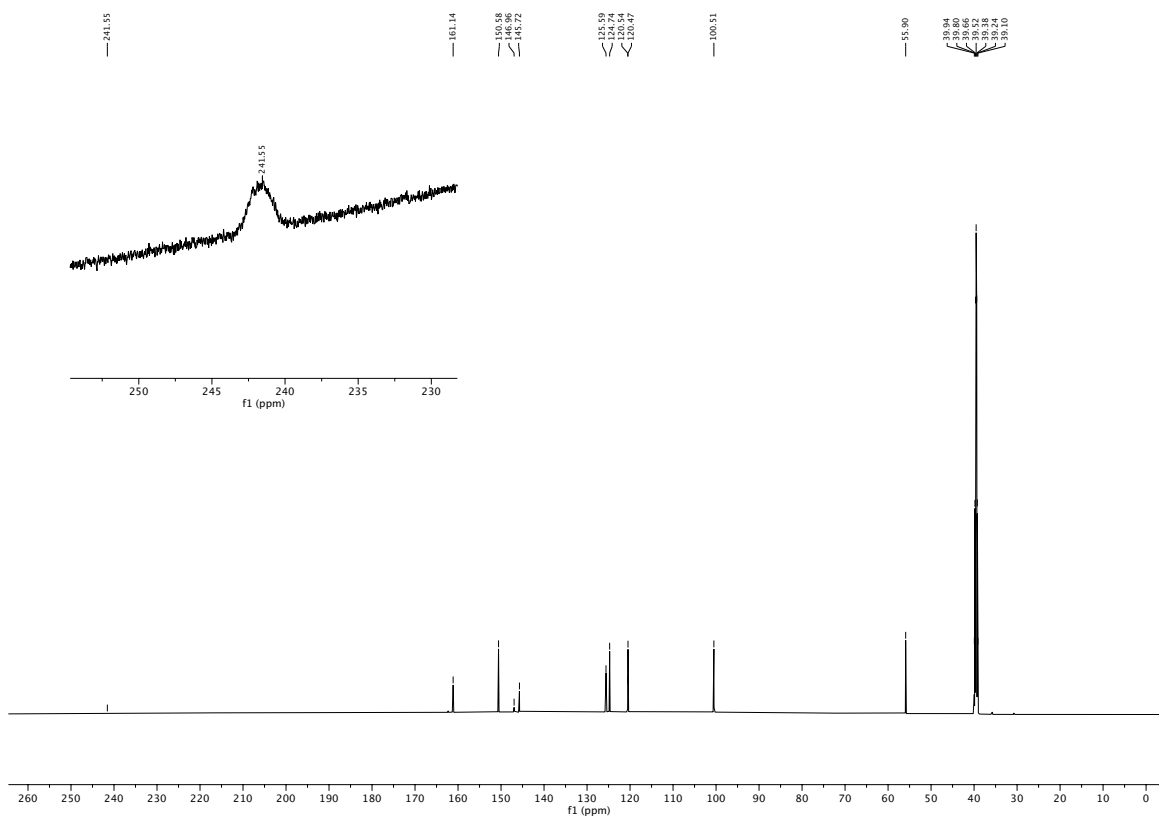
^{13}C -NMR spectrum (151 MHz, DMSO- d_6) **^{19}F -NMR spectrum (470 MHz, DMSO- d_6)**

^{11}B -NMR spectrum (160 MHz, DMSO- d_6) **^1H -NMR spectrum (600 MHz DMSO- d_6)**

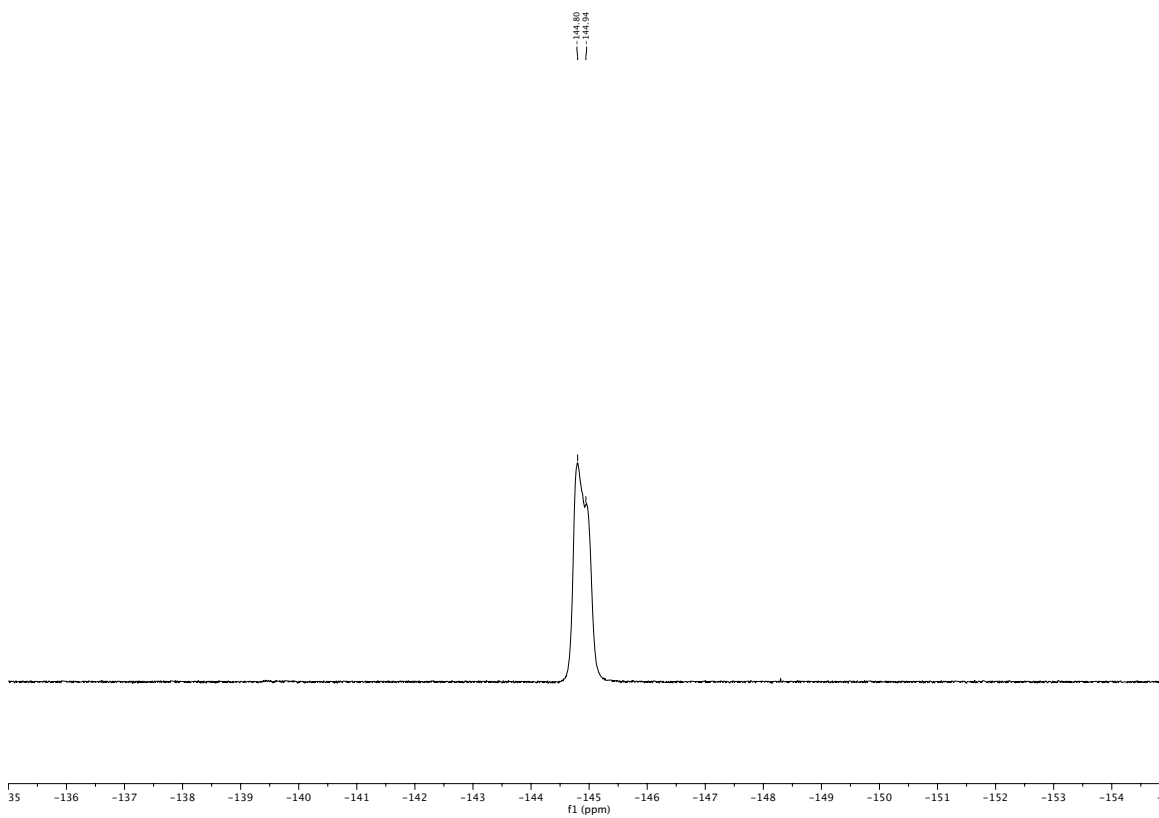
^{13}C -NMR spectrum (151 MHz, DMSO- d_6) **^{19}F -NMR spectrum (470 MHz, DMSO- d_6)**

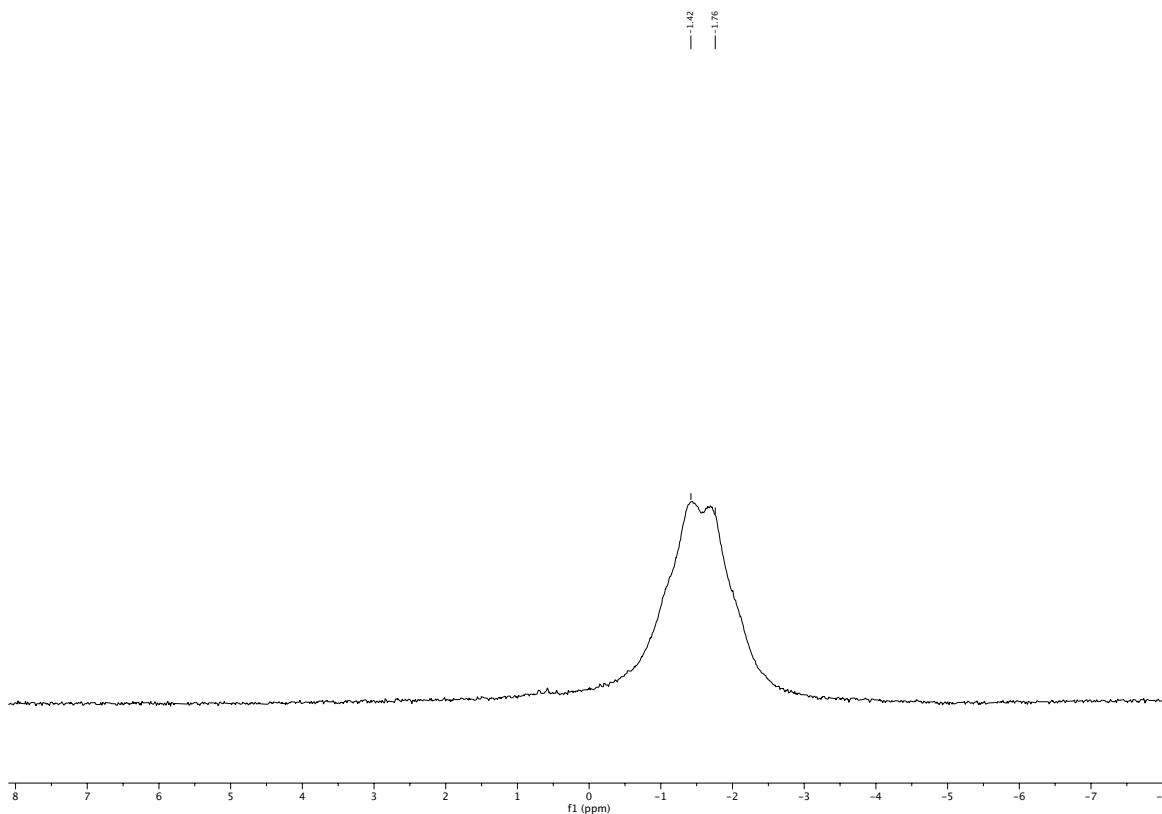
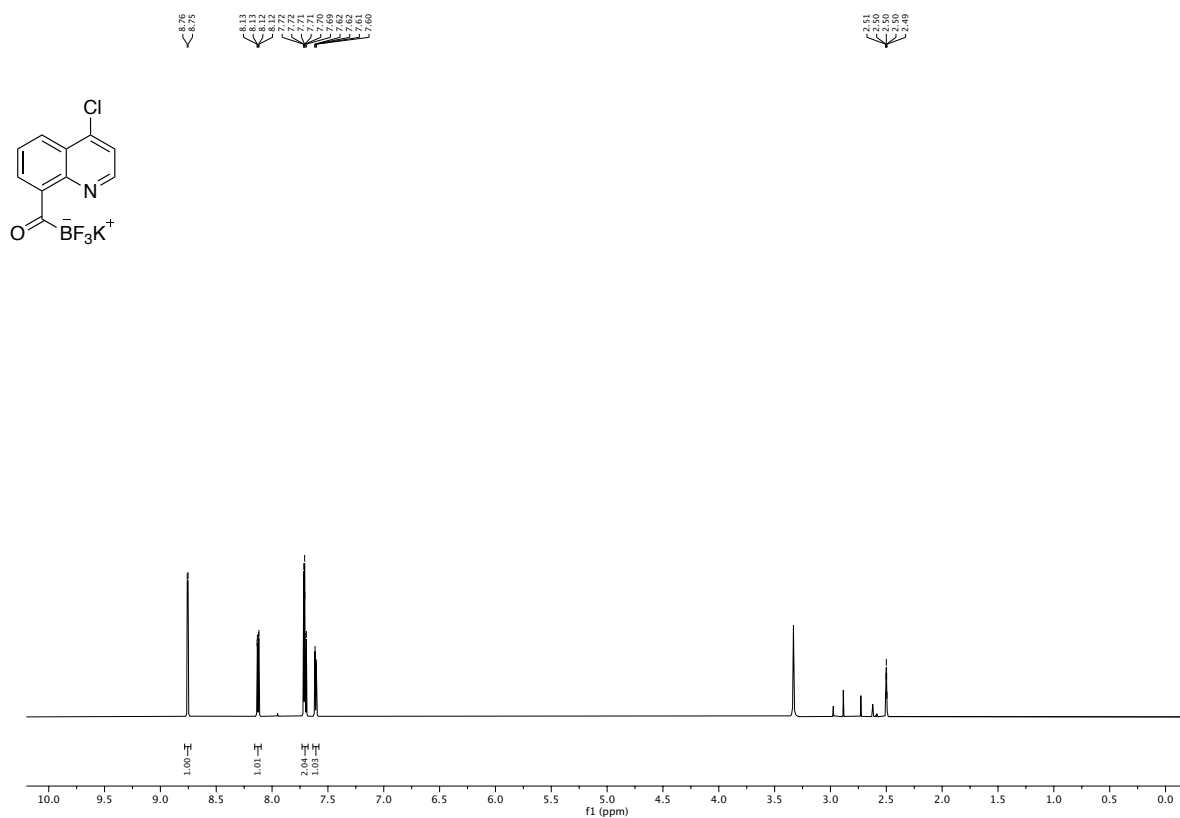
^{11}B -NMR spectrum (160 MHz, DMSO- d_6) **^1H -NMR spectrum (600 MHz DMSO- d_6)**

¹³C-NMR spectrum (151 MHz, DMSO-d₆)

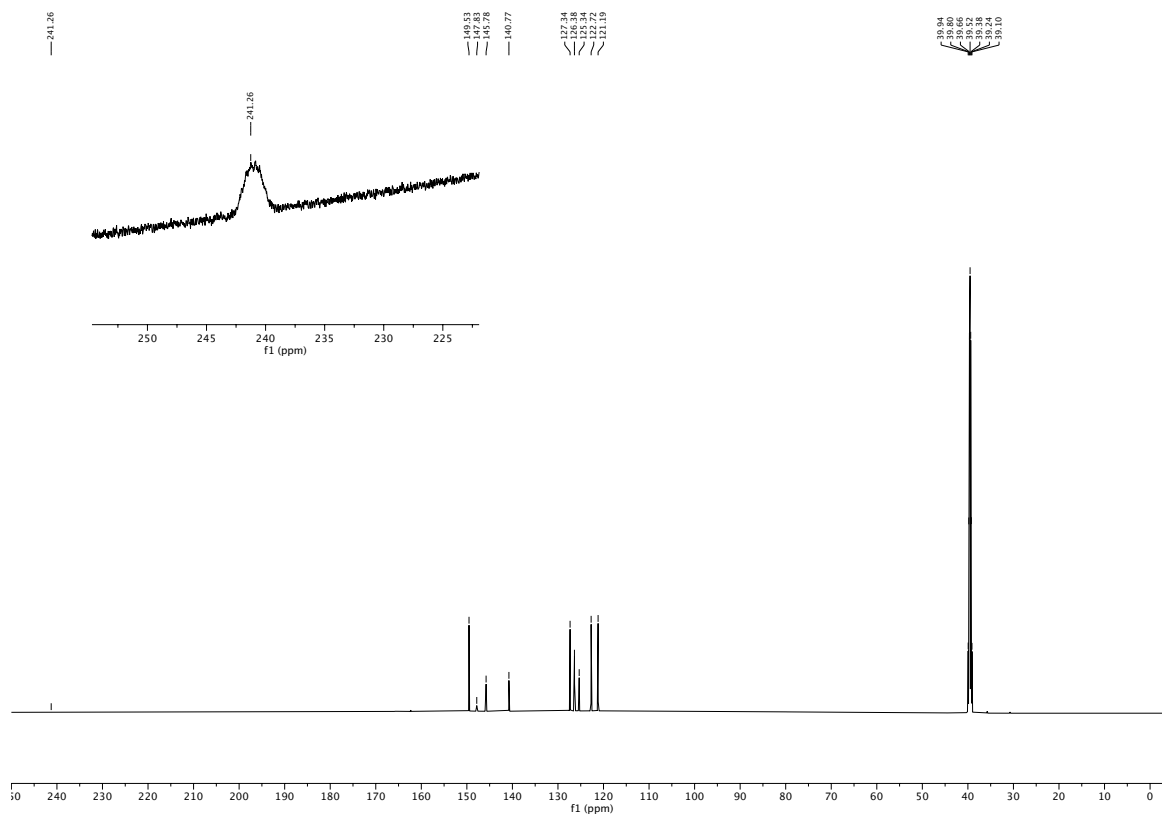


¹⁹F-NMR spectrum (470 MHz, DMSO-d₆)

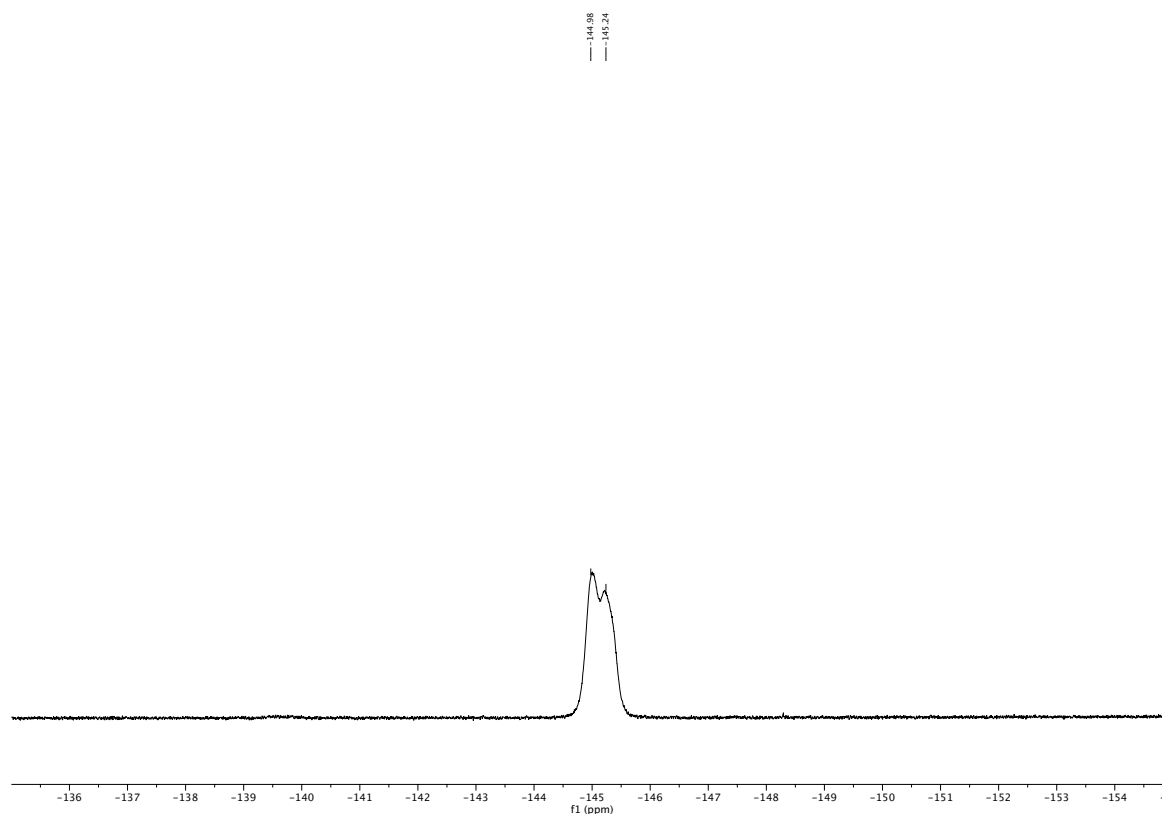


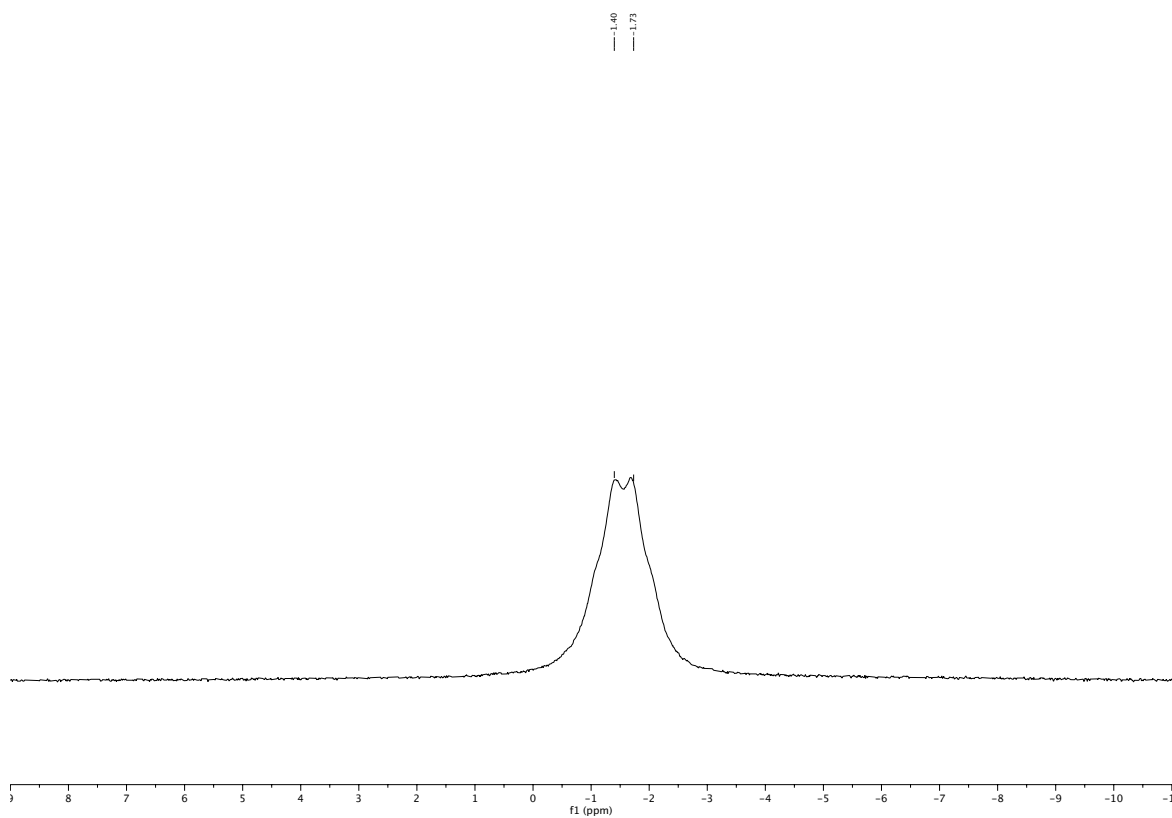
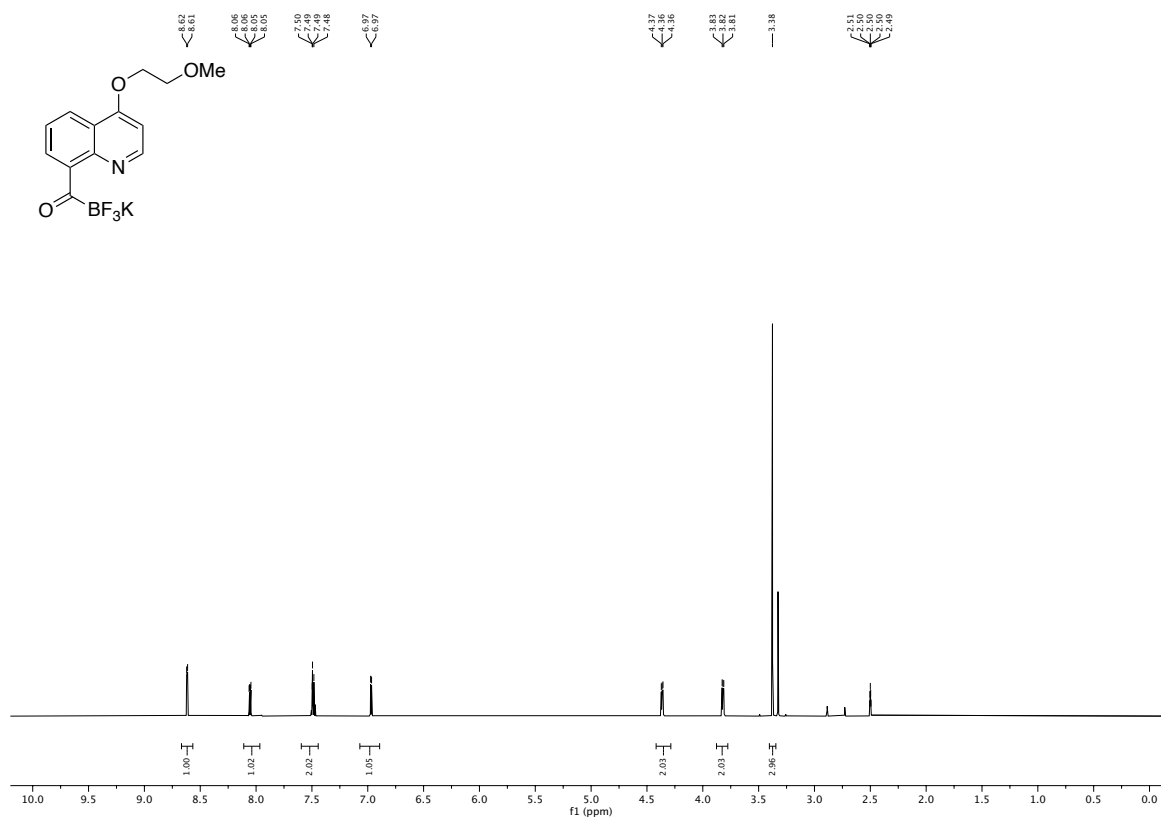
^{11}B -NMR spectrum (160 MHz, DMSO- d_6) **^1H -NMR spectrum (600 MHz DMSO- d_6)**

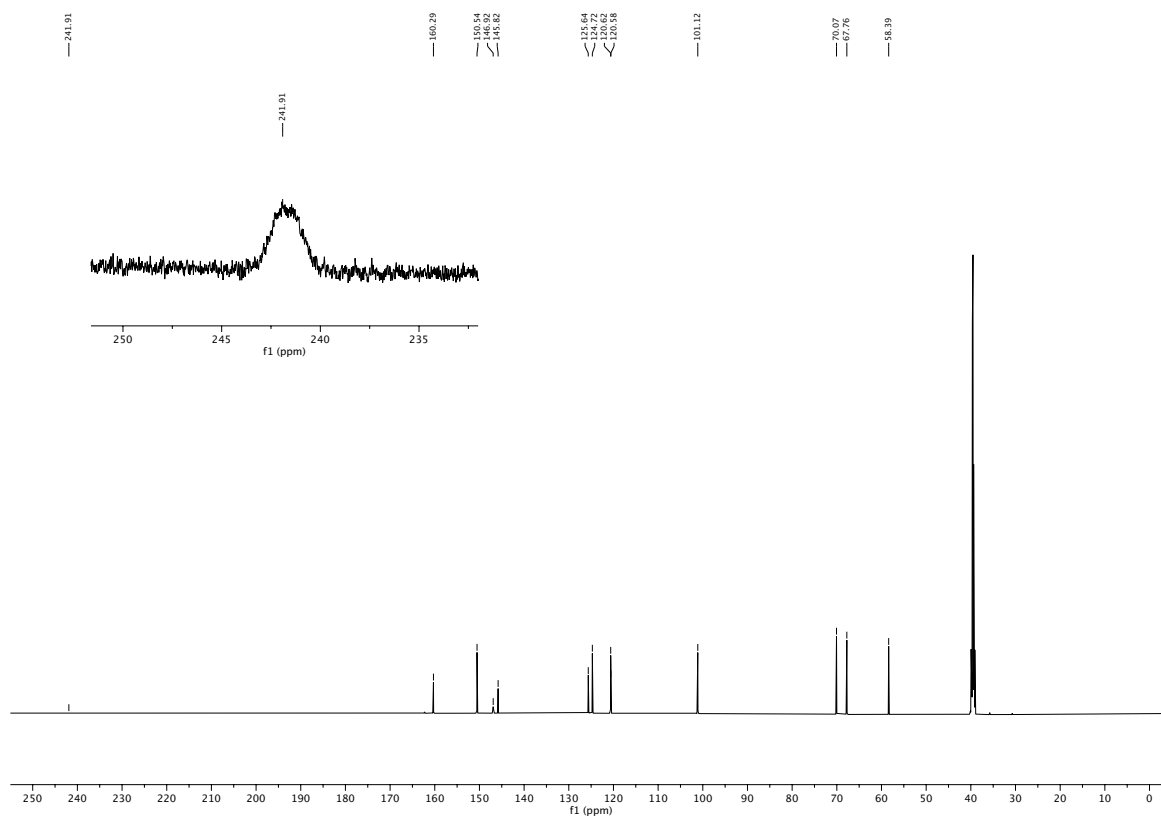
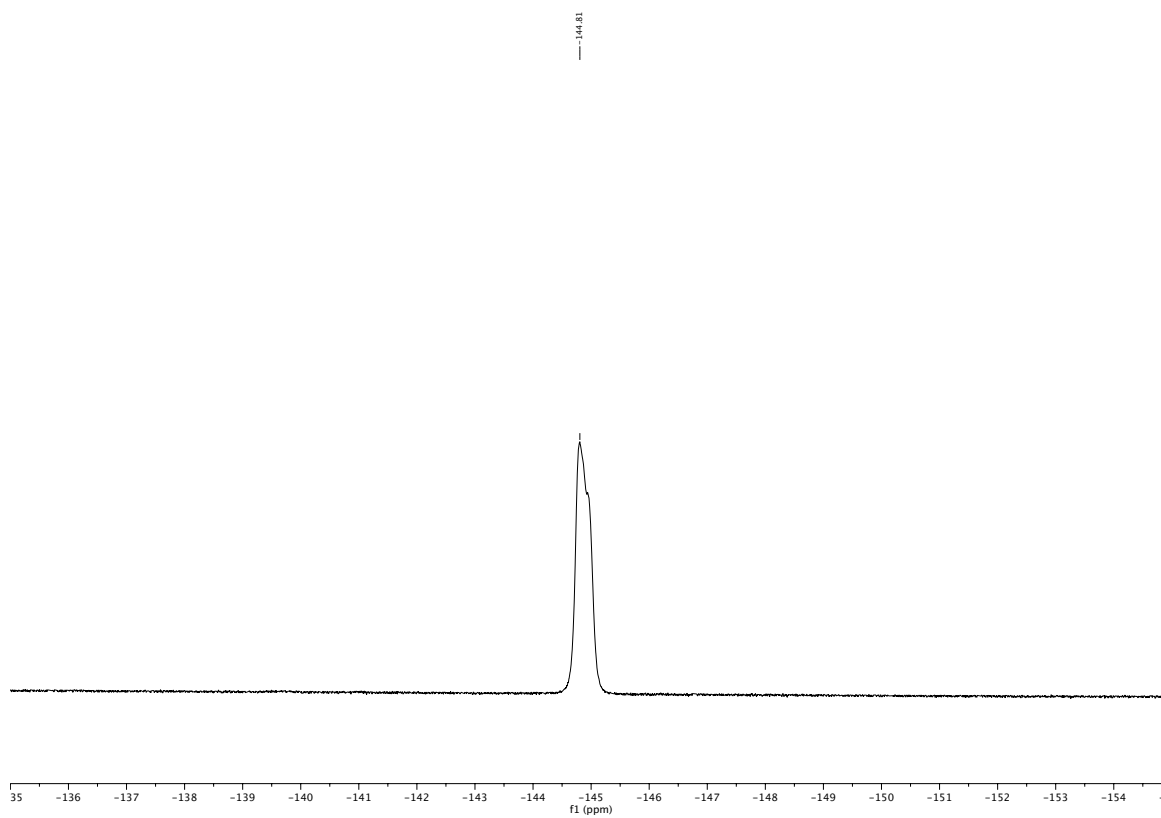
¹³C-NMR spectrum (151 MHz, DMSO-d₆)



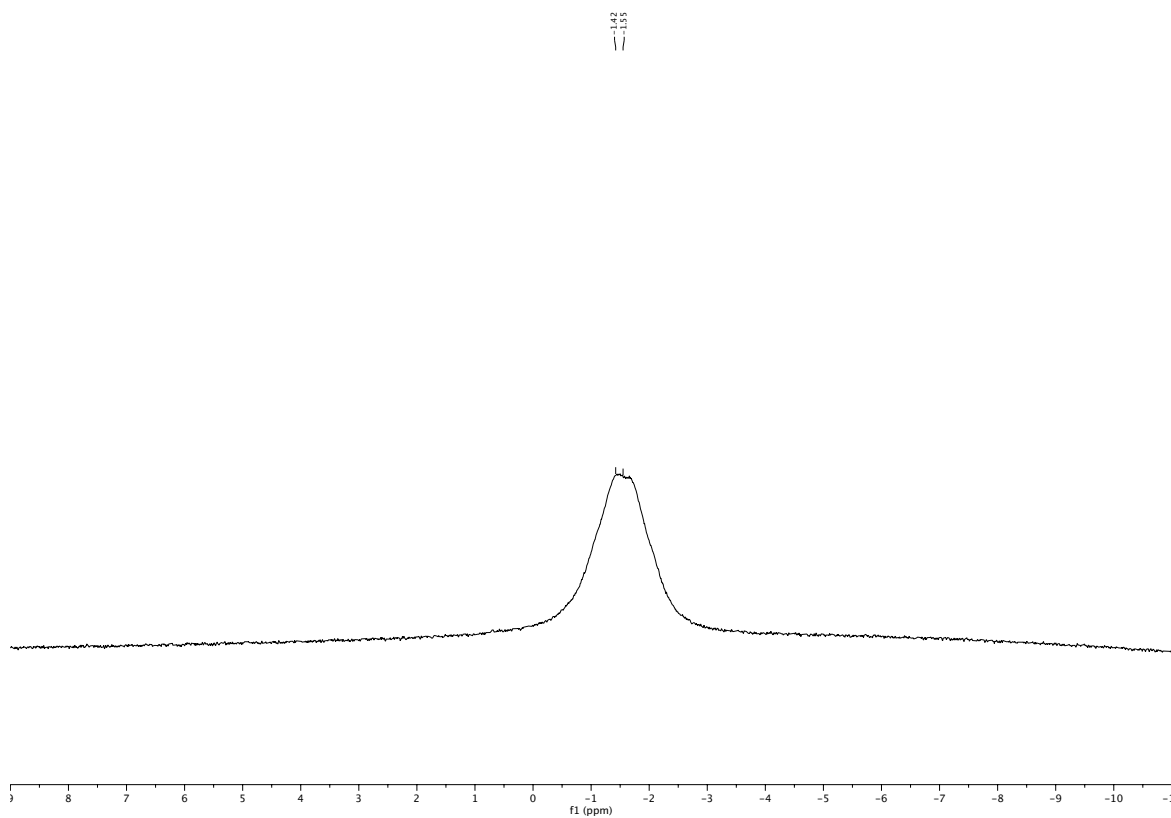
¹⁹F-NMR spectrum (282 MHz, DMSO-d₆)



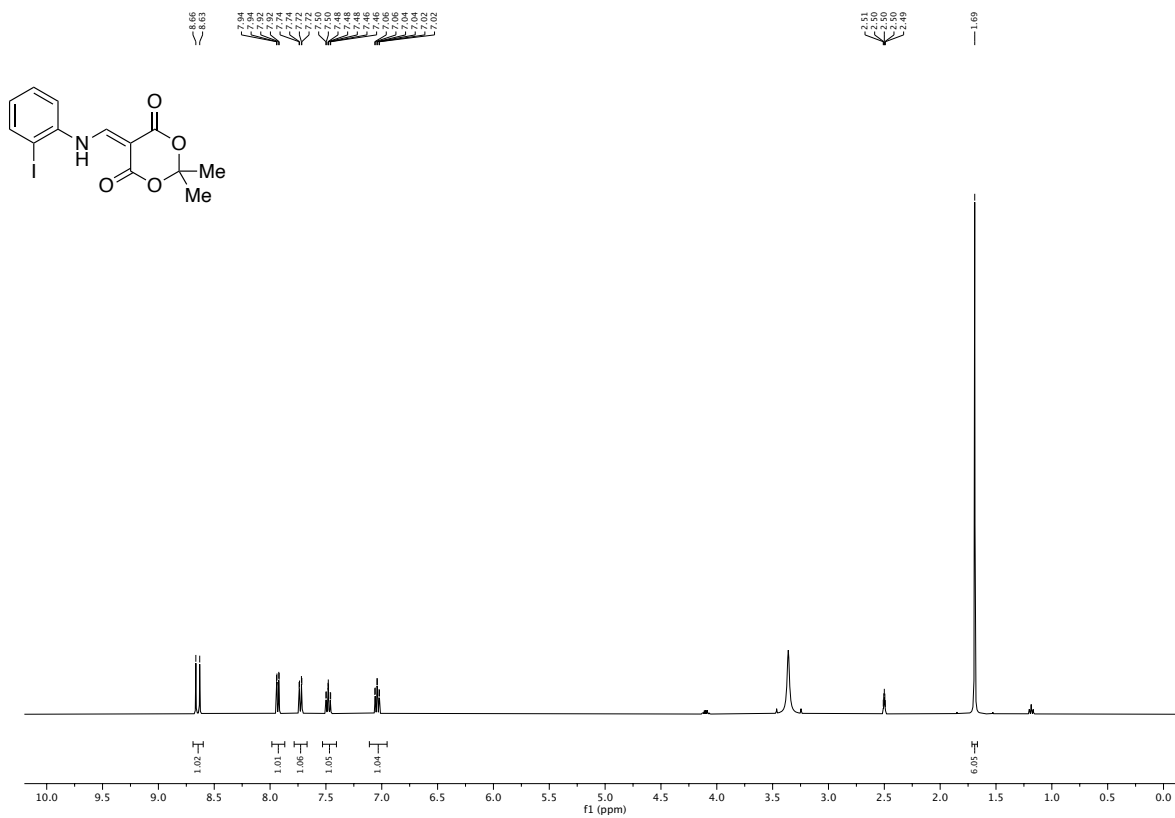
^{11}B -NMR spectrum (160 MHz, DMSO- d_6) **^1H -NMR spectrum (600 MHz DMSO- d_6)**

^{13}C -NMR spectrum (151 MHz, DMSO- d_6) **^{19}F -NMR spectrum (470 MHz, DMSO- d_6)**

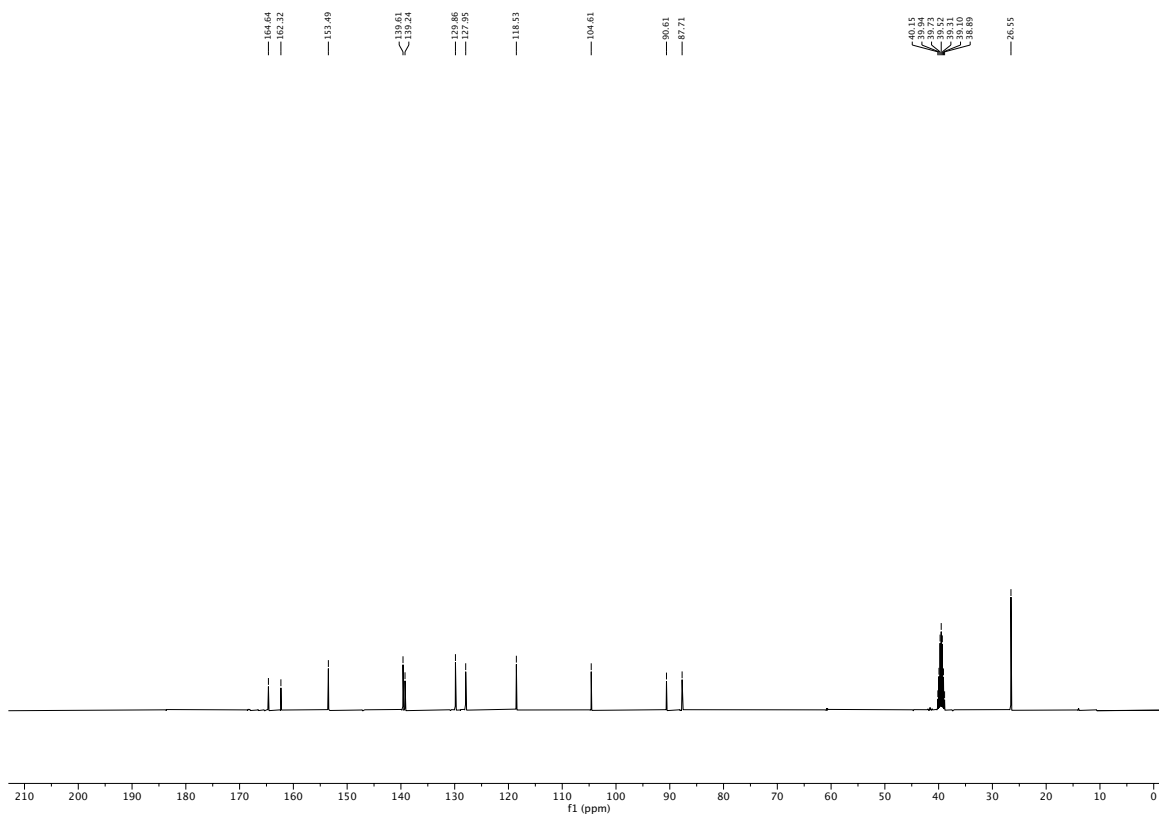
¹¹B-NMR spectrum (160 MHz, DMSO-d₆)



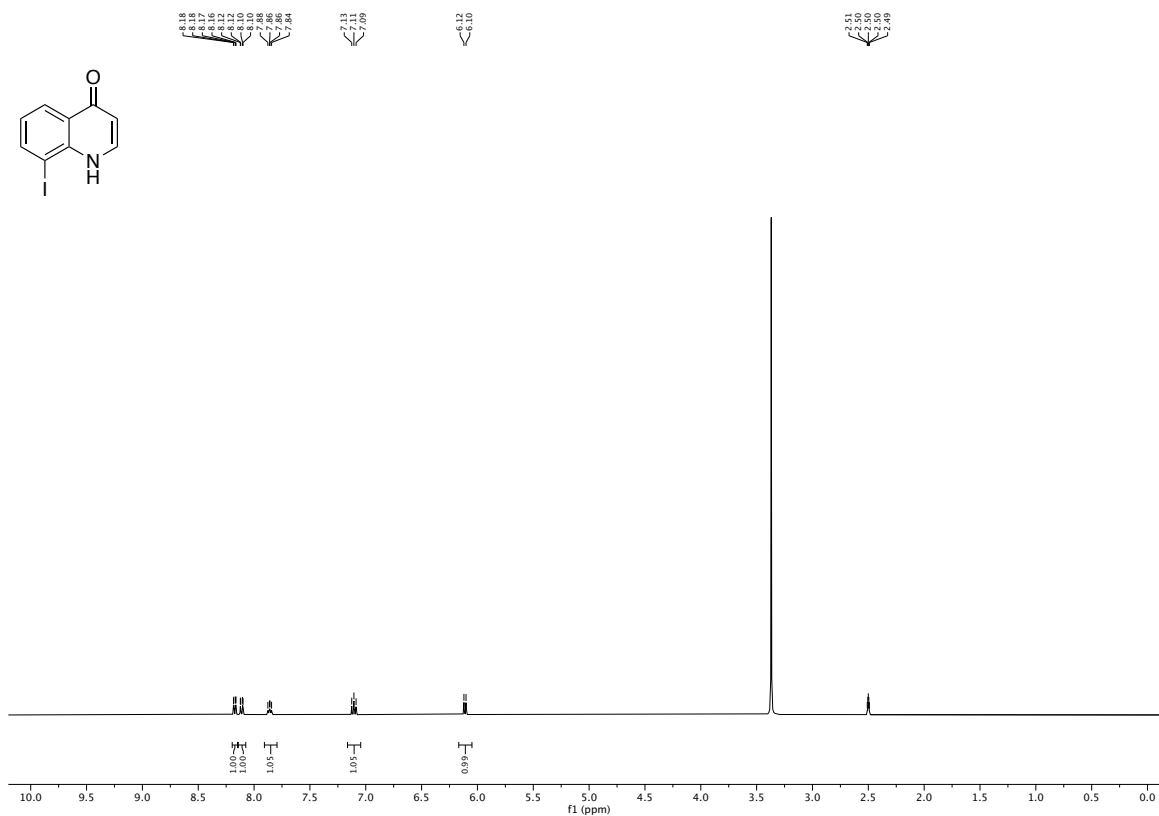
¹H-NMR (400 MHz, DMSO-d₆)

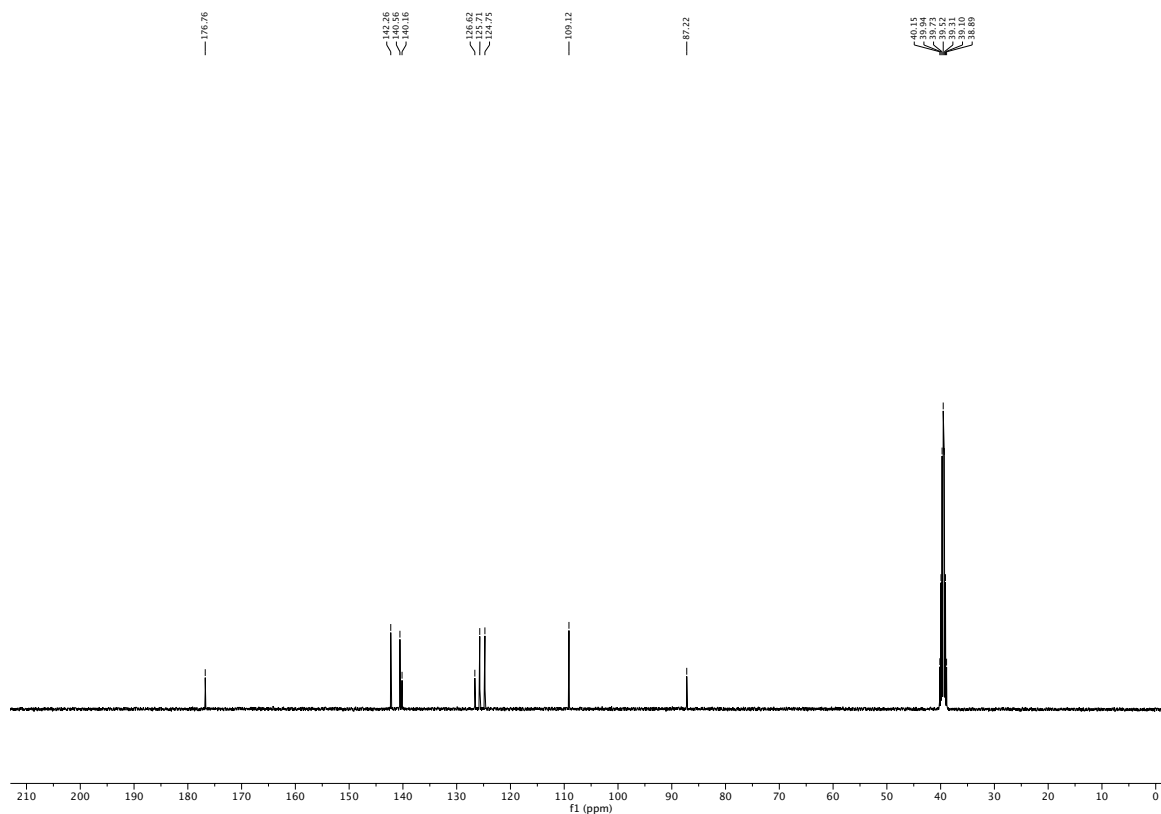
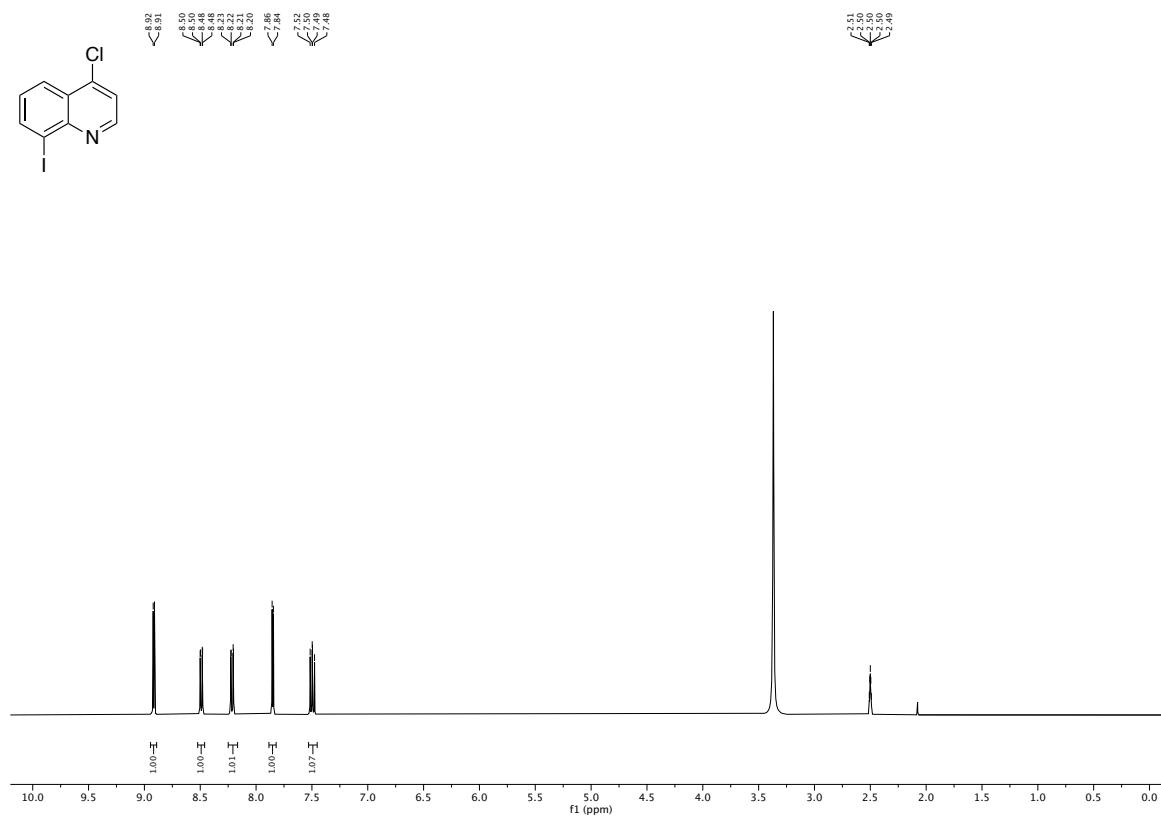


¹³C-NMR (101 MHz, DMSO-d₆)

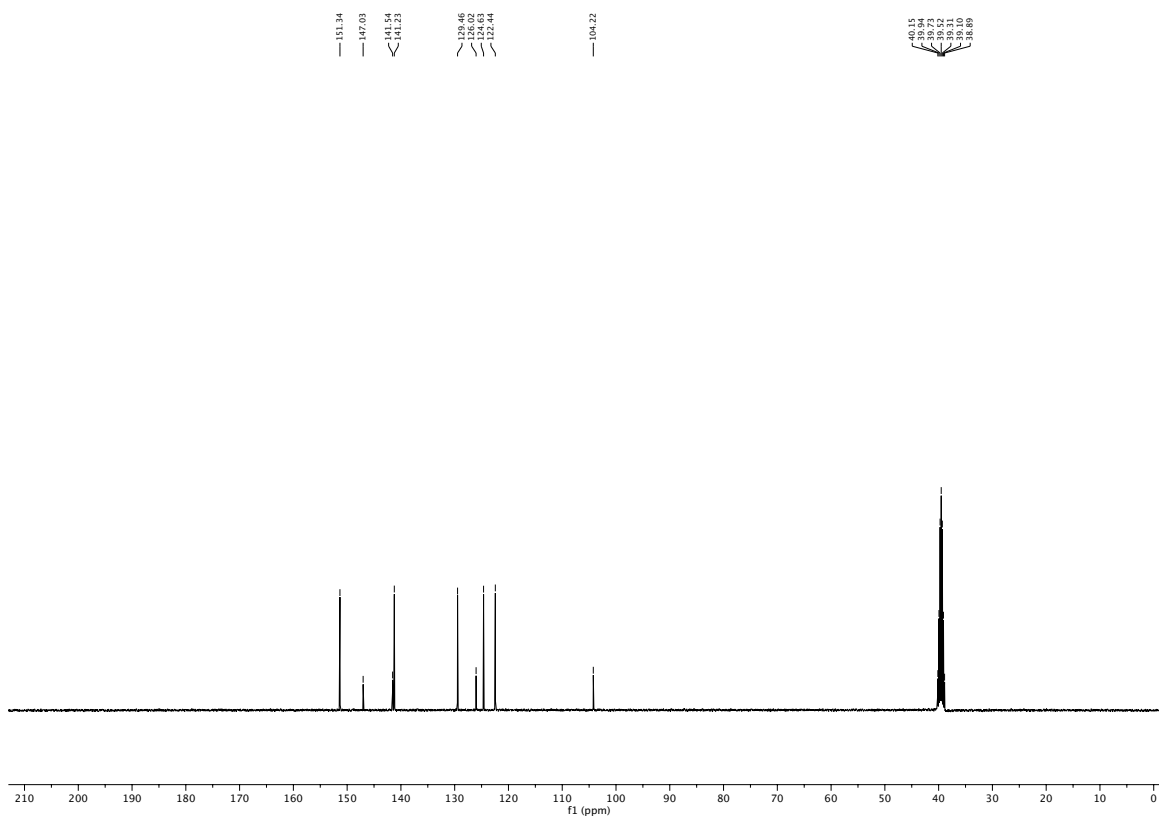


¹H-NMR (400 MHz, DMSO-d₆)

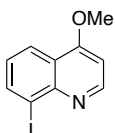
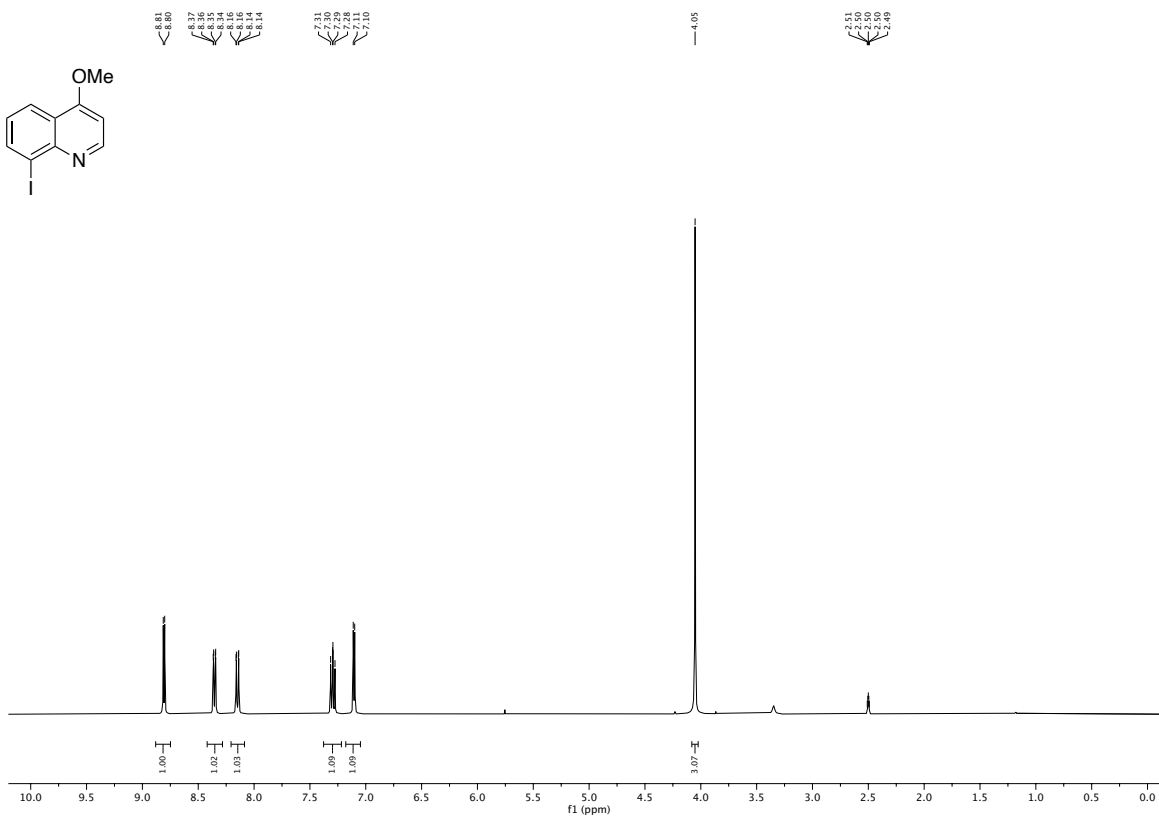


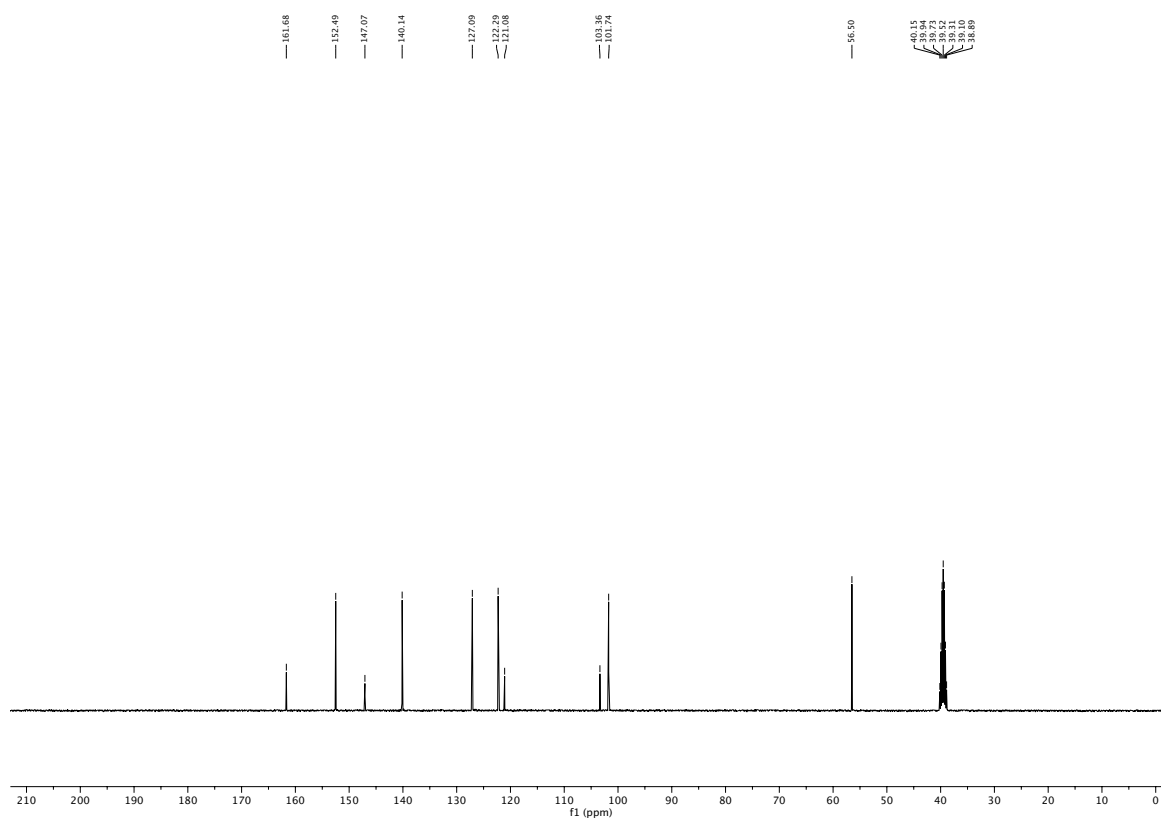
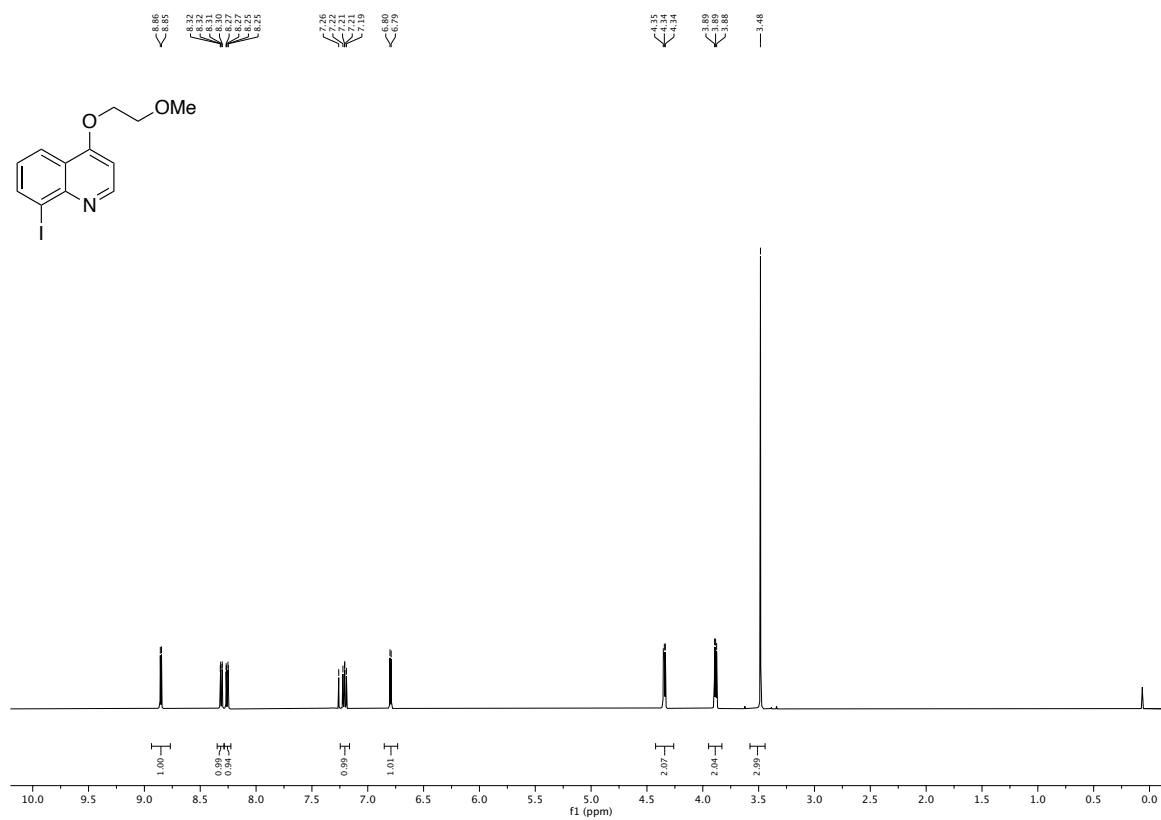
¹³C-NMR (101 MHz, DMSO-d₆)**¹H-NMR (400 MHz, DMSO-d₆)**

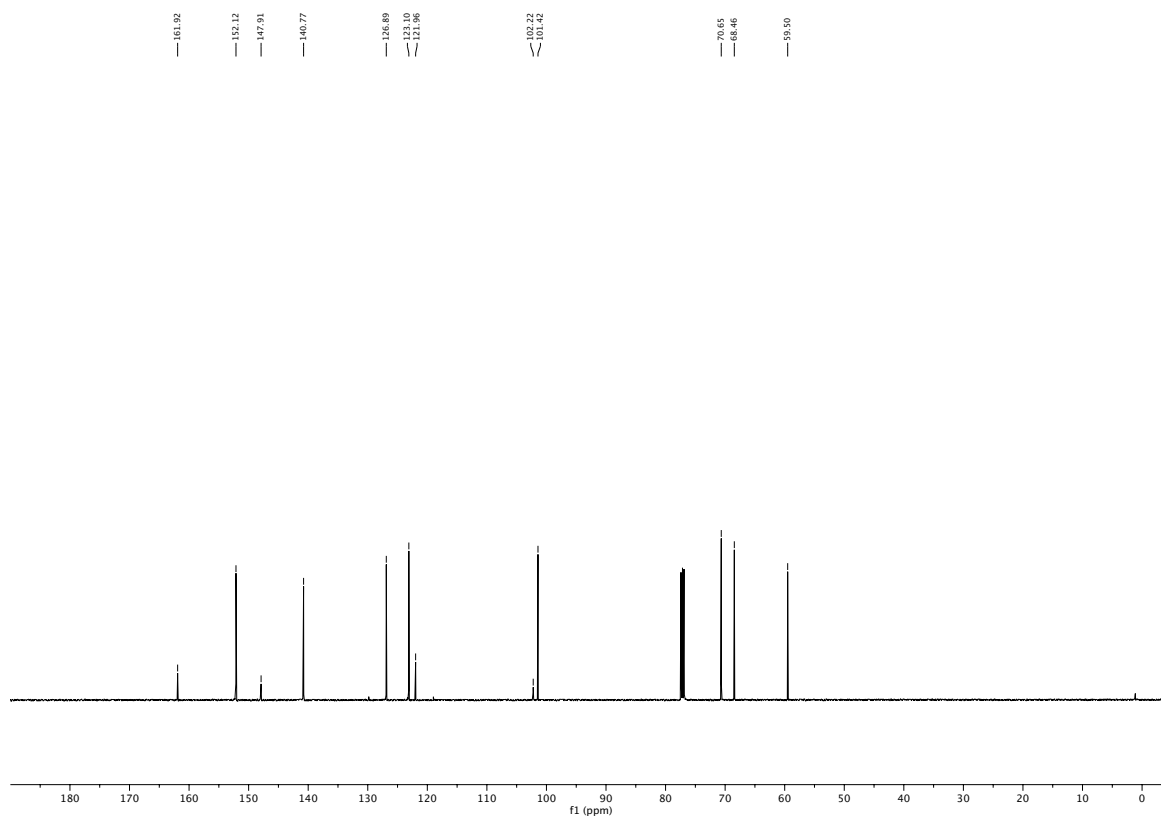
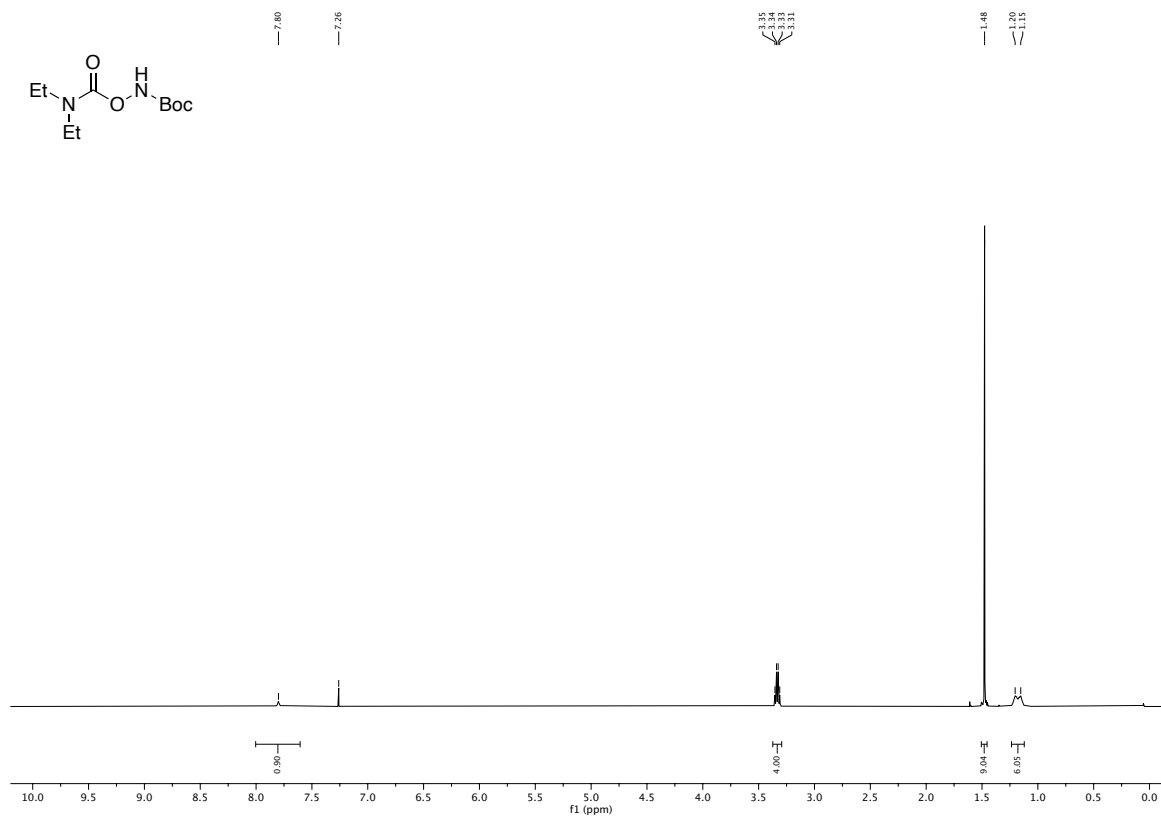
¹³C-NMR (101 MHz, DMSO-d₆)

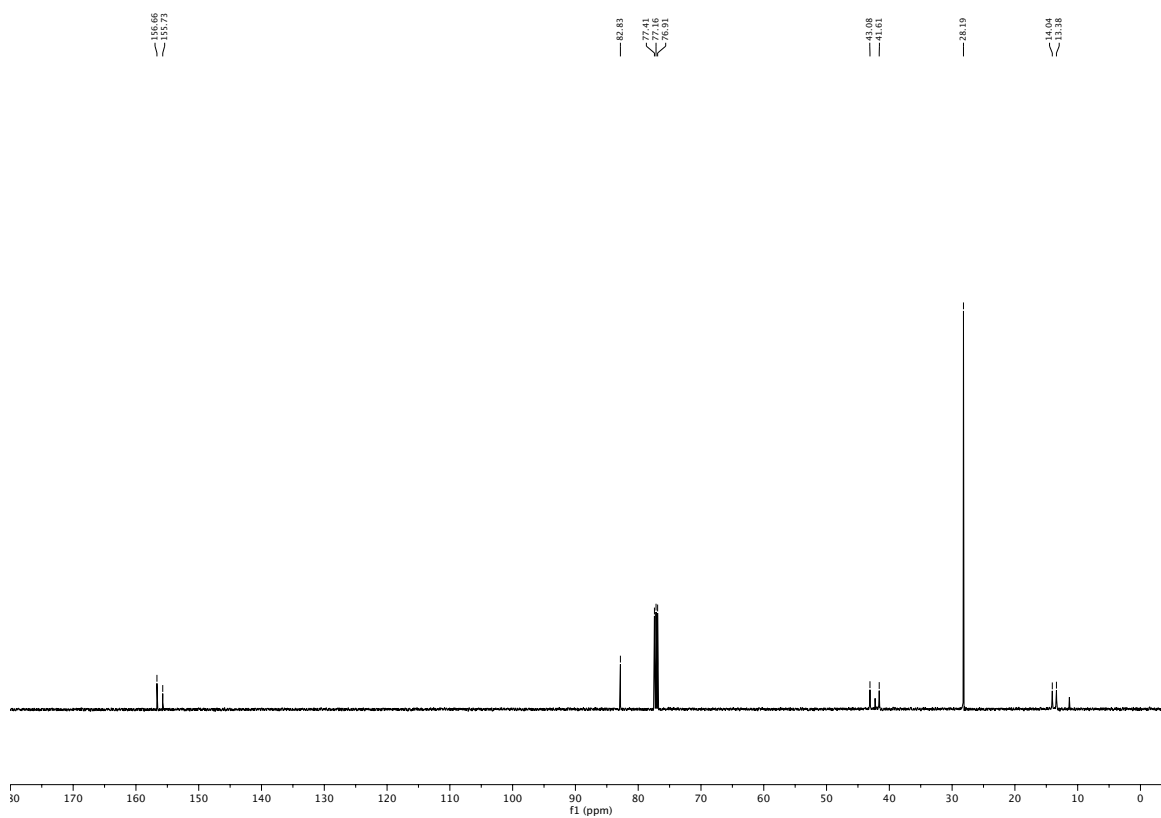
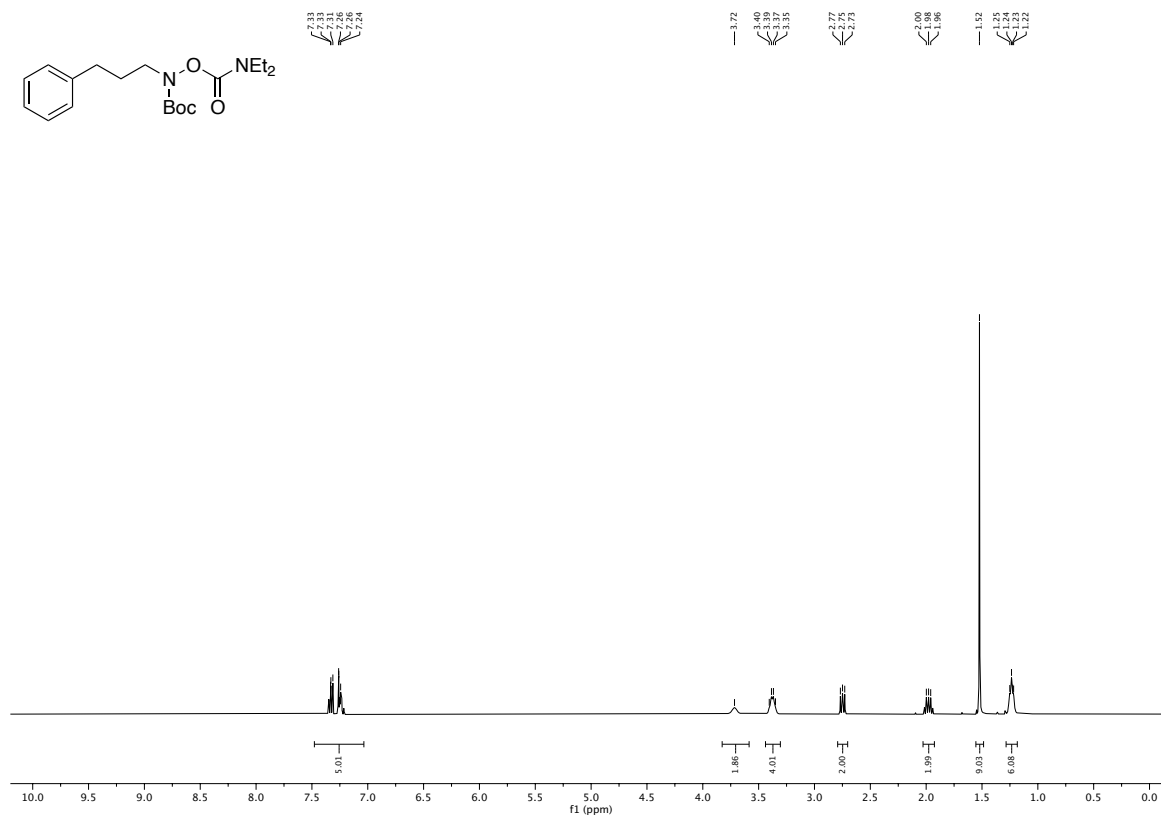


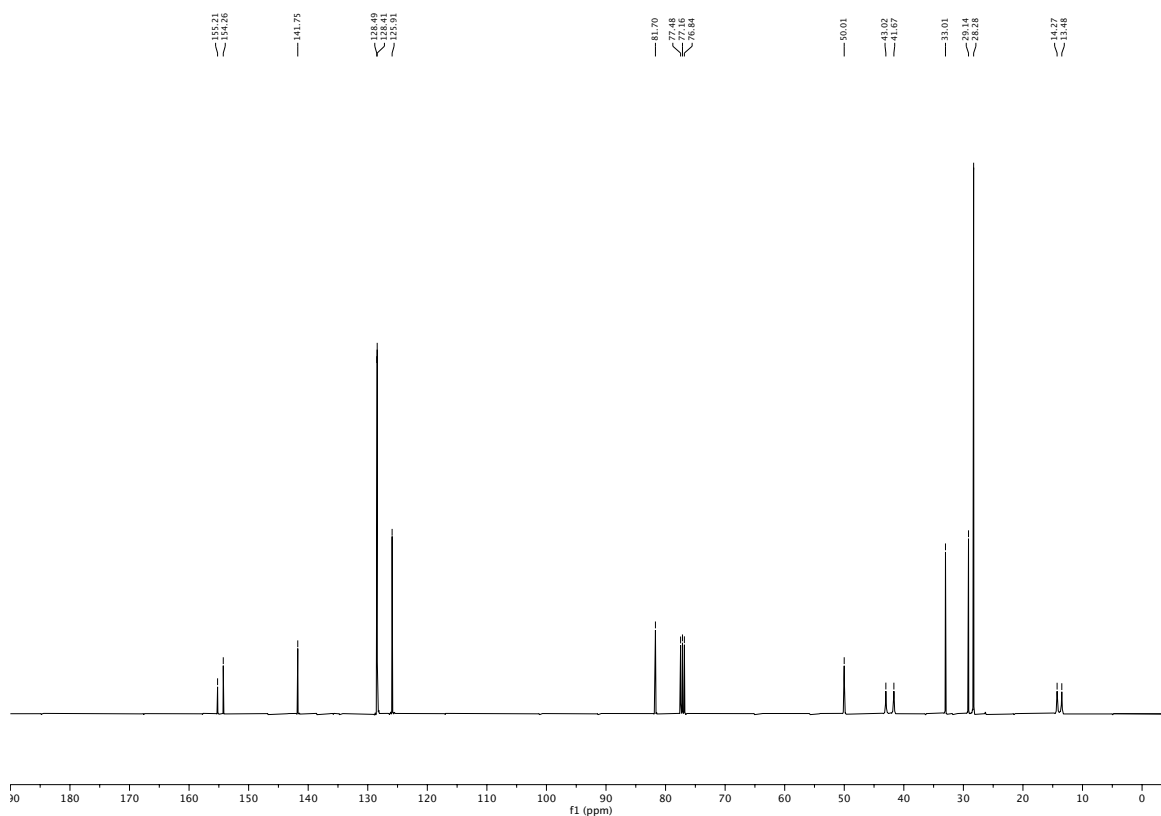
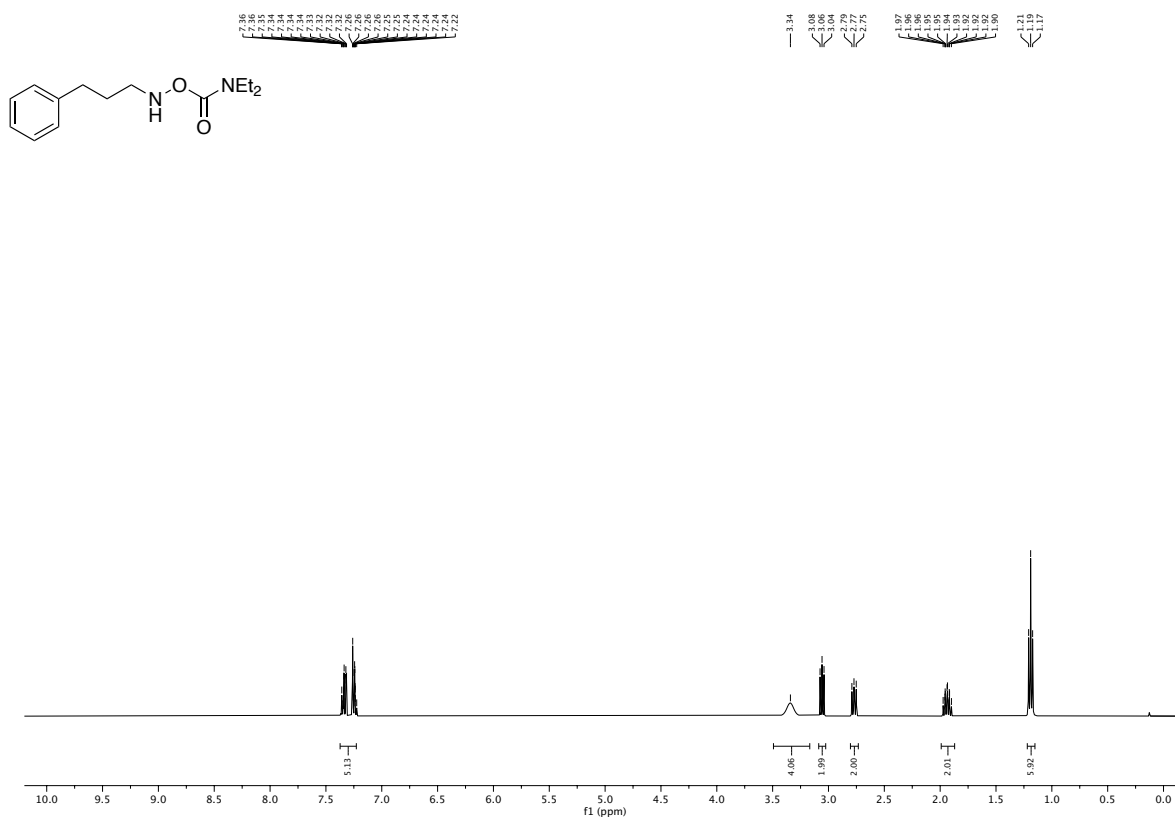
¹H-NMR (400 MHz, DMSO-d₆)

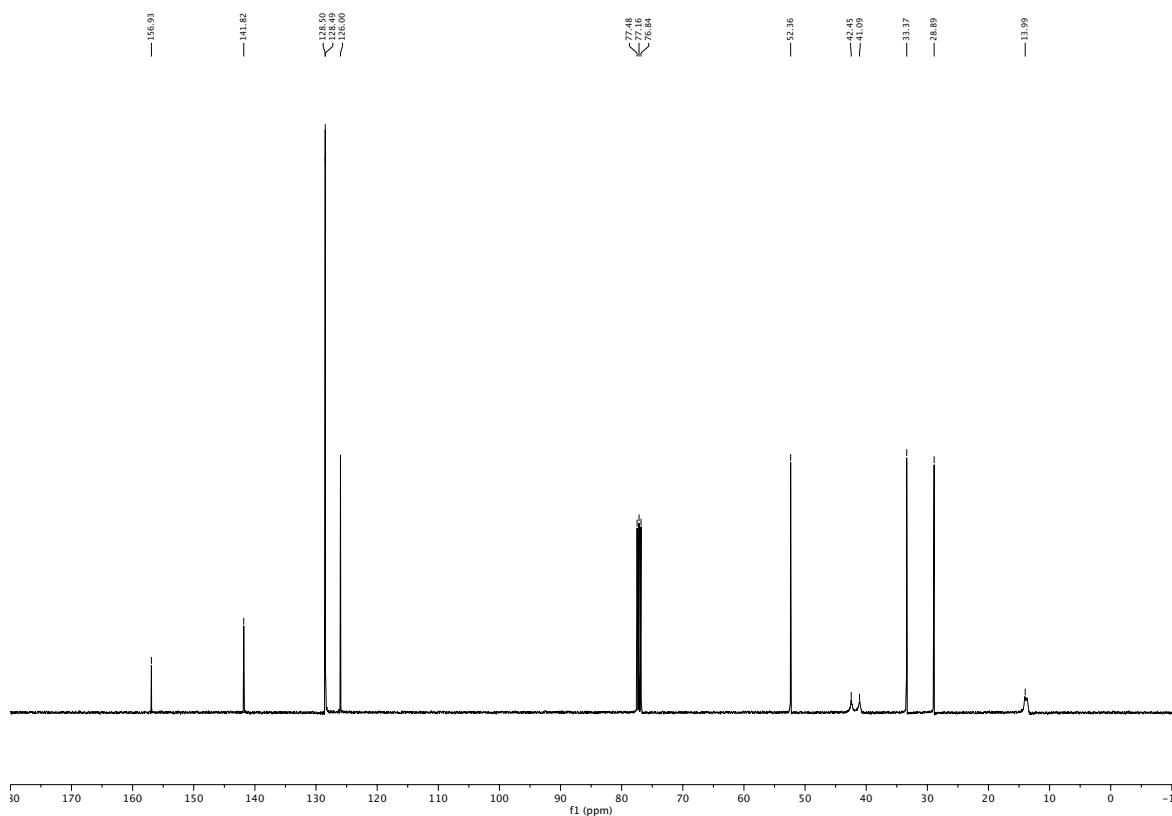
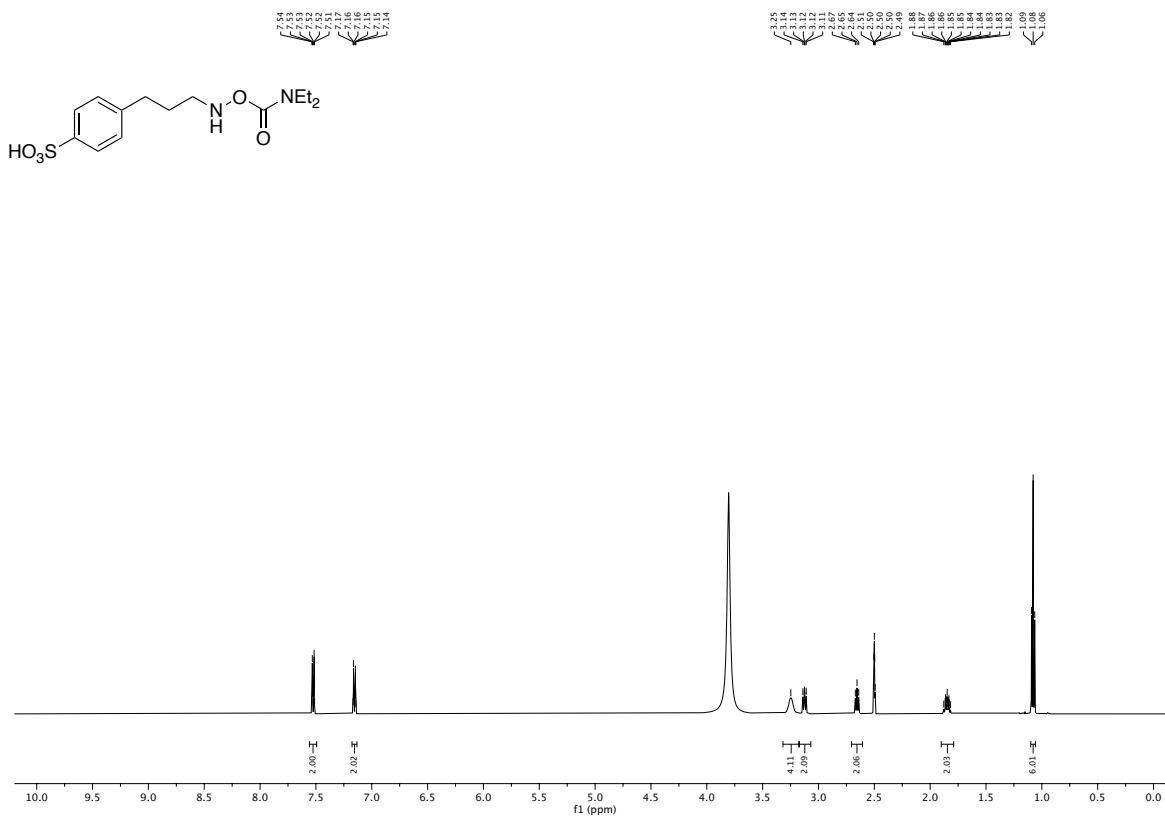


^{13}C -NMR (101 MHz, DMSO- d_6) **^1H NMR (500 MHz, CDCl_3)**

^{13}C -NMR (126 MHz, CDCl_3) **^1H NMR (500 MHz, CDCl_3)**

^{13}C -NMR (126 MHz, CDCl_3) **^1H NMR (400 MHz, CDCl_3)**

¹³C-NMR (101 MHz, CDCl₃)**¹H NMR (400 MHz, CDCl₃)**

^{13}C -NMR (101 MHz, CDCl_3) **^1H -NMR (500 MHz, DMSO-d_6)**

¹³C-NMR (126 MHz, DMSO-d₆)

